NASA TECHNICAL NOTE

NASA TN D-2709

c. 1

NASA TN D-2709

EFFECT OF FIRST-STAGE GEOMETRY ON AERODYNAMIC CHARACTERISTICS IN PITCH OF TWO-STAGE ROCKET VEHICLES FROM MACH 1.57 TO 2.86

by William A. Corlett and Celia S. Richardson

Langley Research Center

Langley Station, Hampton, Va.

NATIONAL AERONAUTICS AND SPACE ADMINISTRATION • WASHINGTON, D. C. • MARCH 1965

EFFECT OF FIRST-STAGE GEOMETRY ON AERODYNAMIC CHARACTERISTICS IN PITCH OF TWO-STAGE ROCKET VEHICLES FROM MACH 1.57 TO 2.86

By William A. Corlett and Celia S. Richardson

Langley Research Center
Langley Station, Hampton, Va.

NATIONAL AERONAUTICS AND SPACE ADMINISTRATION

For sale by the Office of Technical Services, Department of Commerce, Washington, D.C. 20230 -- Price $3.00

EFFECT OF FIRST-STAGE GEOMETRY ON AERODYNAMIC CHARACTERISTICS IN PITCH OF TWO-STAGE ROCKET VEHICLES FROM MACH 1.57 TO 2.86

By William A. Corlett and Celia S. Richardson
Langley Research Center

SUMMARY

An investigation has been conducted to determine the effects of first-stage geometry on the longitudinal aerodynamic characteristics of two-stage rocket vehicles at Mach numbers 1.57, 2.16, 2.50, and 2.86. The results indicate that reducing the diameter of the first-stage configuration or varying the length of a conical fairing between stages has only small effects on the normal-force and pitching-moment coefficients. However, a decrease in the first-stage diameter results in a large increase in the axial-force coefficient, but this increase can be significantly reduced by the addition of boattail fairings.

INTRODUCTION

The National Aeronautics and Space Administration has for some time been staging launch vehicles for specific payload missions. The staging of a launch vehicle is dependent upon the diameter and the thrust characteristics of available rocket engines, and often vehicles are staged so that the payload has a greater diameter than the rocket engine or engines of the previous stages. For vehicles in which the stability and performance are critical to the mission requirements, geometric differences between stages have been a matter of concern to the designer. Examples of such configurations are the Trailblazer I (ref. 1), the Trailblazer II (refs. 2 and 3), and the Little Joe-Apollo combination (ref. 4).

A series of two-stage launch vehicles were designed and tested to provide some information of general usefulness on staged vehicles with geometric differences between stages. Geometric differences consisted of systematic variations in the first-stage length, diameter, and boattail fairing. The tests were performed in the Langley Unitary Plan wind tunnel at Mach numbers of 1.57, 2.16, 2.50, and 2.86 at a constant Reynolds number per foot of 2.4×10^6. The angle-of-attack range was from about -5° to 10°.

SYMBOLS

The coefficients of forces and moments are referred to the body-axis system. (See fig. 1.) Aerodynamic moments for all configurations are presented about a point 11.069 inches aft of the model nose. All coefficients are based on the maximum cross-sectional area and diameter of the second stage.

A	maximum cross-sectional area of second stage, 0.08727 sq ft
C_A	axial-force coefficient, $\frac{\text{Axial force}}{qA}$
$C_{A,b}$	base axial-force coefficient, $\frac{\text{Base axial force}}{qA}$
$C_{A,c}$	chamber axial-force coefficient, $\frac{\text{Chamber axial force}}{qA}$
$C_{A,0}$	axial-force coefficient at angle of attack of 0°
C_m	pitching-moment coefficient, $\frac{\text{Pitching moment}}{qAd}$
C_{m_α}	slope of pitching-moment curve at $\alpha = 0^{\circ}$, $\frac{\partial C_m}{\partial \alpha}$, per deg
C_N	normal-force coefficient, $\frac{\text{Normal force}}{qA}$
C_{N_α}	slope of normal-force curve at $\alpha = 0^{\circ}$, $\frac{\partial C_N}{\partial \alpha}$, per deg
d	maximum diameter of second stage, 4.00 in.
d_a	base diameter of first stage, in.
l_B	length of boattail measured parallel to body axis, in.
l_a	length of first stage, in.
M	free-stream Mach number
q	free-stream dynamic pressure, lb/sq ft
r	radius, in.
α	angle of attack, deg
θ	angle of boattail taper, deg

MODEL

Dimensional details of the model are presented in figure 2. Photographs of two different test configurations are shown in figure 3. Each configuration utilized the same second-stage or payload section which consisted of a blunted 24° half-angle nose cone followed by a 12-inch cylinder with a diameter of 4.00 inches.

The geometry of the first stage was varied both in length and in diameter. The 20-inch, 12-inch, and 8-inch first stages, referred to herein as long, intermediate, and short first stages, respectively, were tested with diameters of 2.20 and 3.00 inches; the long and intermediate configurations were also tested with a base diameter of 4.00 inches. The length of the first-stage fairing, which is referred to as boattail length, was varied from 0 (i.e., sharp break in diameter between stages) to 4, 8, 12, or 20 inches, depending on first-stage length. Two sizes of cruciform fins oriented in the horizontal and vertical planes were tested. The larger fins had areas of 12.62 square inches, and the smaller fins had areas of 5.16 square inches. (See fig. 2.)

TESTS, CORRECTIONS, AND ACCURACY

The investigation was conducted in the low Mach number test section of the Langley Unitary Plan wind tunnel. The test section is about 4 by 4 feet square and about 7 feet long. The nozzle leading to the test section is of the asymmetric-sliding-block type, which permits a continuous variation in Mach number from 1.47 to 2.86 without tunnel shutdown. Aerodynamic forces and moments were determined with an electrical strain-gage balance mounted within the model.

Tests were made through an angle-of-attack range from approximately -5° to 10° at an angle of sideslip of 0°. Angles of attack have been corrected for both tunnel flow angularity and deflection of the balance and sting due to aerodynamic loads. The axial-force data have been adjusted to free-stream static pressure acting over the model base and chamber. Typical values of combined base and chamber axial-force coefficients are presented in figure 4.

The test conditions for the investigation were as follows:

Mach number	Stagnation temperature, $^\circ$F	Stagnation pressure, lb/sq ft
1.57	125	1283
2.16	125	1610
2.50	150	2028
2.86	150	2458

The Reynolds number per foot was maintained constant at 2.4×10^6. The stagnation dewpoint was maintained below -30° F in order to avoid condensation effects. Carborundum grains with a diameter of approximately 0.012 inch were affixed around the model 1 inch aft of the nose in a 1/16-inch-wide strip to assure turbulent flow over the model.

The estimated accuracies of the data, based on calibrations and data repeatability, are within the following limits:

C_A	±0.003
C_N	±0.020
C_m	±0.018
M	±0.015
α, deg	±0.10

RESULTS AND DISCUSSION

The aerodynamic characteristics in pitch for various configurations of the model are presented in figures 5 to 8 for the long first stages, in figures 9 to 12 for the intermediate first stages, and in figures 13 and 14 for the short first stages. The effect of the ratio of the first-stage diameter to second-stage diameter on the longitudinal aerodynamic parameters is presented in figure 15 and the effect of boattail length on the longitudinal aerodynamic parameters is presented in figures 16 to 21. An outline of the contents of these data figures is as follows:

	Figure
Aerodynamic characteristics in pitch:	
Long first stage:	
Fins off	5
Small fins; $l_B/d = 2$	6
Large fins	7
$d_a/d = 1.00$	8
Intermediate first stage:	
Fins off	9
Small fins	10
Large fins	11
$d_a/d = 1.00$	12
Short first stage:	
Fins off	13
Large fins	14
Effect of the ratio of first-stage diameter to second-stage diameter on the longitudinal aerodynamic parameters.	
Fins off; $l_B/d = 0$	15

	Figure
Effect of boattail length on longitudinal aerodynamic parameters:	
Fins off; $d_a/d = 0.55$	16
Fins off; $d_a/d = 0.75$	17
Small fins; $d_a/d = 0.55$	18
Small fins; $d_a/d = 0.75$	19
Large fins; $d_a/d = 0.55$	20
Large fins; $d_a/d = 0.75$	21

The summarized data in figure 15 indicate that there is no significant effect of first-stage diameter on C_{N_α} and little effect on C_{m_α} except for a slight reduction in stability as the first-stage diameter is decreased. However, a decrease in first-stage diameter causes a significant increase in axial force. It should be noted that these axial-force data are adjusted for base pressures corresponding to free-stream static pressure, and therefore they represent the net external axial force on the configurations. For these data to be comparable, the base must be completely filled with rocket exhaust. Essentially the same results were obtained with fins on. (See, for example, figs. 10 and 11.)

The effect of boattail length on the longitudinal aerodynamic parameters is presented in figures 16 to 21. The addition of a boattail produces a small reduction in C_{N_α} and generally causes a destabilizing increment of C_{m_α}. The major effect of the addition of a boattail is that it provides a substantial reduction in axial force which becomes more pronounced as the boattail length is increased. The effects of boattail addition are essentially the same for fins off or on.

CONCLUDING REMARKS

An investigation has been conducted to determine the effects of first-stage geometry on the longitudinal aerodynamic characteristics of two-stage rocket vehicles at Mach numbers 1.57, 2.16, 2.50, and 2.86. The results indicate that reducing the diameter of the first-stage configuration or varying the length of a conical fairing between stages has only small effects on the normal-force and pitching-moment coefficients. However, a decrease in the first-stage diameter results in a large increase in the axial-force coefficient, but this increase can be significantly reduced by the addition of boattail fairings.

Langley Research Center,
National Aeronautics and Space Administration,
Langley Station, Hampton, Va., December 8, 1964.

REFERENCES

1. Gregory, Donald T.; and Carraway, Ausley B.: Investigation of the Static Longitudinal Stability and Roll Characteristics of a Three-Stage Missile Configuration at Mach Numbers From 1.77 to 2.87. NASA TM X-124, 1959.

2. Carraway, Ausley B.; Edwards, Frederick G.; and Keating, Jean C.: Investigation of the Static Stability Characteristics of Two Stages of a Three-Stage Missile at a Mach Number of 4.00. NASA TN D-651, 1961.

3. Lundstrom, Reginald R.; Henning, Allen B.; and Hook, W. Ray: Description and Performance of Three Trailblazer II Reentry Research Vehicles. NASA TN D-1866, 1964.

4. Fournier, Roger H.: Static Longitudinal Aerodynamic Characteristics of a 0.028-Scale Model of a Proposed Little Joe-Apollo Space Vehicle at Mach Numbers From 1.50 to 2.16. NASA TM X-730, 1962.

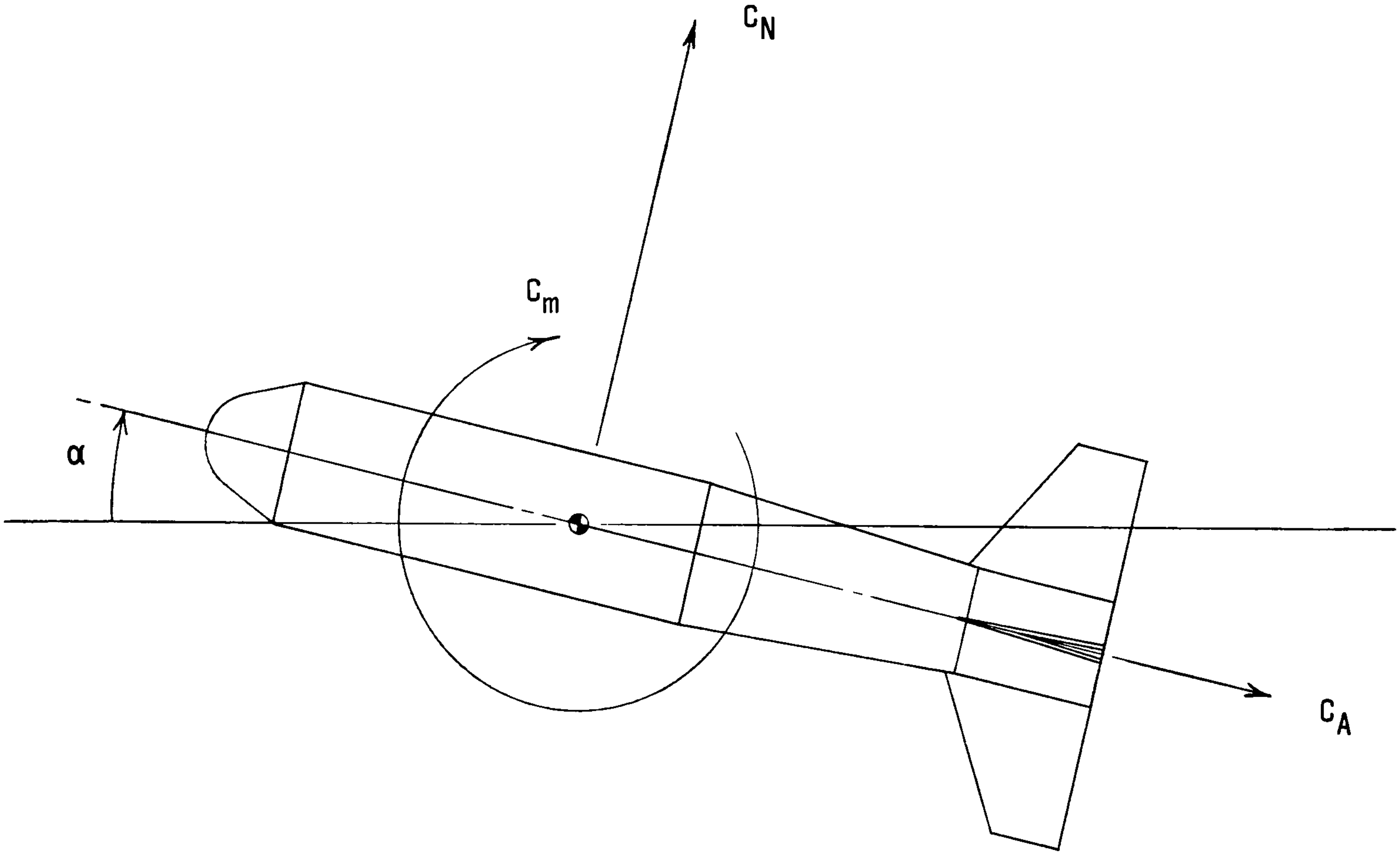

Figure 1.- Body system of axes with positive coefficients and angle of attack shown.

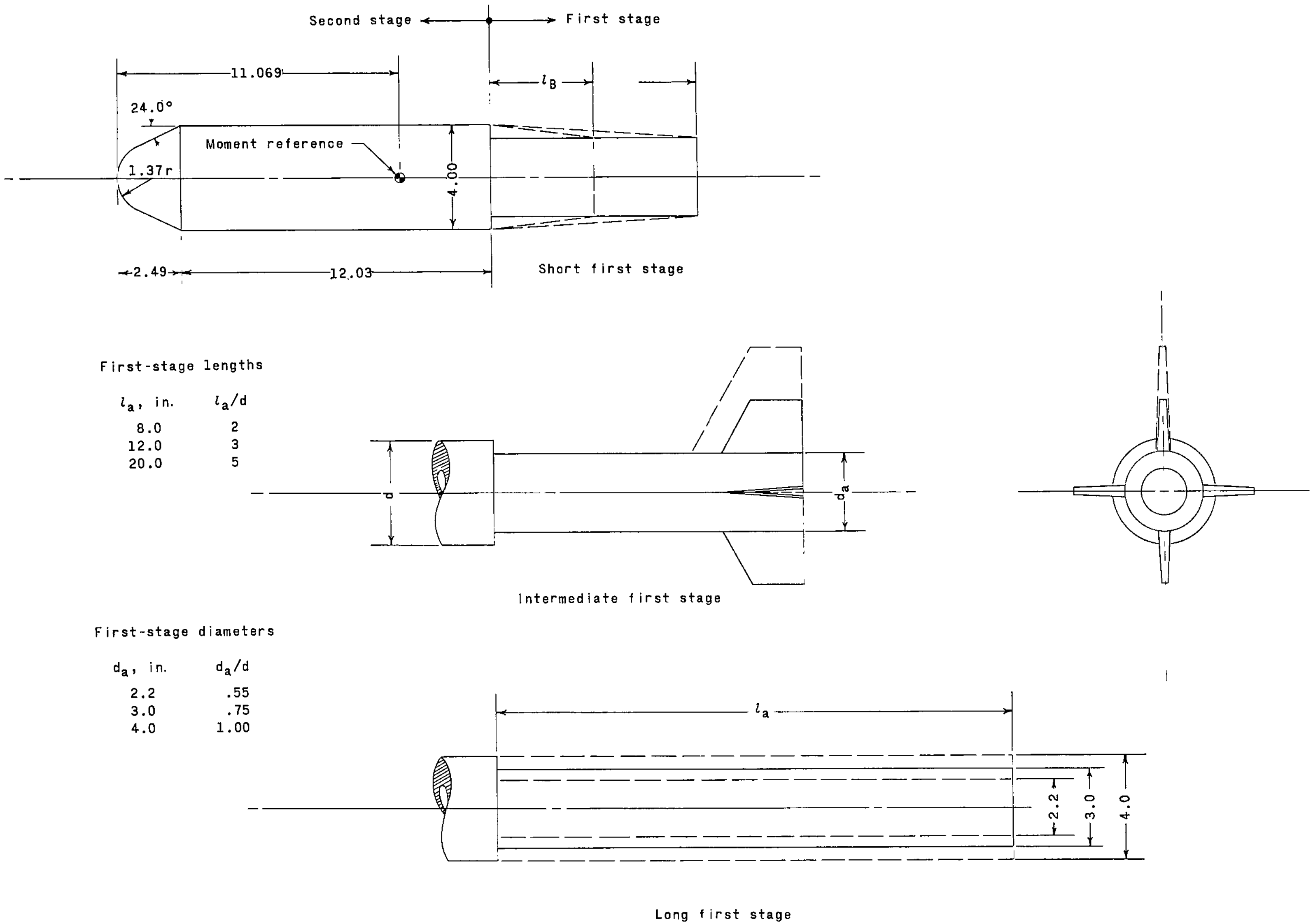

Figure 2.- Dimensional details of model. All dimensions in inches unless otherwise indicated.

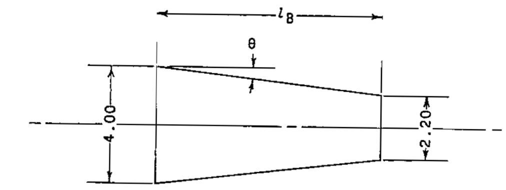

l_B, in	l_B/d	θ, deg
4.0	1	14.03
8.0	2	7.12
12.0	3	4.76
20.0	5	2.86

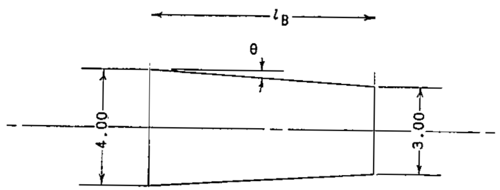

l_B, in	l_B/d	θ, deg
4.0	1	7.12
8.0	2	3.57
12.0	3	2.38
20.0	5	1.43

Boattail fairings

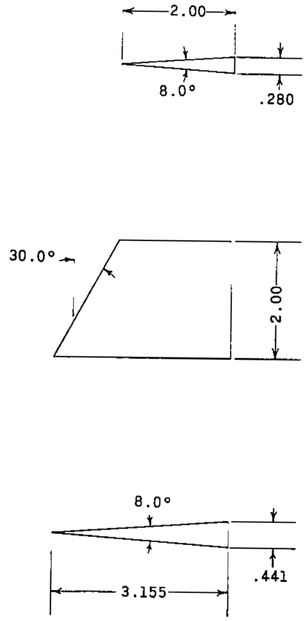

Small fin

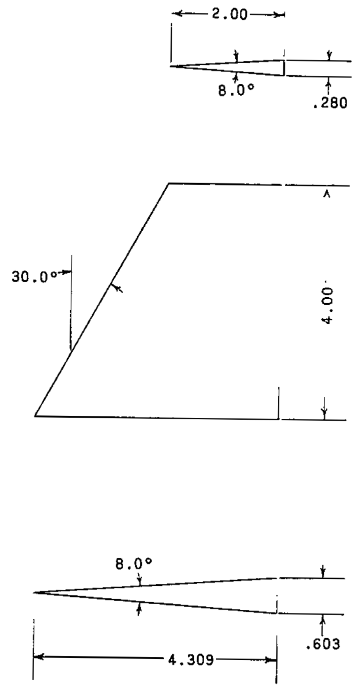

Large fin

Figure 2.- Concluded.

(a) Long first stage; large fins; $d_a/d = 0.55$; $l_B/d = 2$. L-62-3438

(b) Intermediate first stage; small fins; $d_a/d = 0.55$; $l_B/d = 3$. L-62-8807

Figure 3.- Photographs of model mounted in wind tunnel.

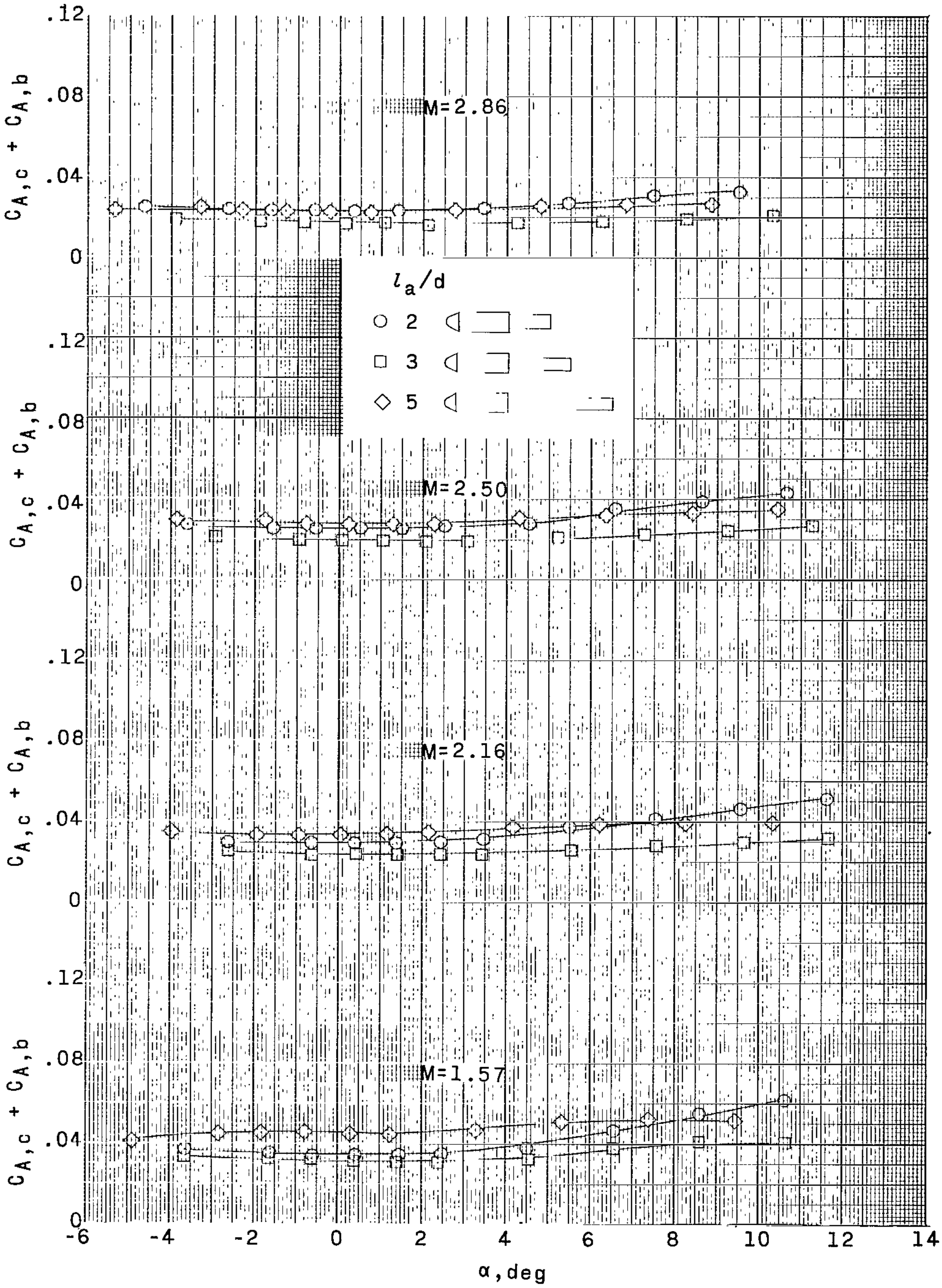

(a) $l_B/d = 0$; fins off; $d_a/d = 0.55$.

Figure 4.- Variation of combined base and chamber axial-force coefficients with angle of attack.

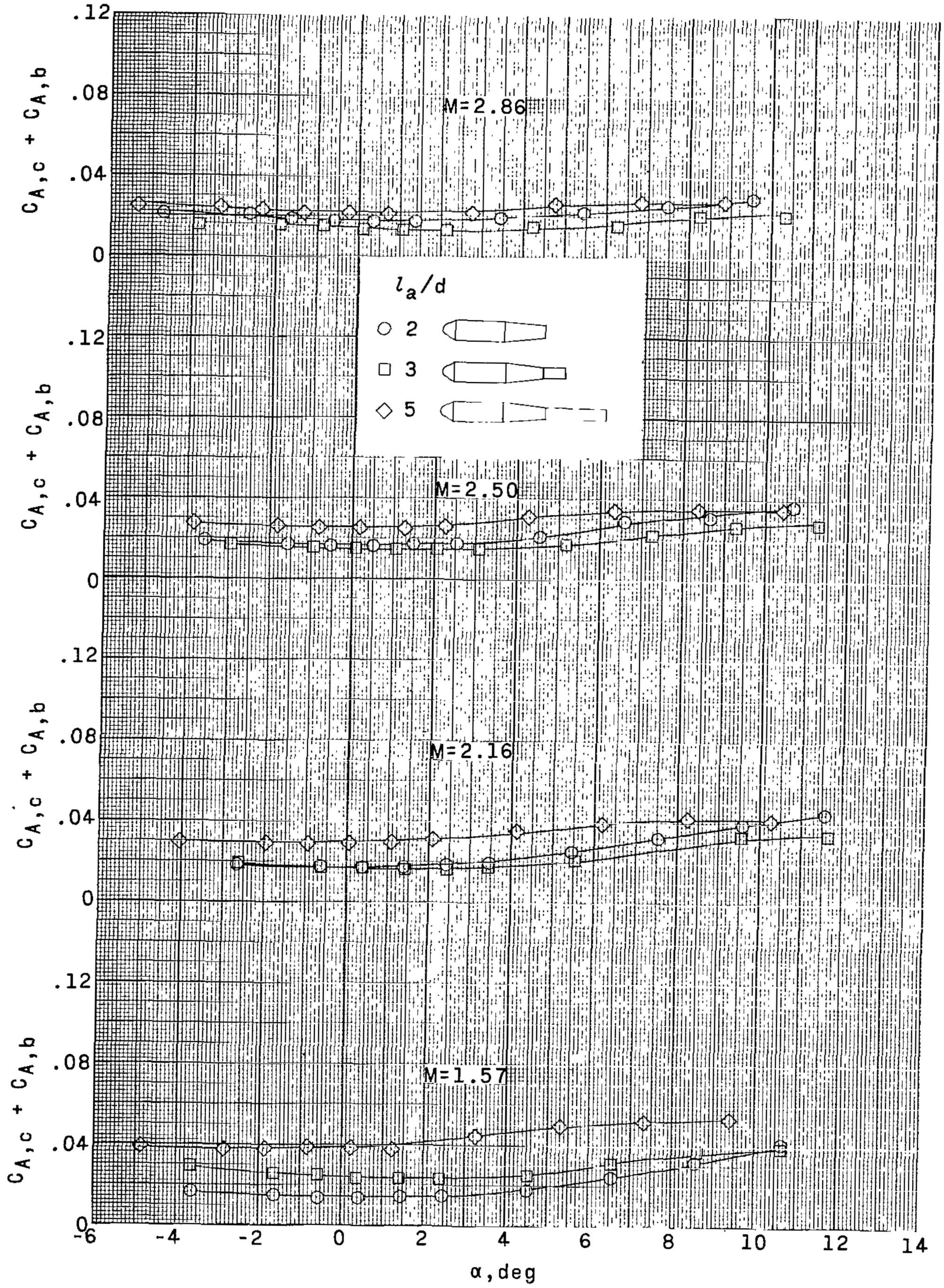

(b) $l_B/d = 2$; fins off; $d_a/d = 0.55$.

Figure 4.- Continued.

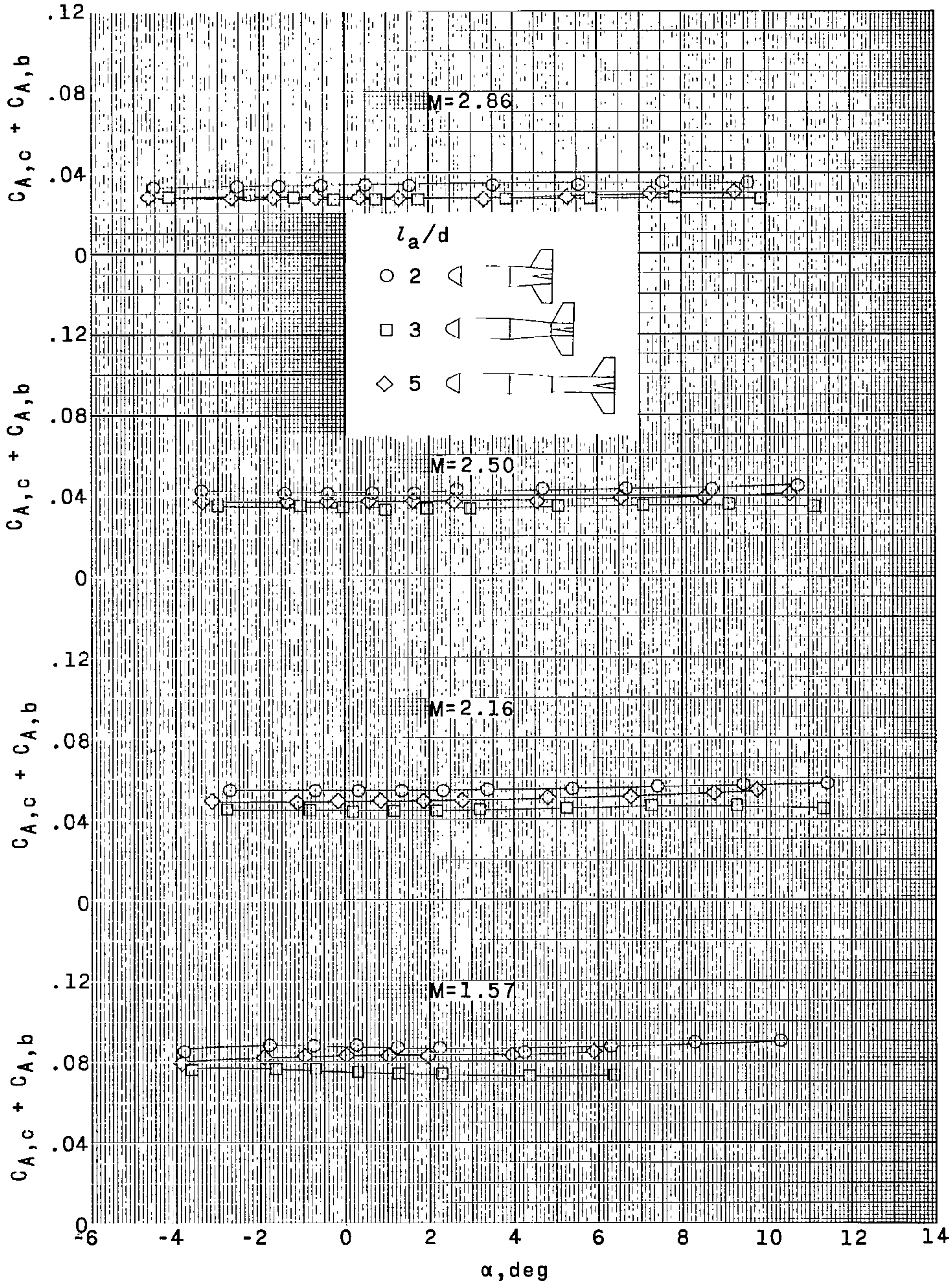

(c) $l_B/d = 2$; large fins; $d_a/d = 0.55$.

Figure 4.- Continued.

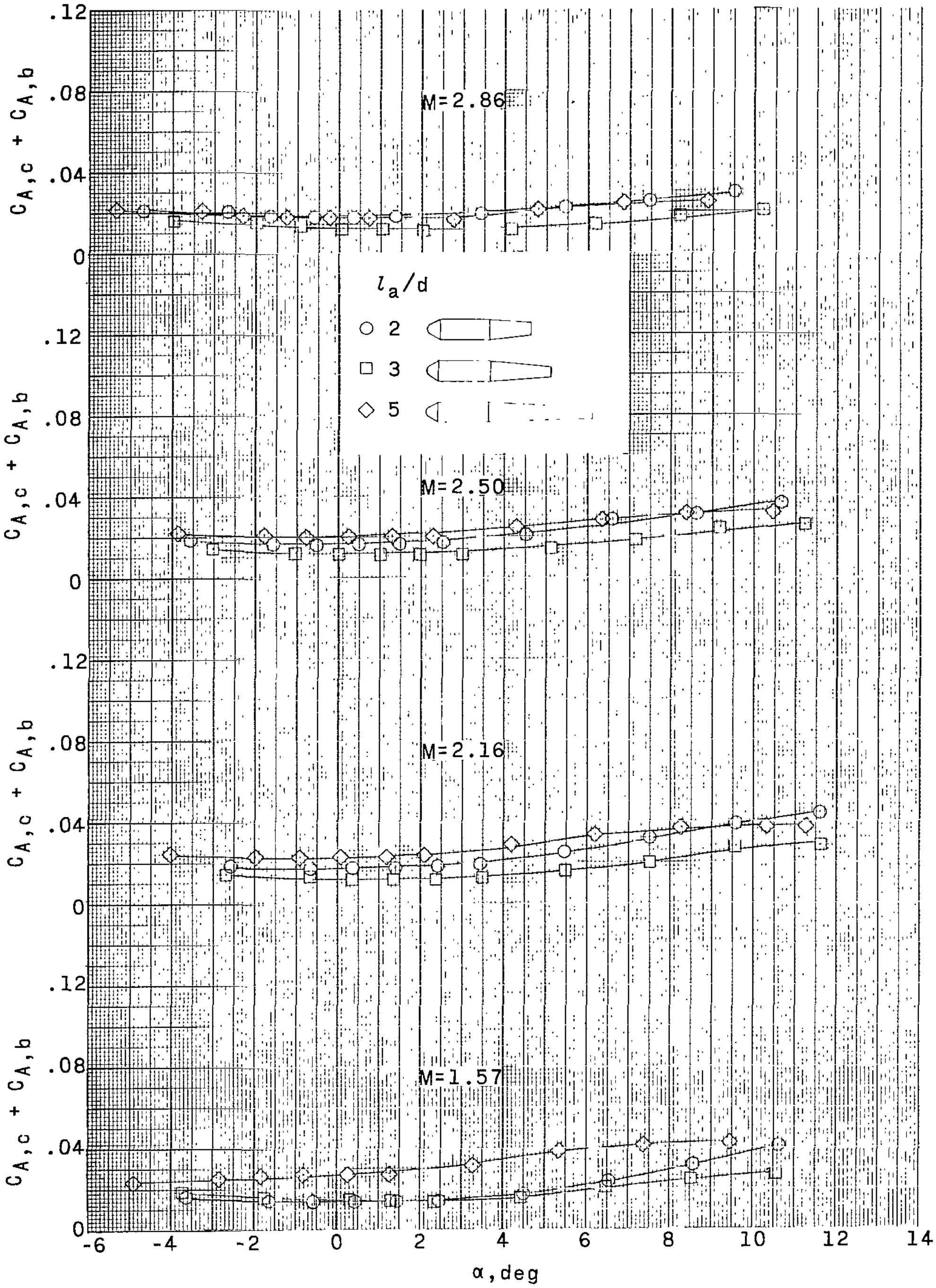

(d) Full boattails; fins off; $d_a/d = 0.55$.

Figure 4.- Continued.

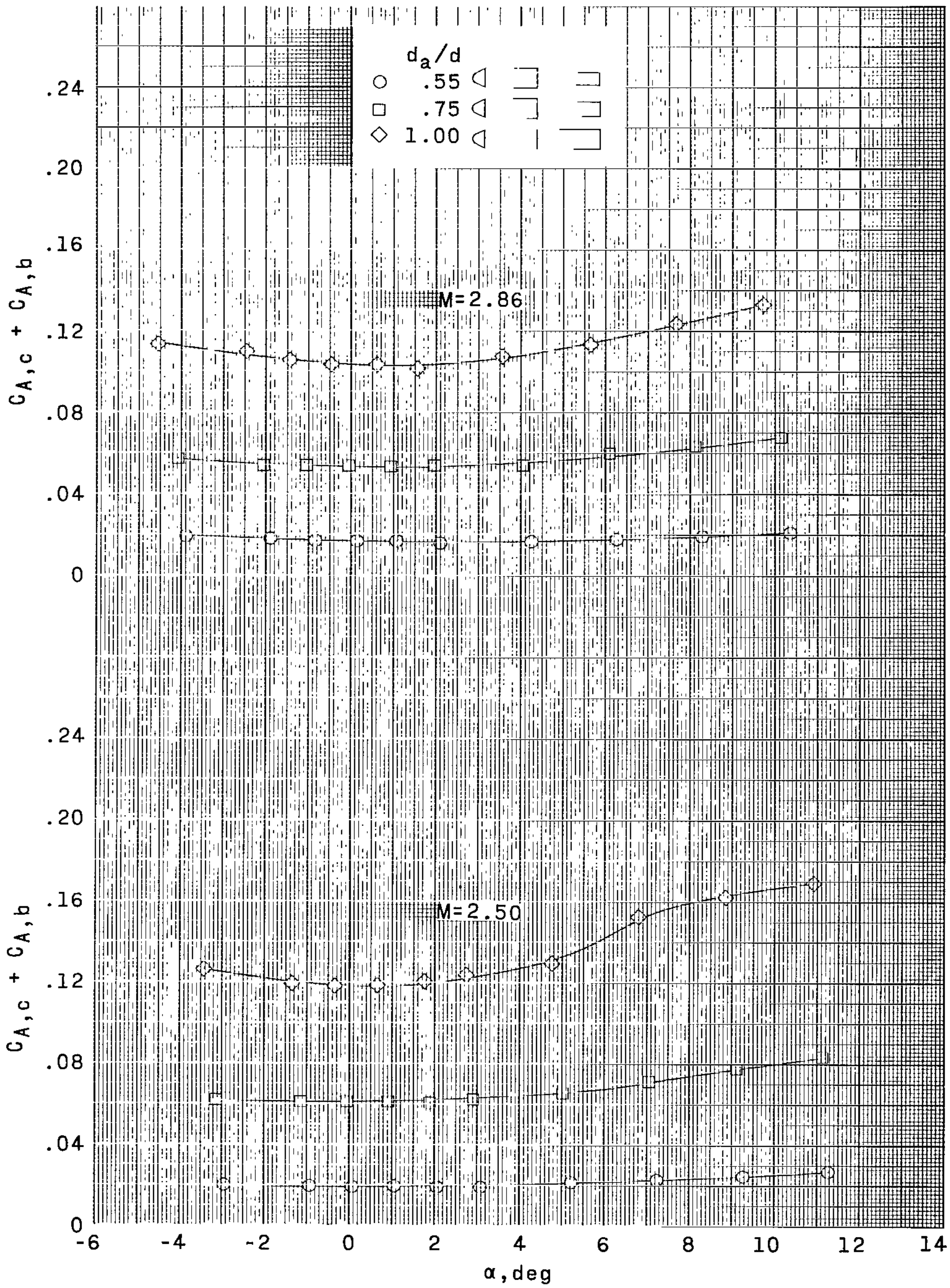

(e) Intermediate first stage; $l_B/d = 0$; fins off.

Figure 4.- Continued.

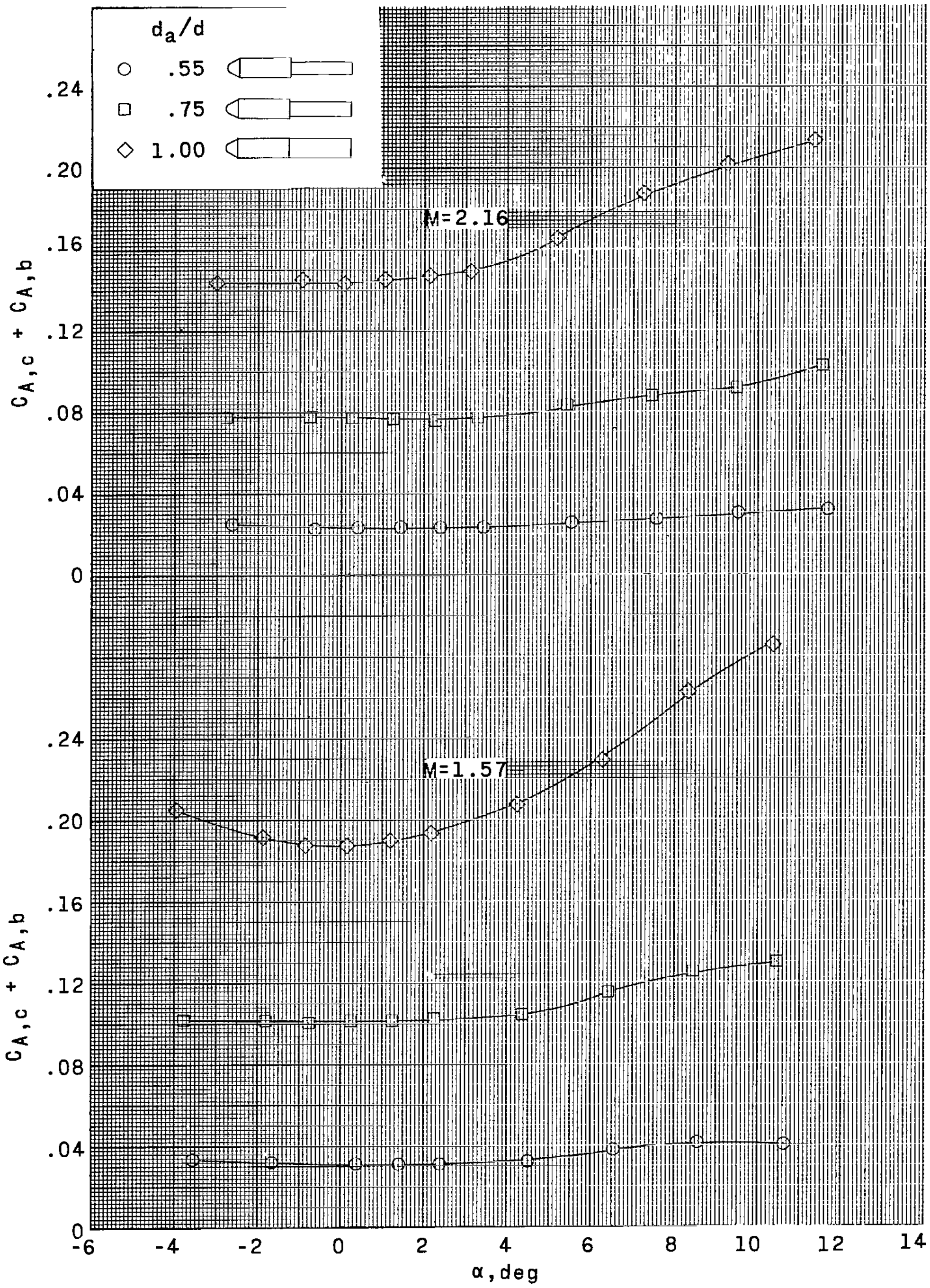

(e) Concluded.

Figure 4.- Concluded.

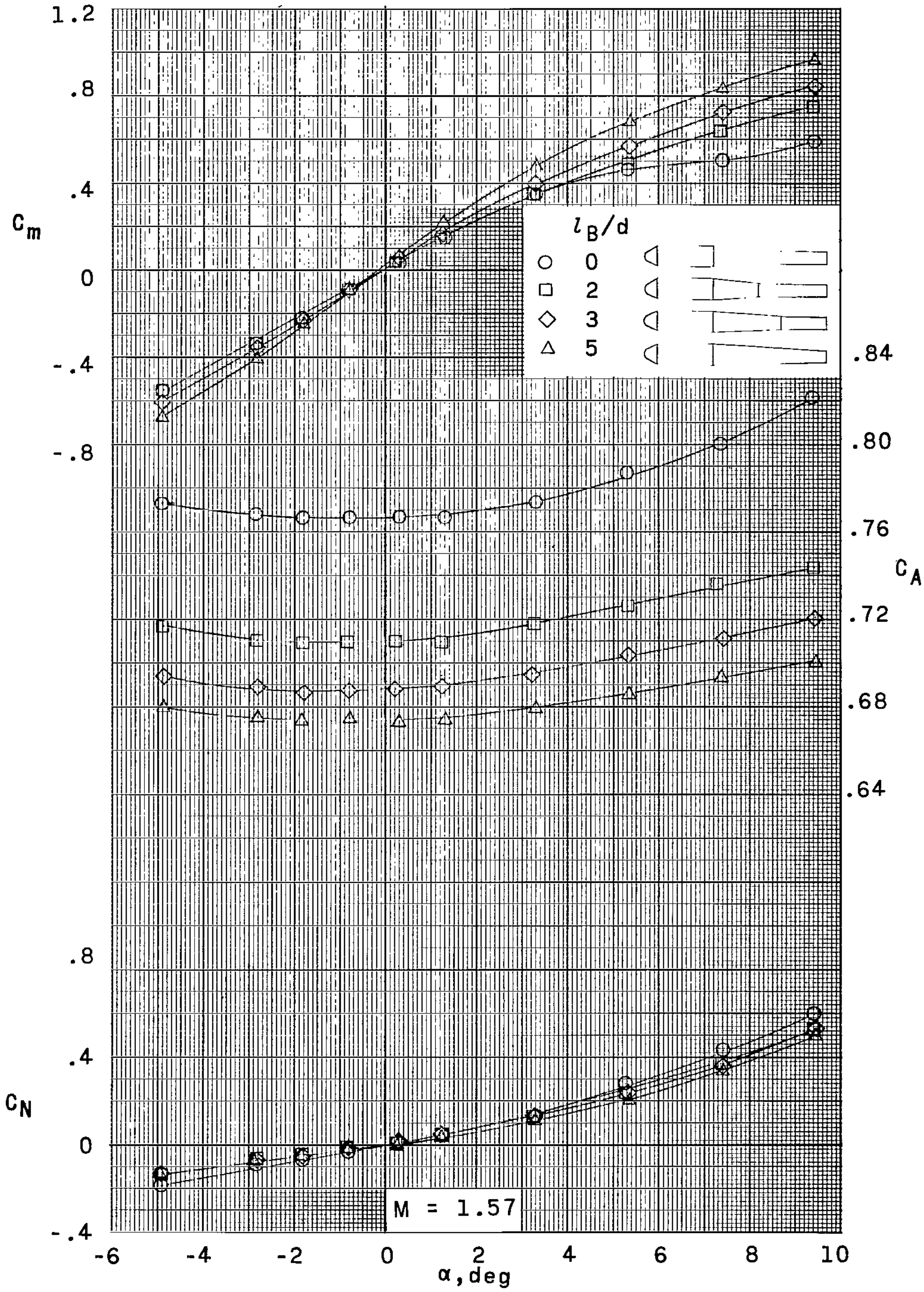

(a) $d_a/d = 0.55$.

Figure 5.- Aerodynamic characteristics in pitch. Long first stage; fins off.

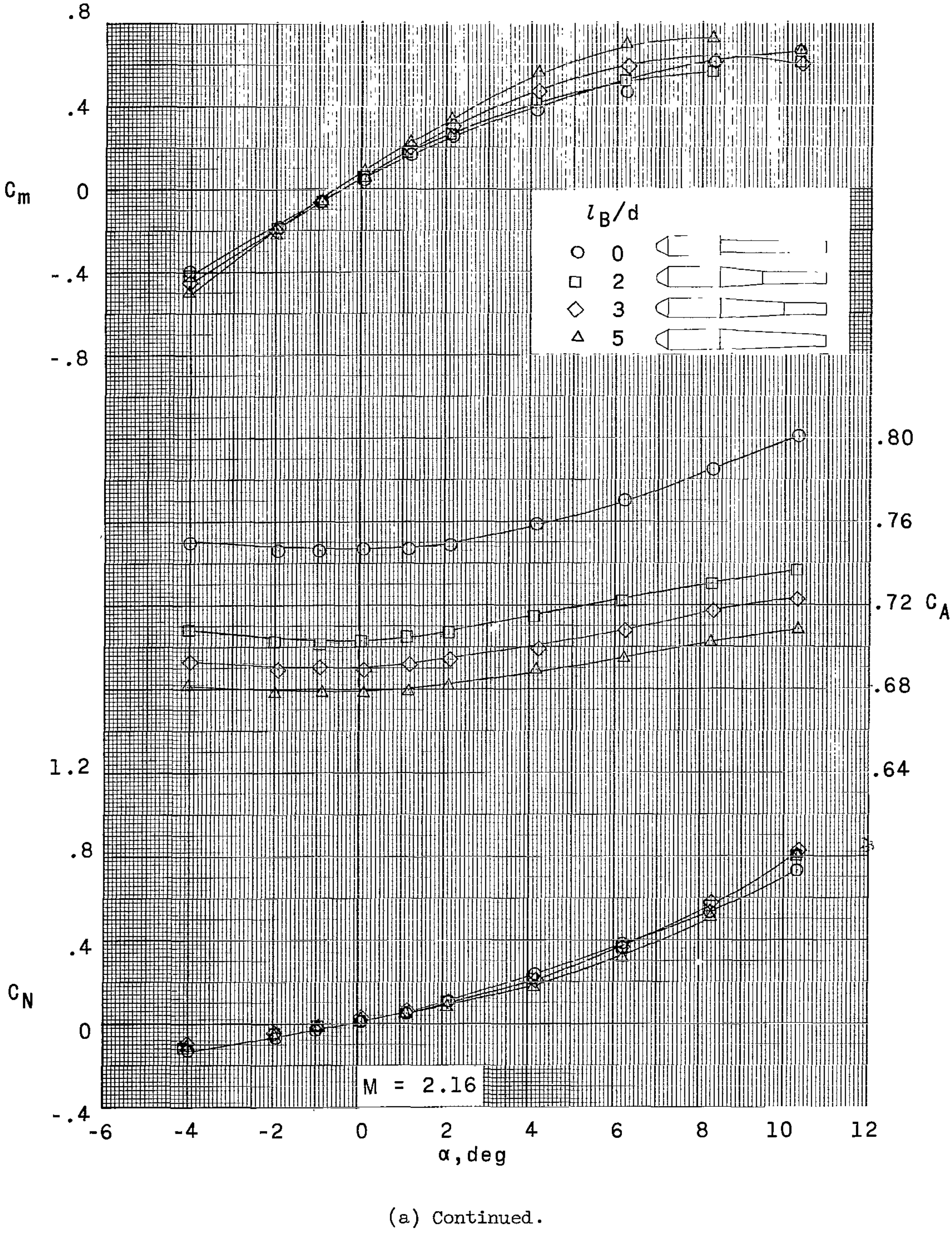

(a) Continued.

Figure 5.- Continued.

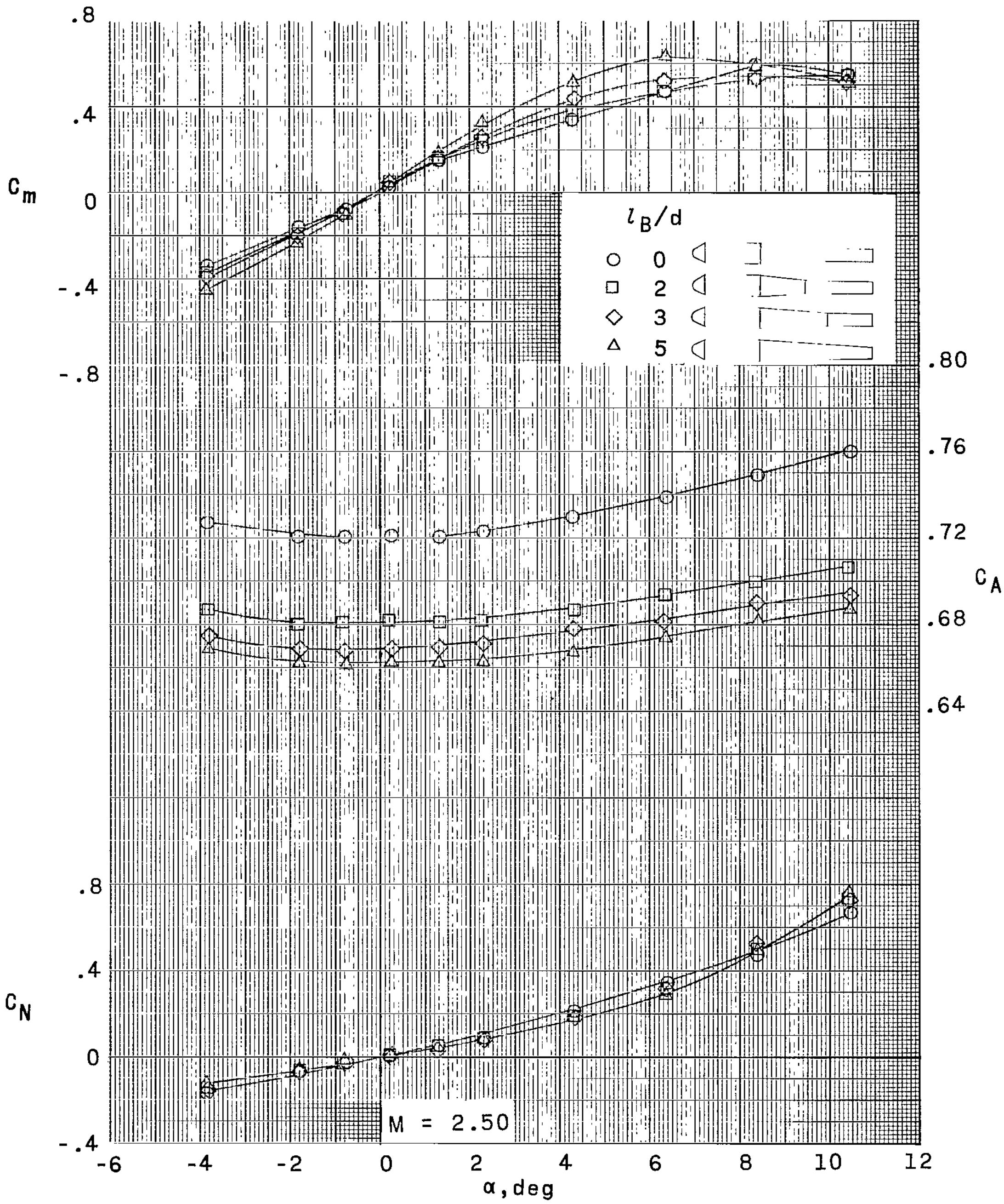

(a) Continued.

Figure 5.- Continued.

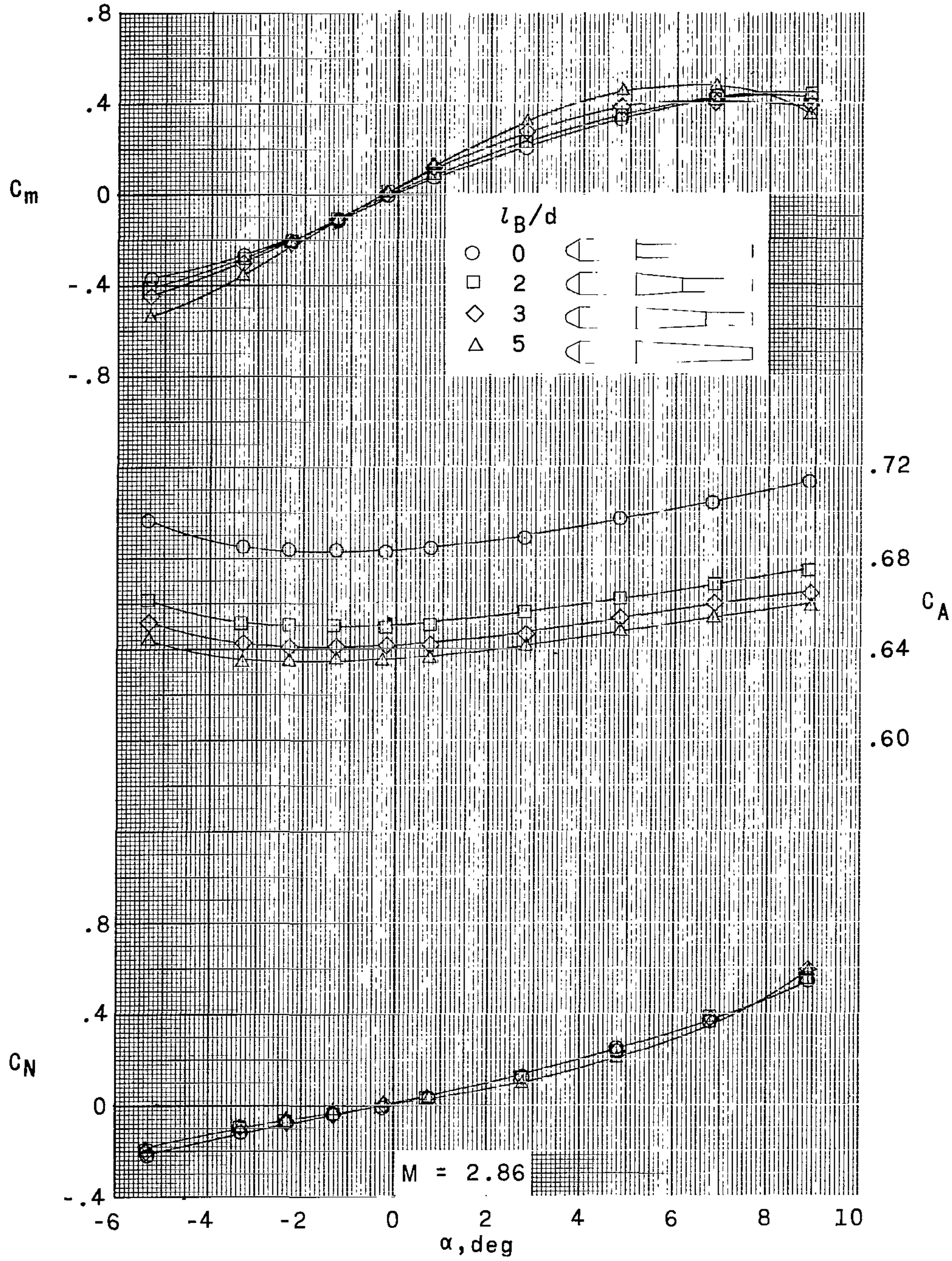

(a) Concluded.

Figure 5.- Continued.

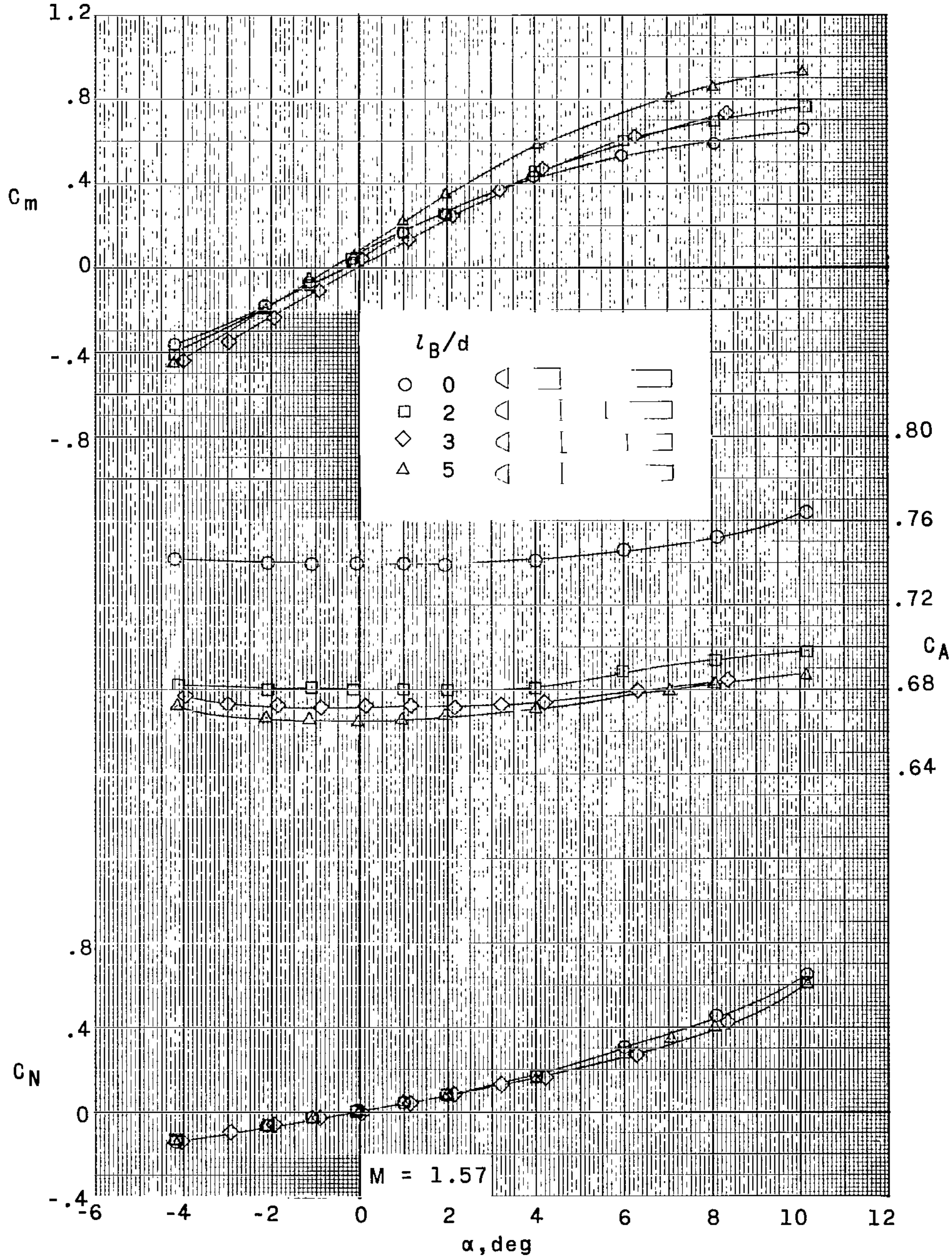

(b) $d_a/d = 0.75$.

Figure 5.- Continued.

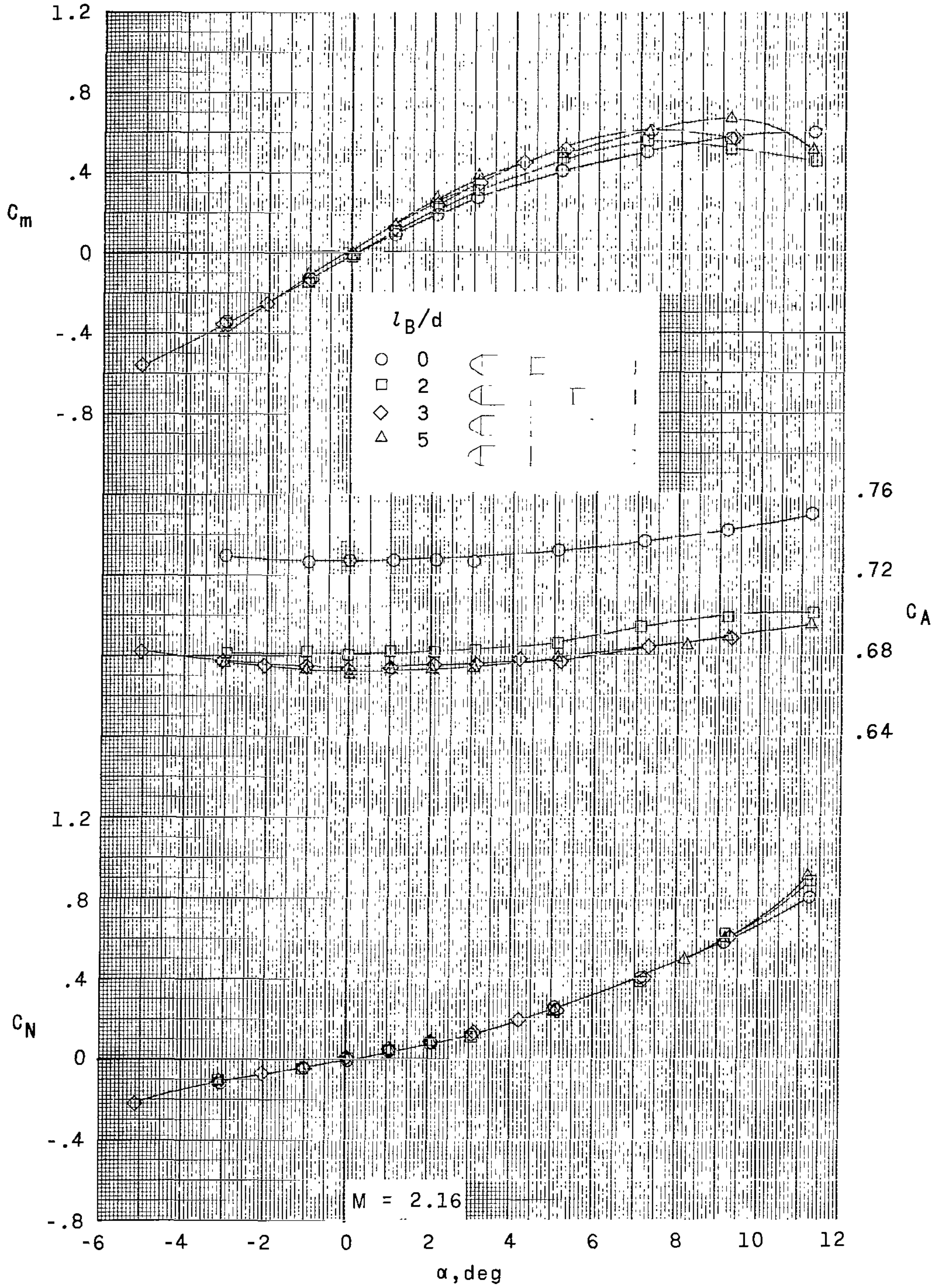

(b) Continued.

Figure 5.- Continued.

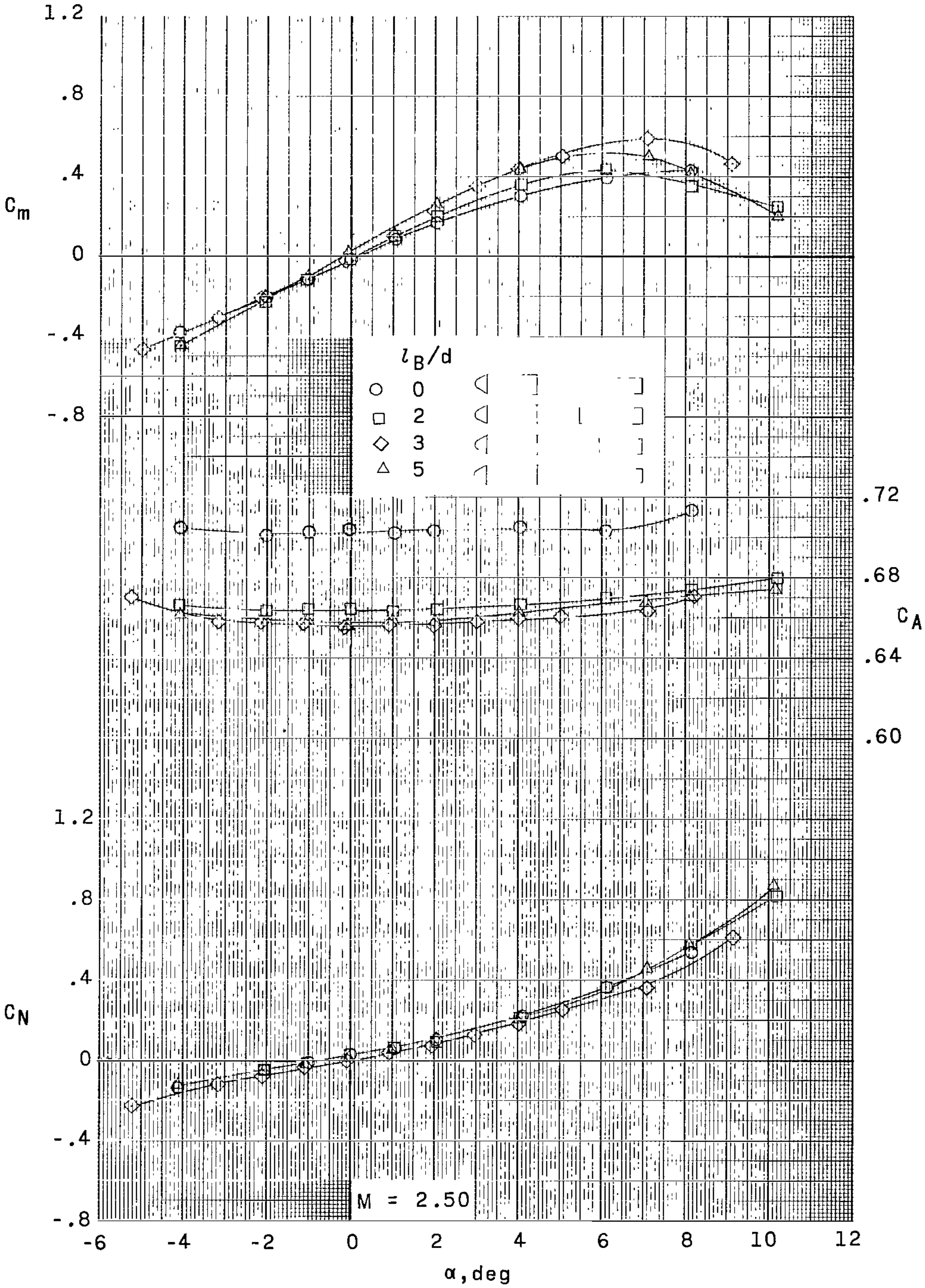

(b) Continued.

Figure 5.- Continued.

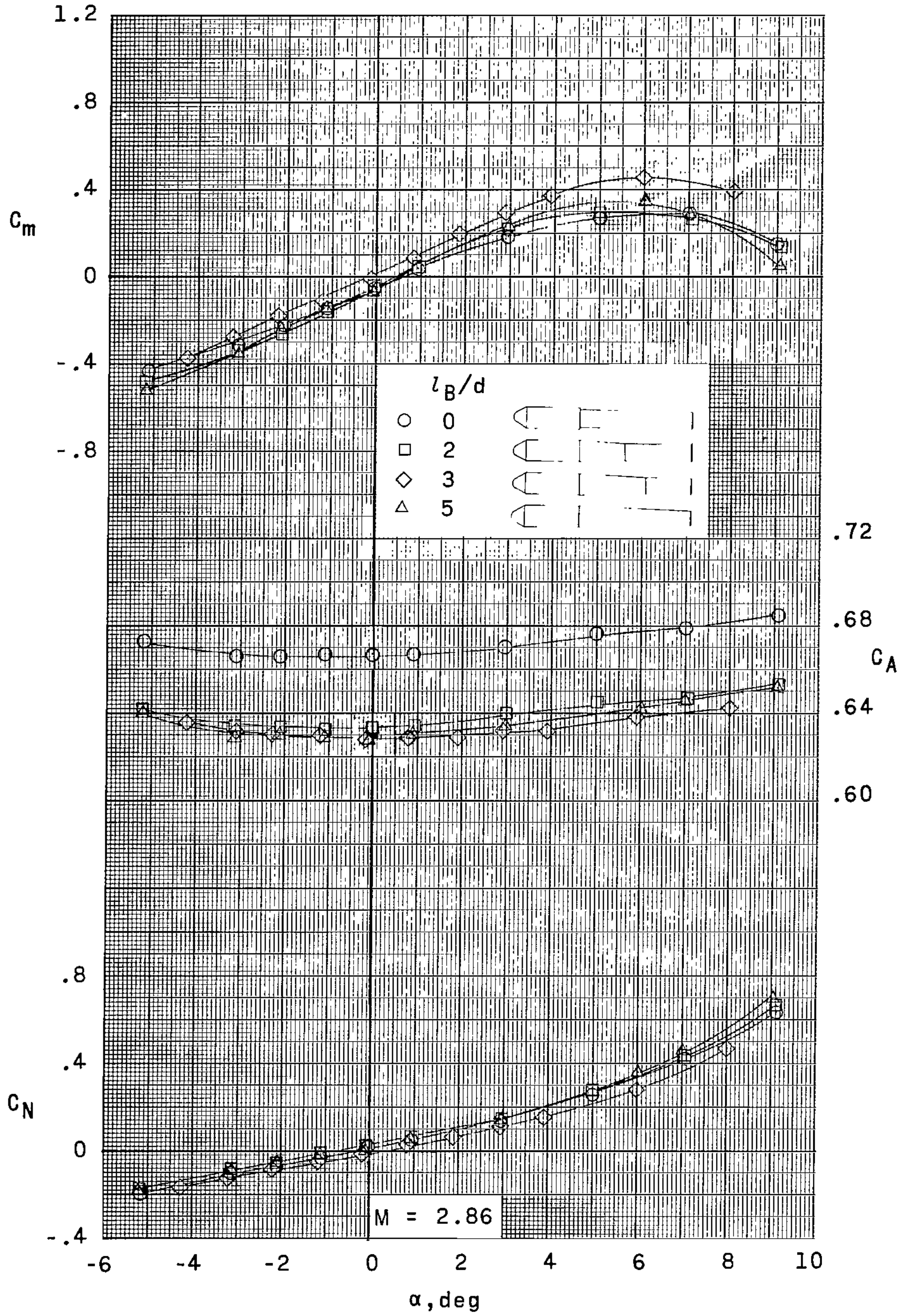

(b) Concluded.

Figure 5.- Concluded.

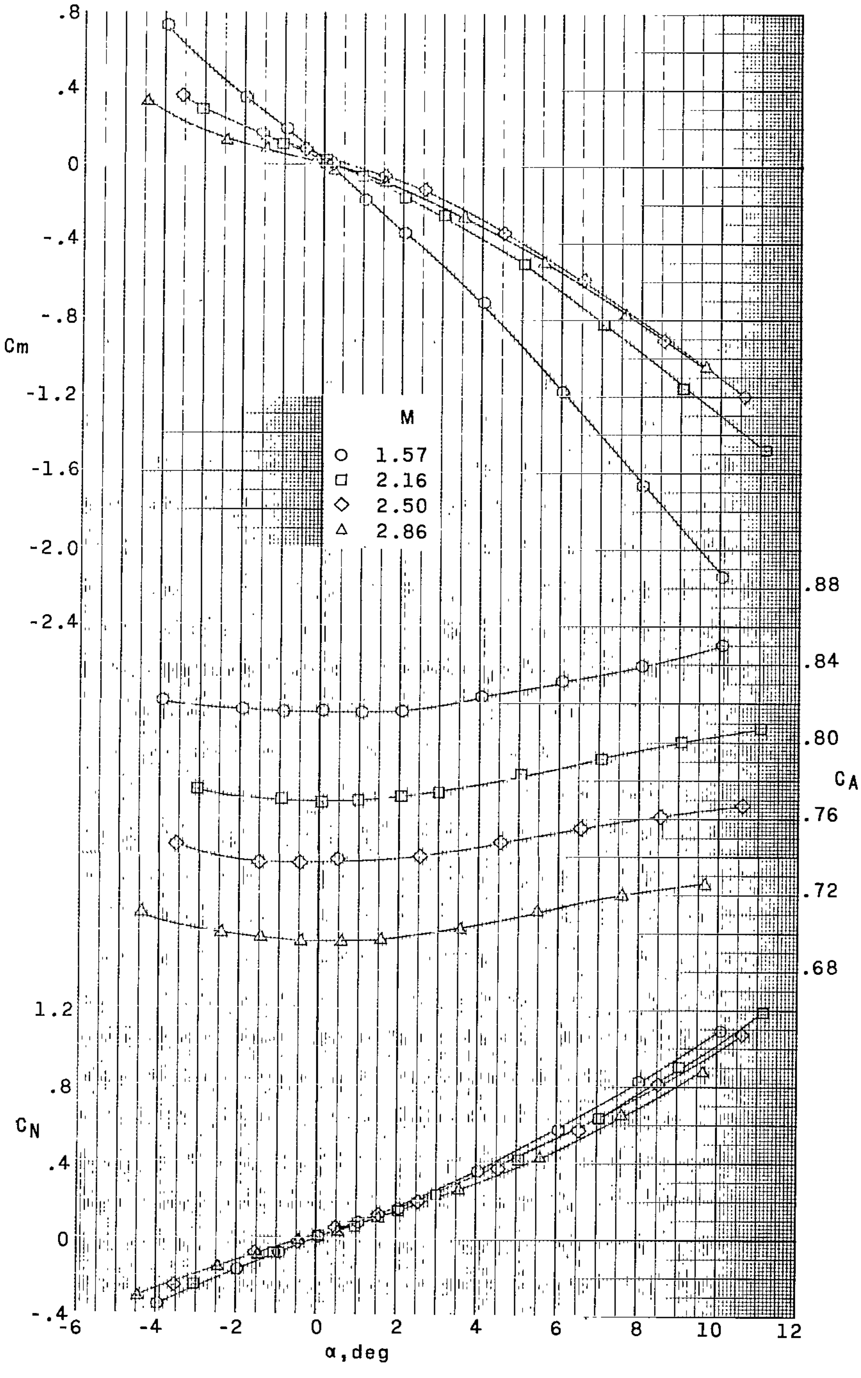

(a) $d_a/d = 0.55$.

Figure 6.- Aerodynamic characteristics in pitch. Long first stage; small fins. $l_B/d = 2$.

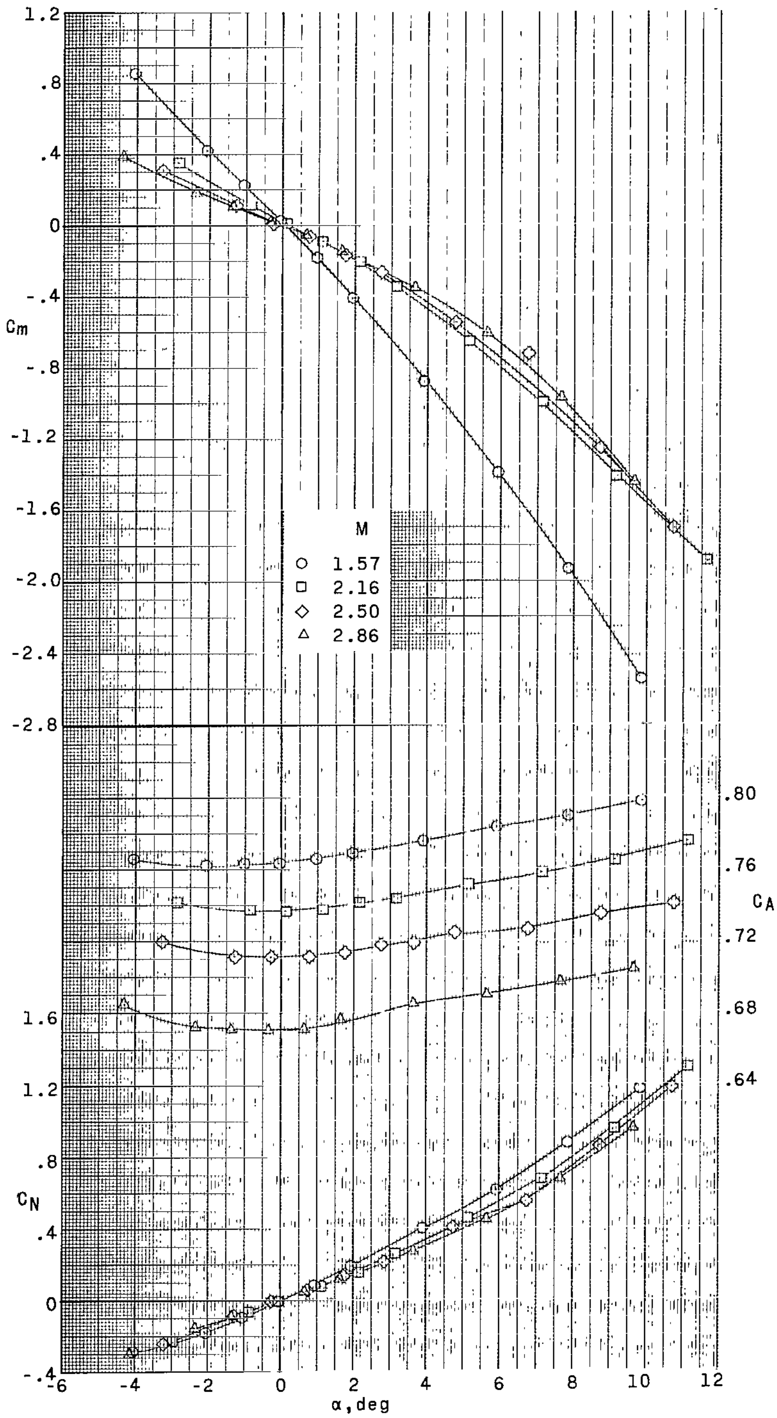

(b) $d_a/d = 0.75$.

Figure 6.- Concluded.

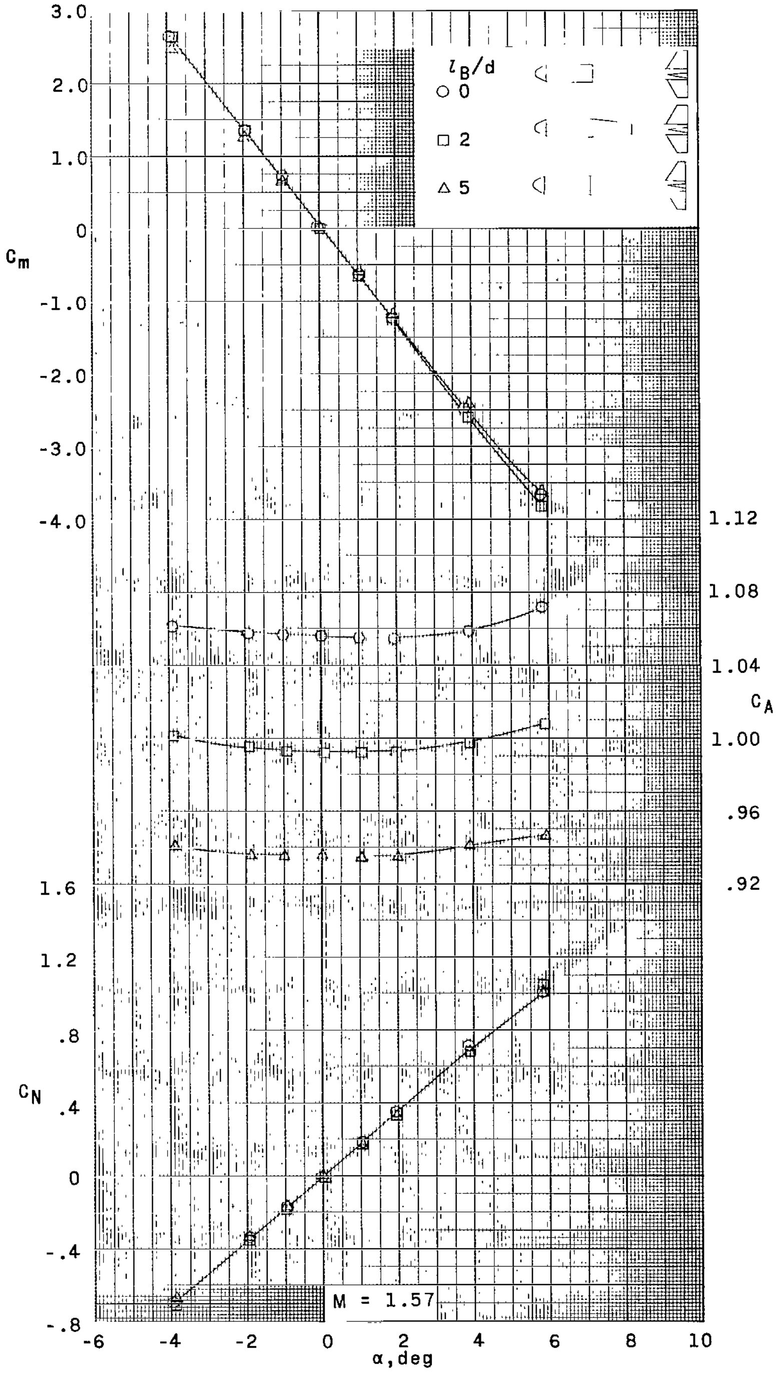

(a) $d_a/d = 0.55$.

Figure 7.- Aerodynamic characteristics in pitch. Long first stage; large fins.

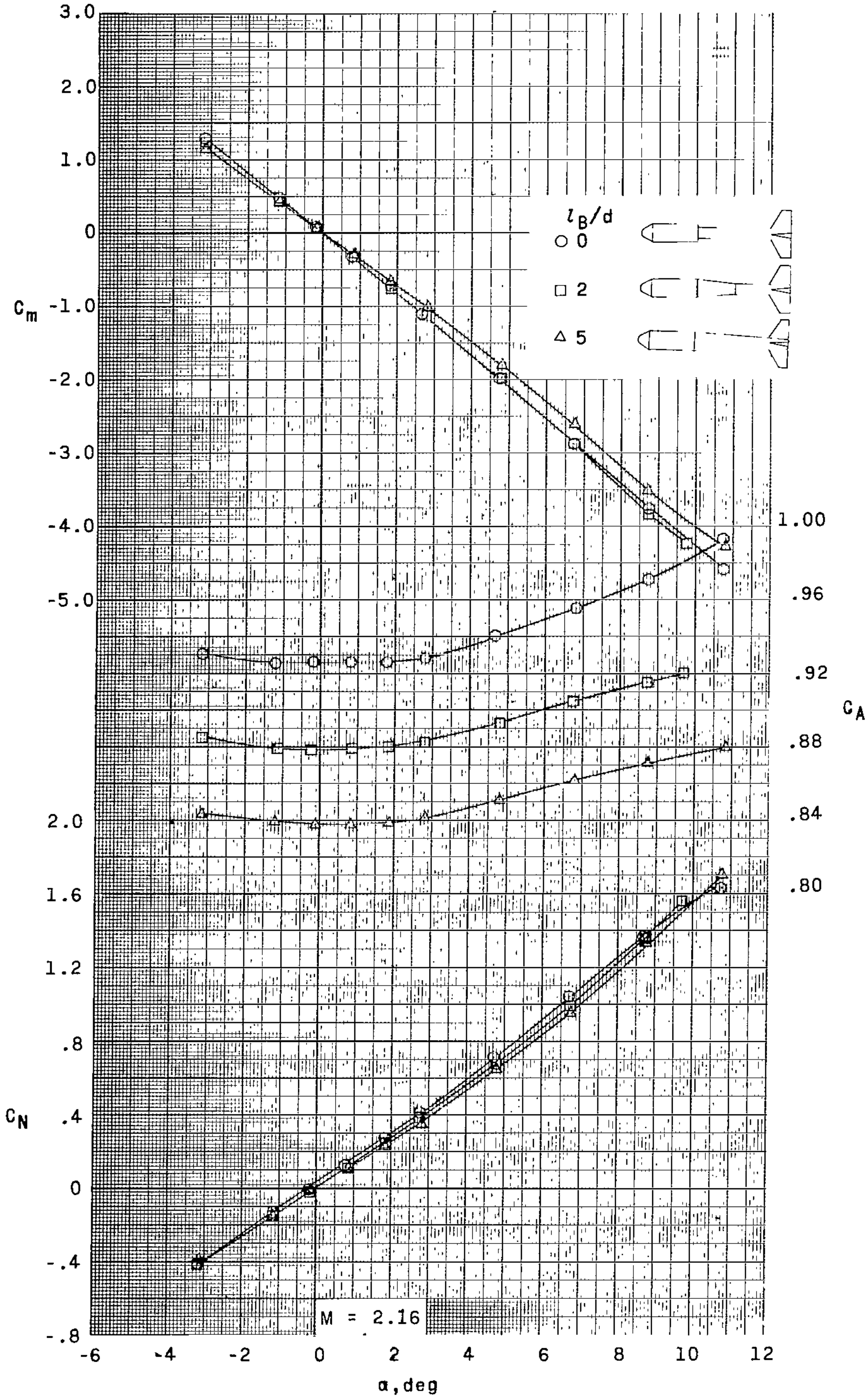

(a) Continued.

Figure 7.- Continued.

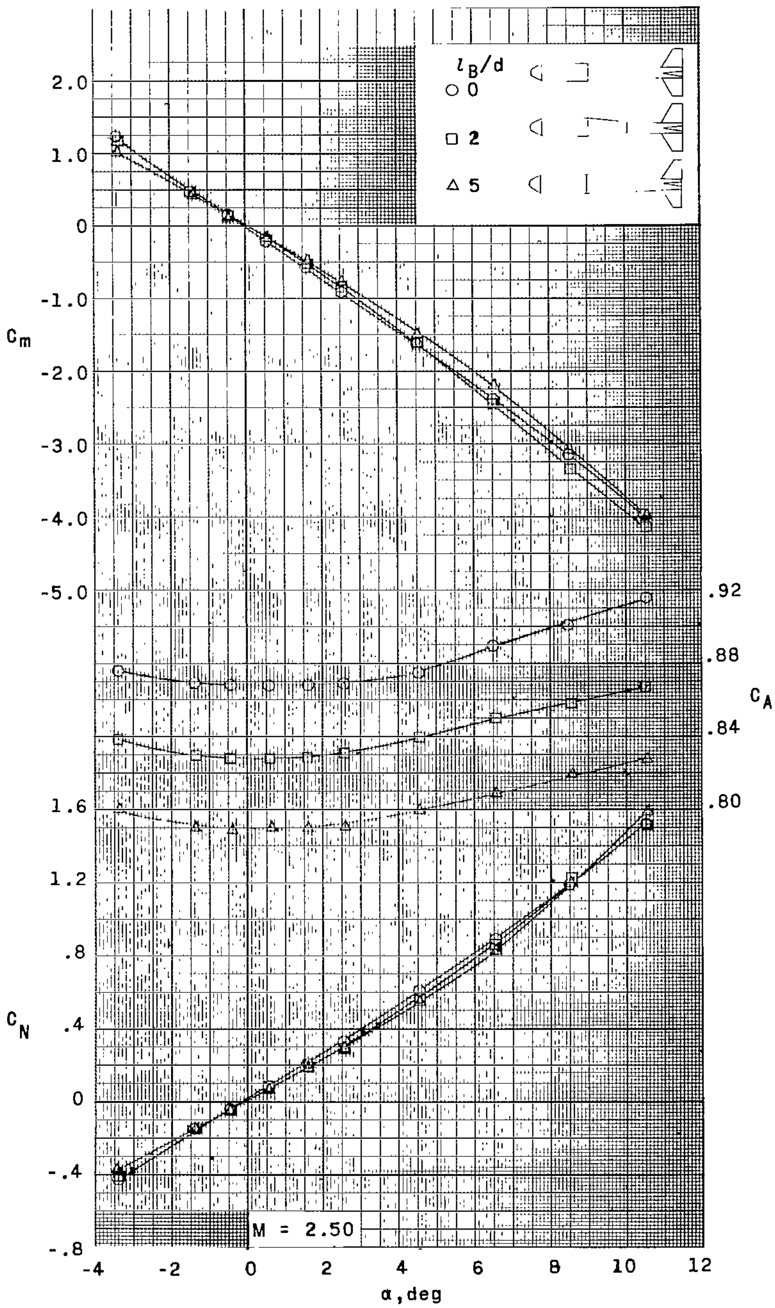

(a) Continued.

Figure 7.- Continued.

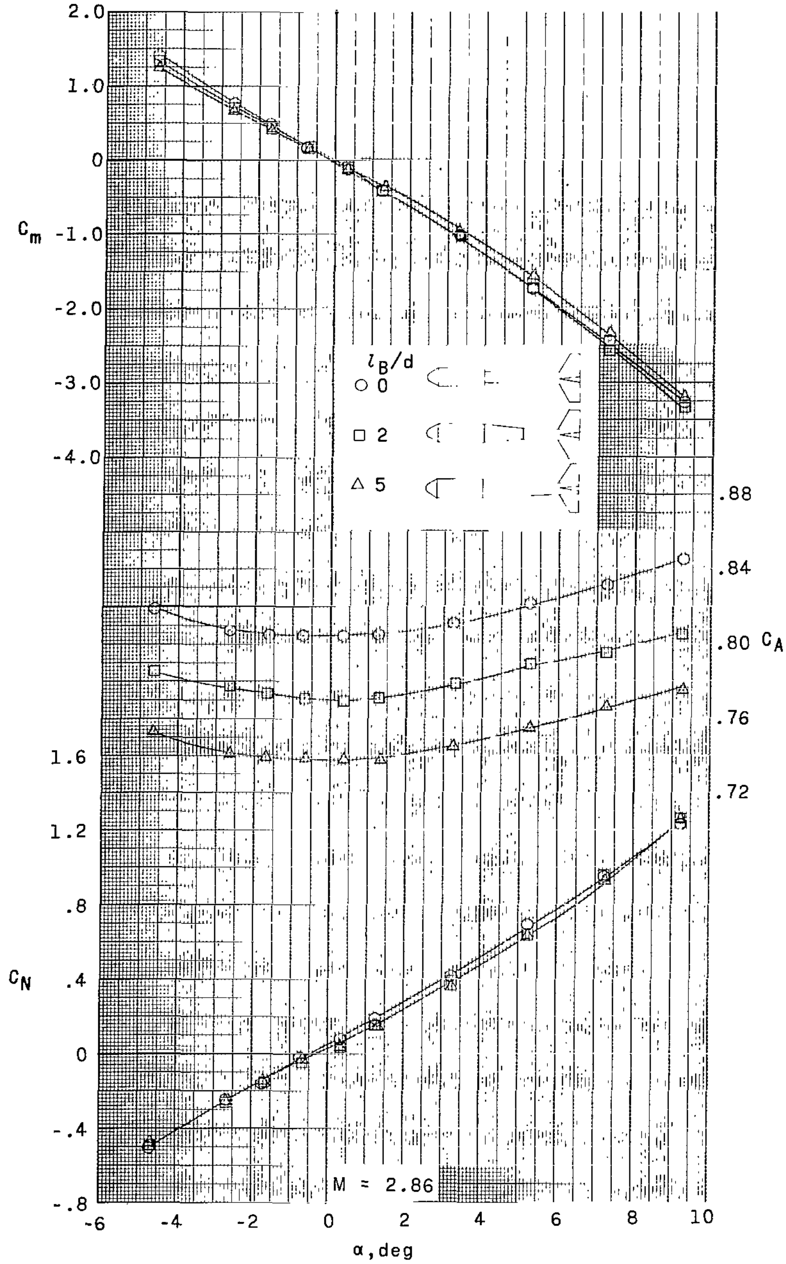

(a) Concluded.

Figure 7.- Continued.

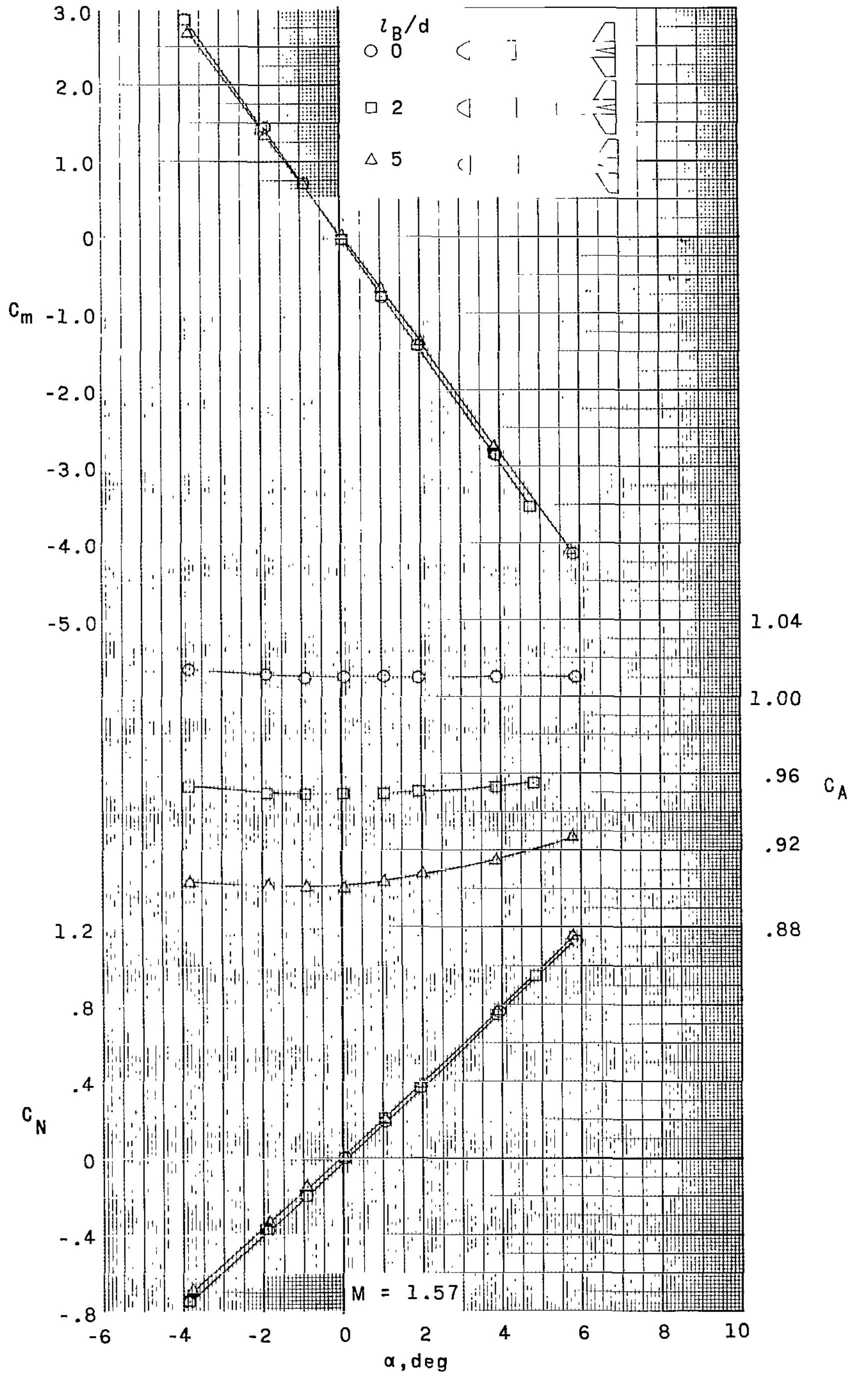

(b) $d_a/d = 0.75$.

Figure 7.- Continued.

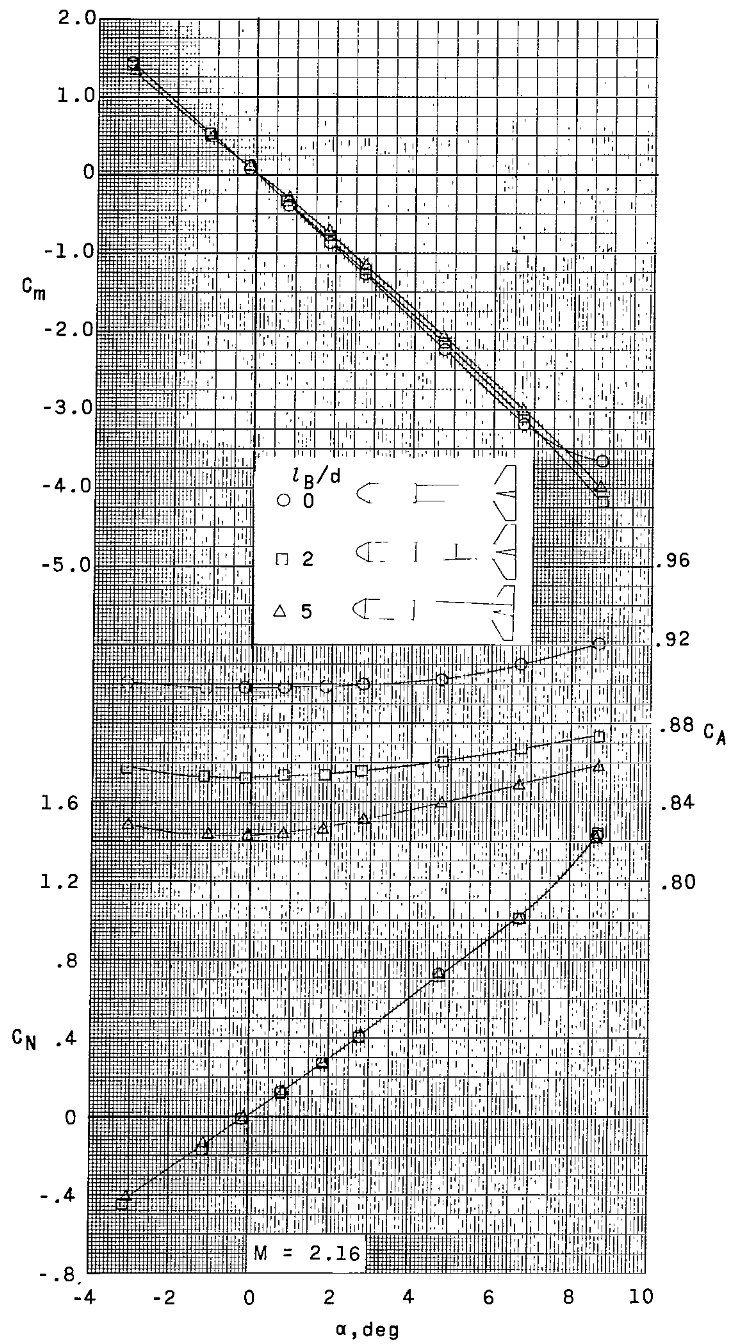

(b) Continued.

Figure 7.- Continued.

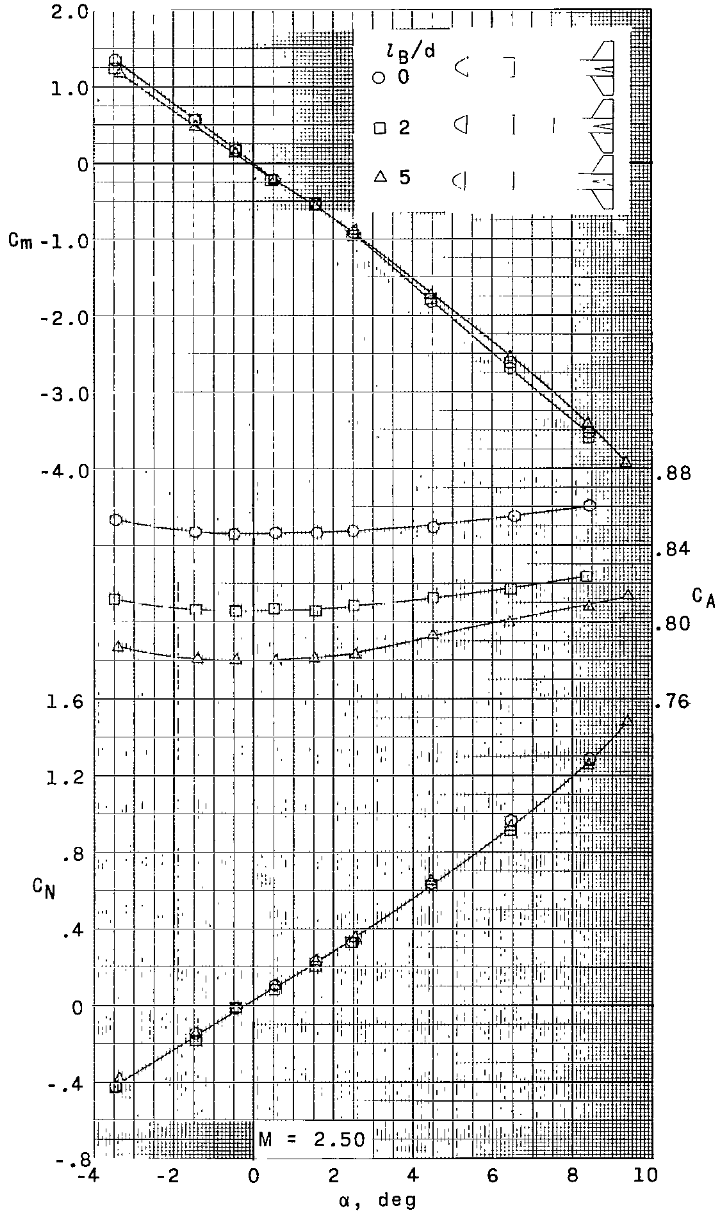

(b) Continued.

Figure 7.- Continued.

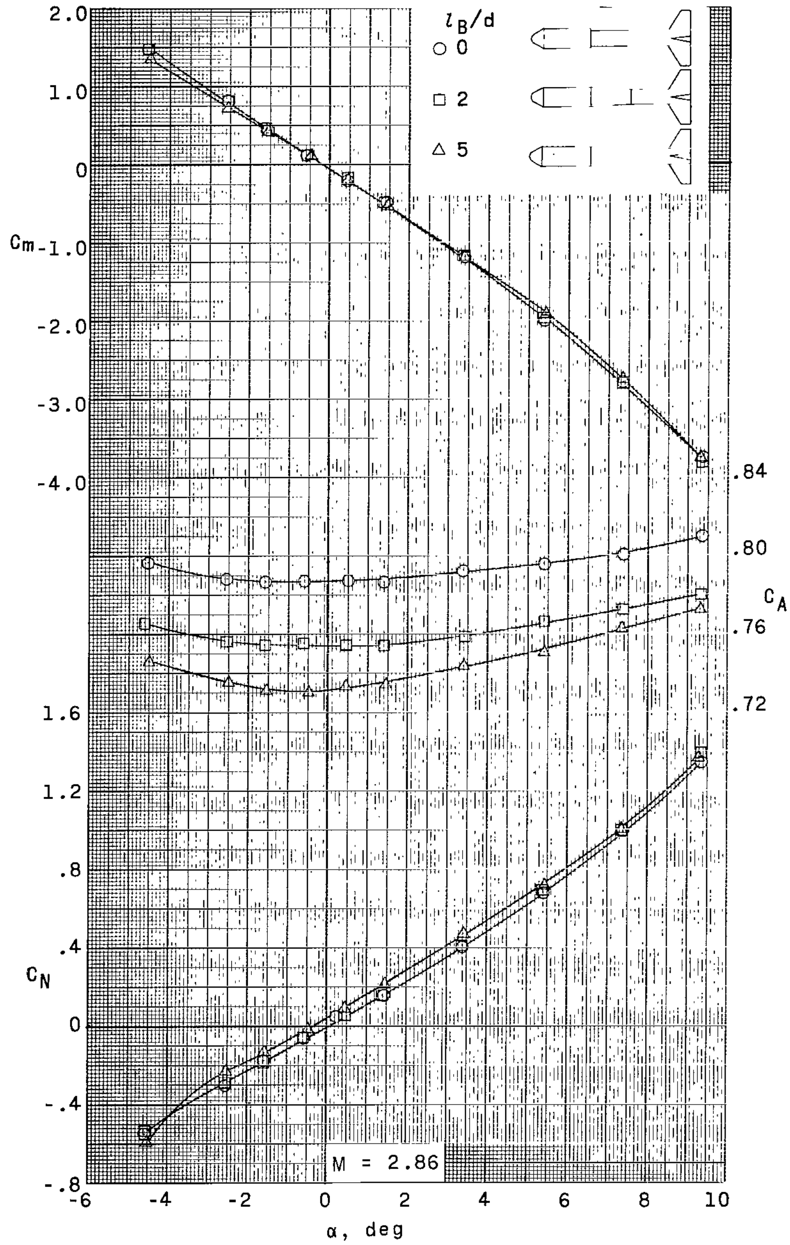

(b) Concluded.

Figure 7.- Concluded.

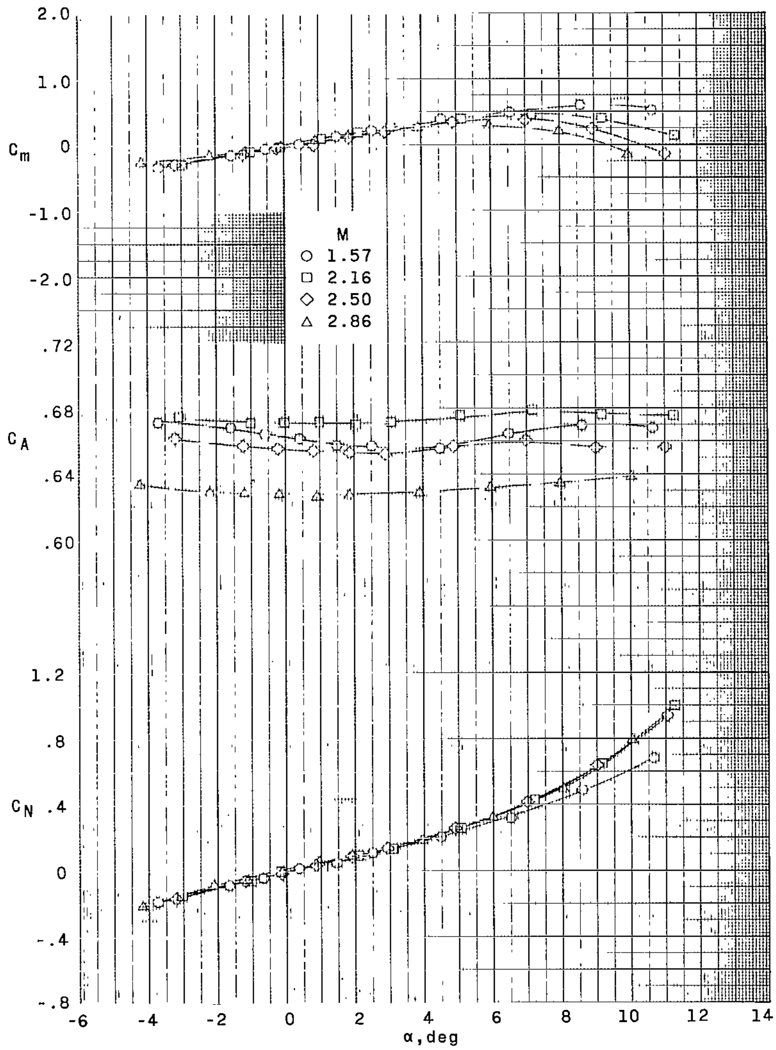

(a) Fins off.

Figure 8.- Aerodynamic characteristics in pitch. Long first stage; $d_a/d = 1.00$.

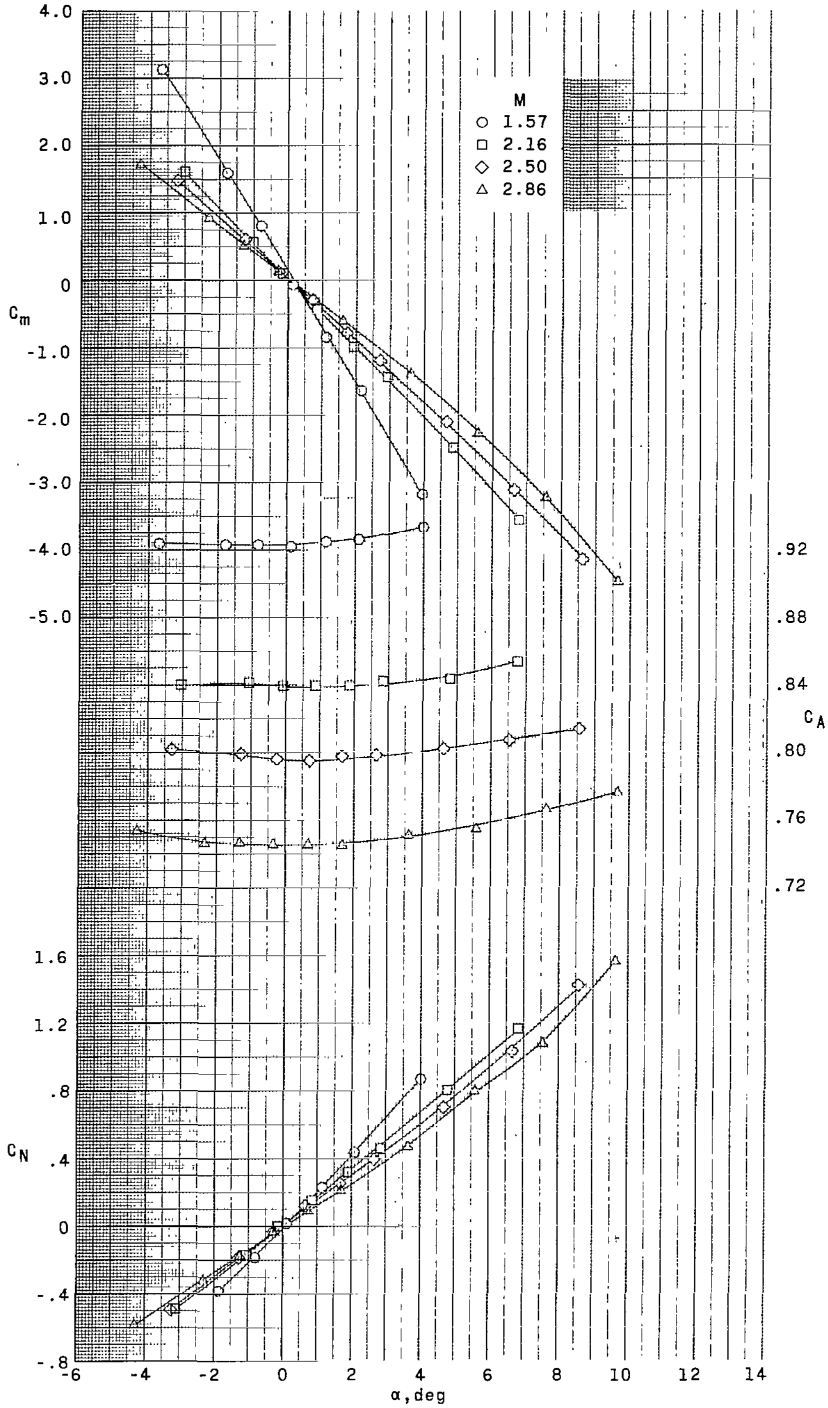

(b) Large fins.

Figure 8.- Concluded.

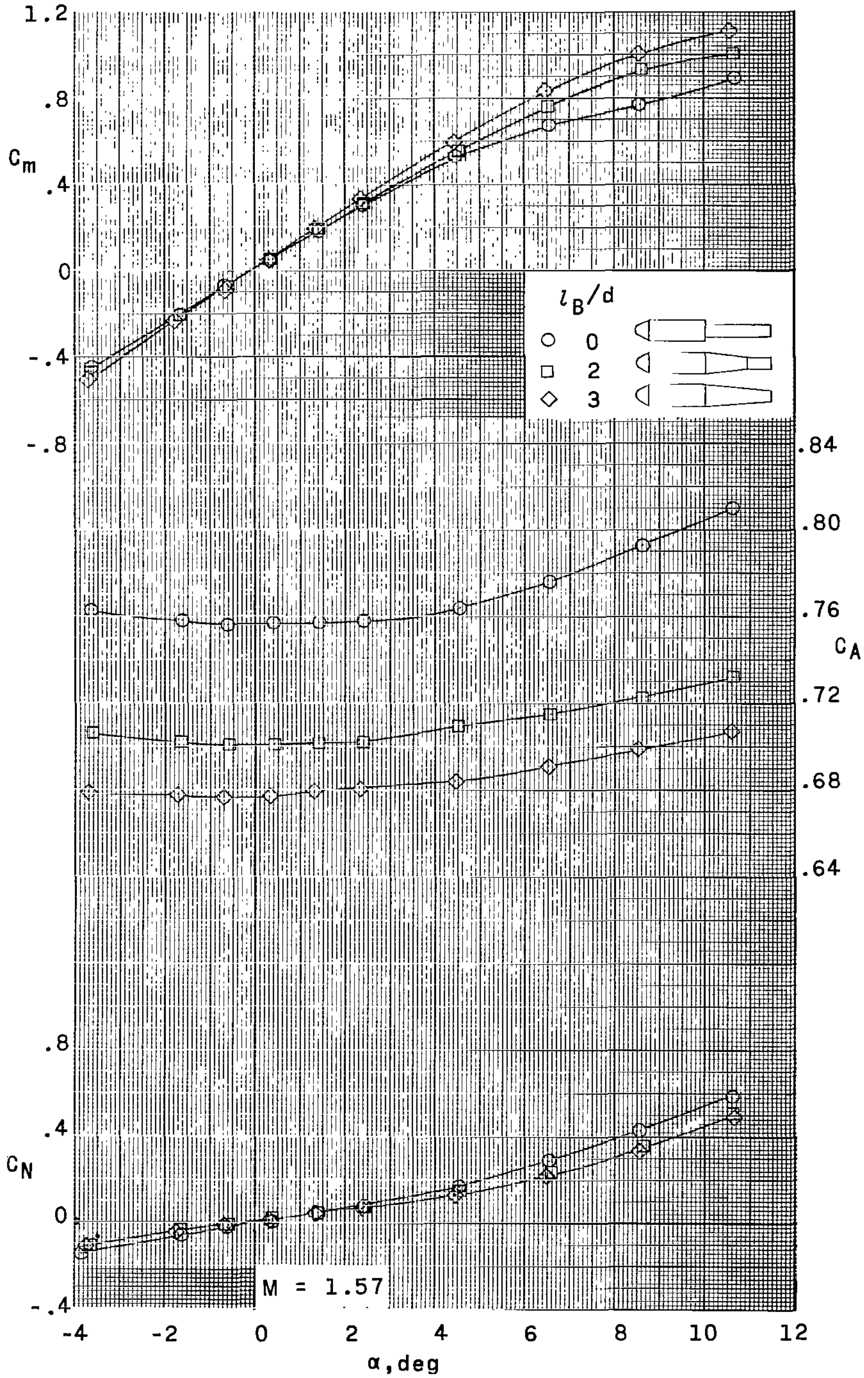

(a) $d_a/d = 0.55$.

Figure 9.- Aerodynamic characteristics in pitch. Intermediate first stage; fins off.

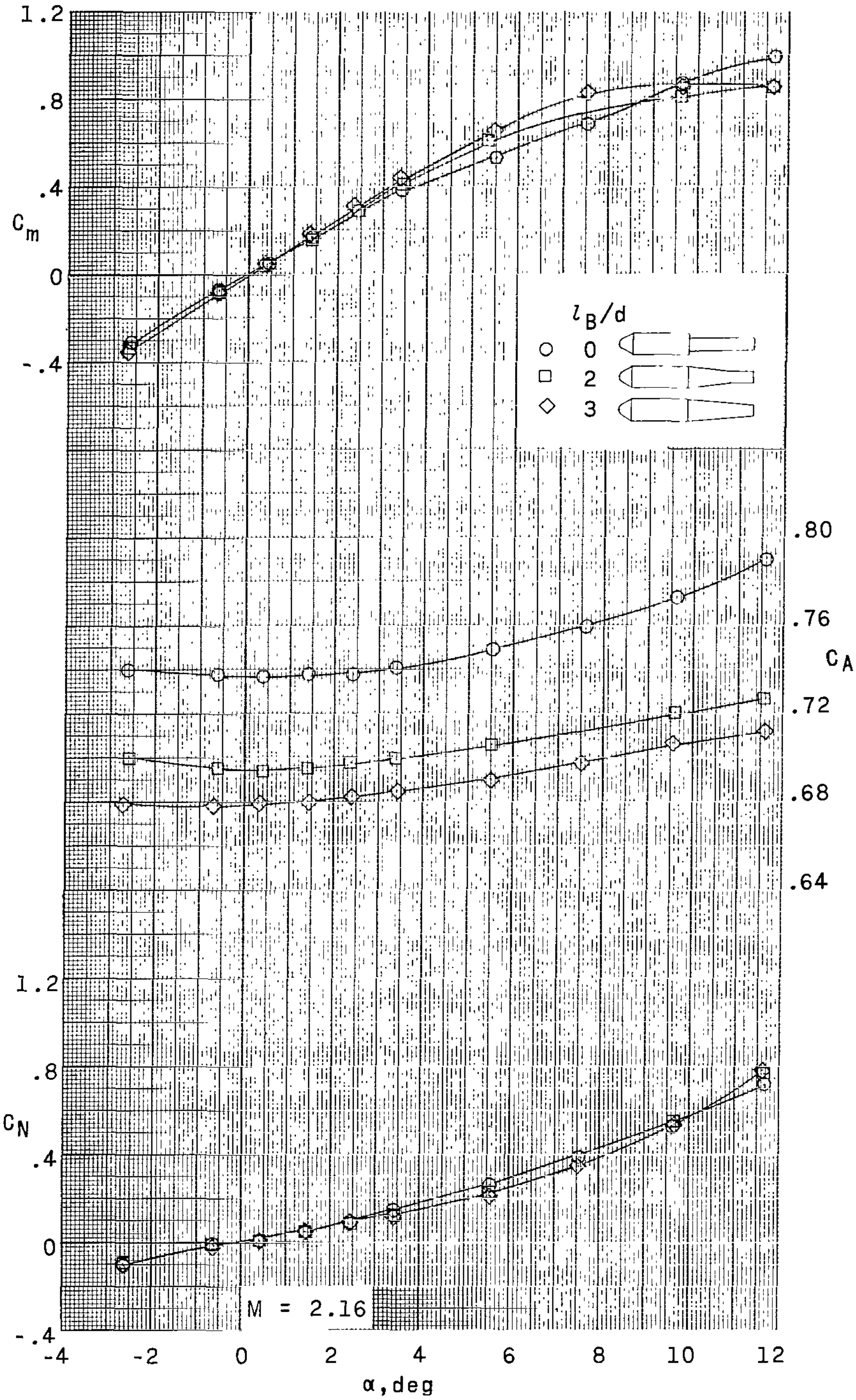

(a) Continued.

Figure 9.- Continued.

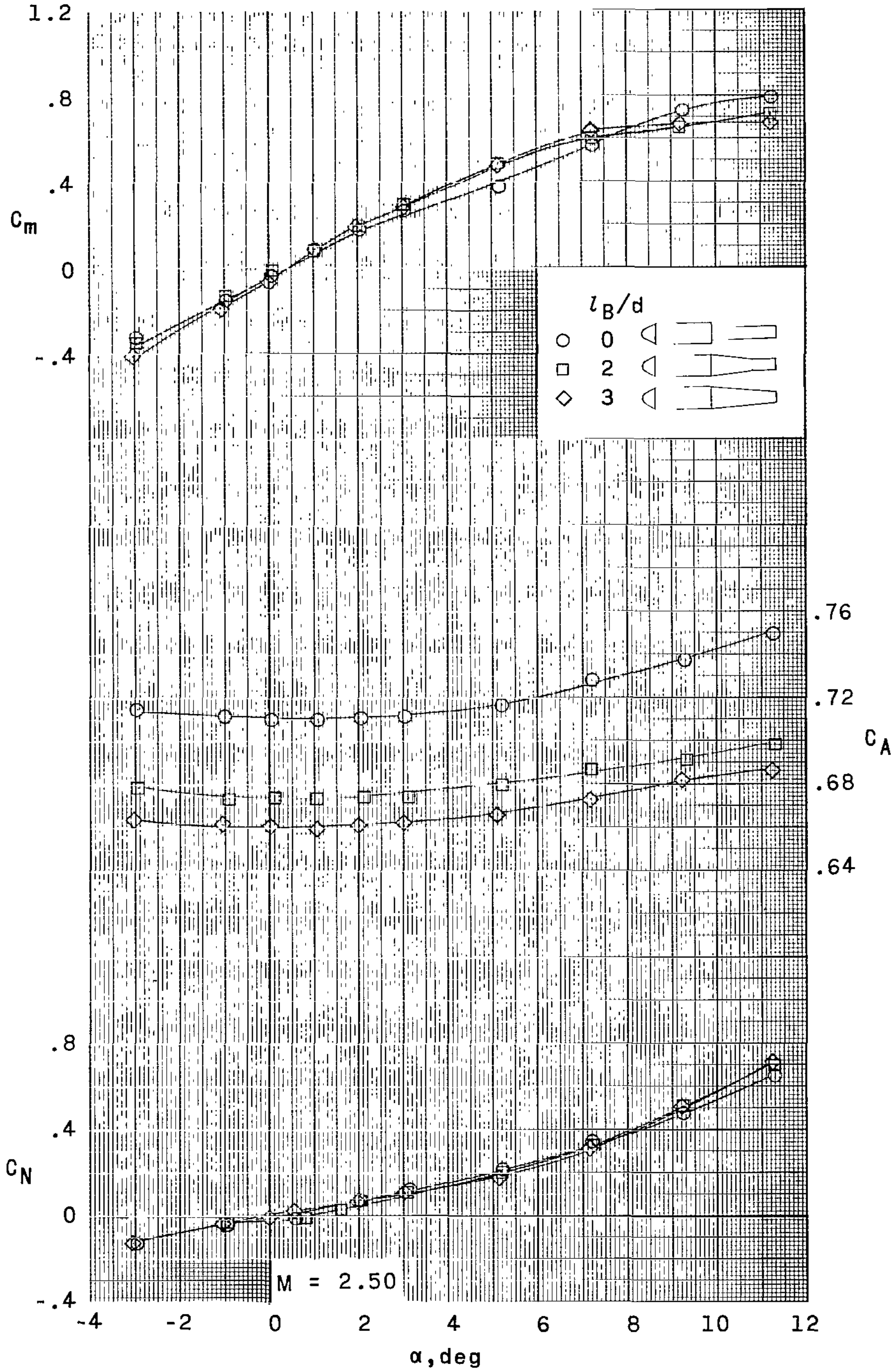

(a) Continued.

Figure 9.- Continued.

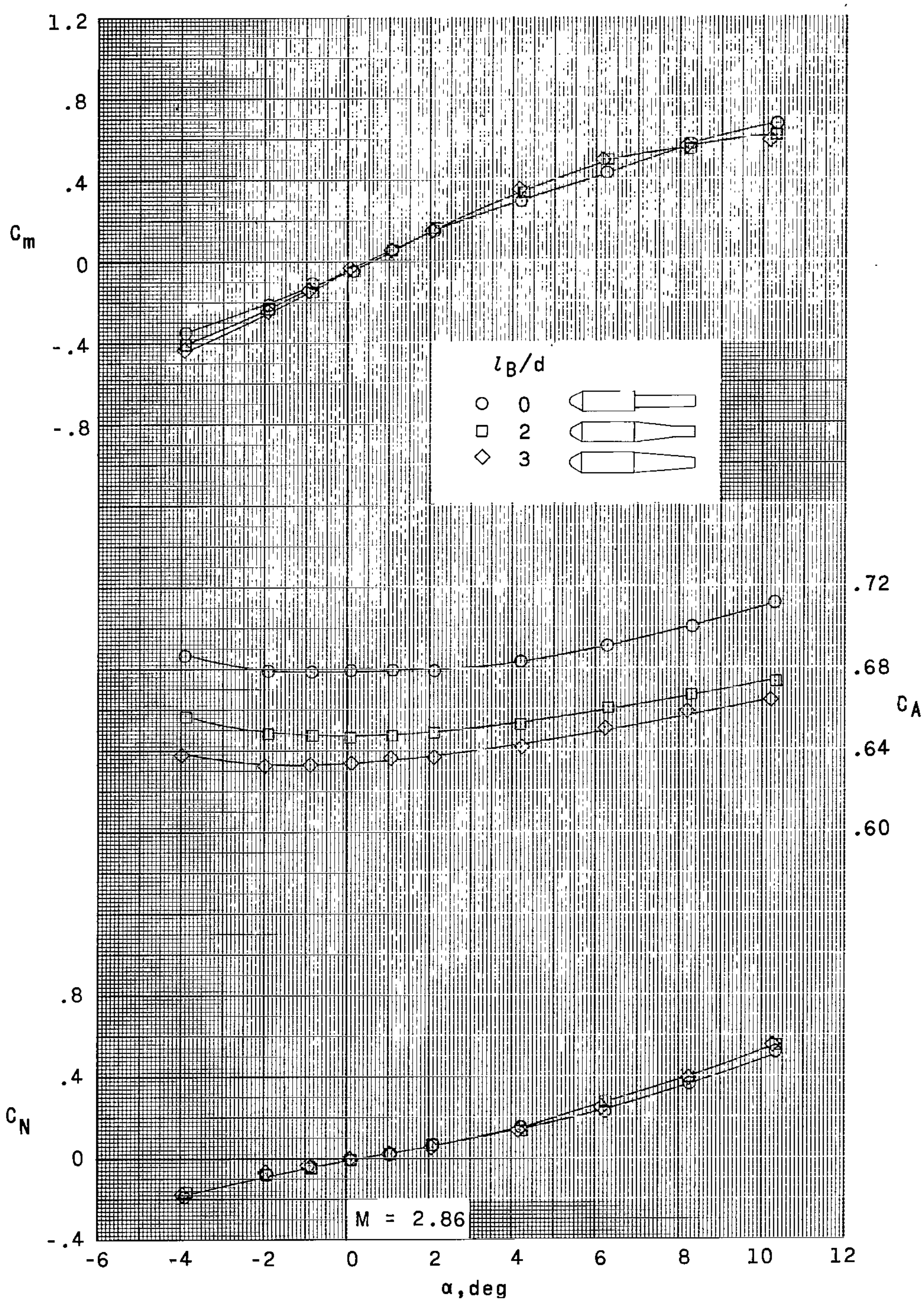

(a) Concluded.

Figure 9.- Continued.

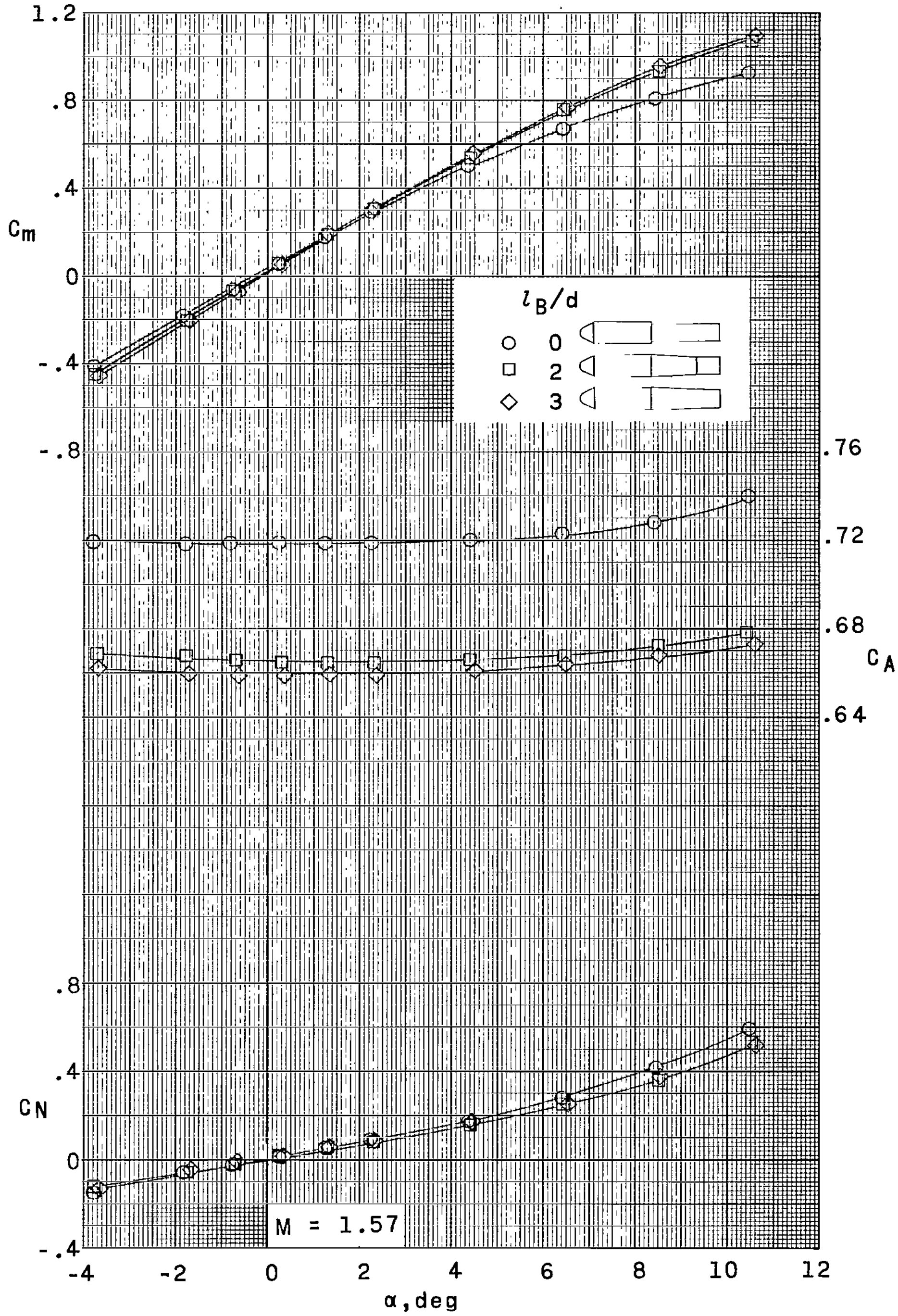

(b) $d_a/d = 0.75$.

Figure 9.- Continued.

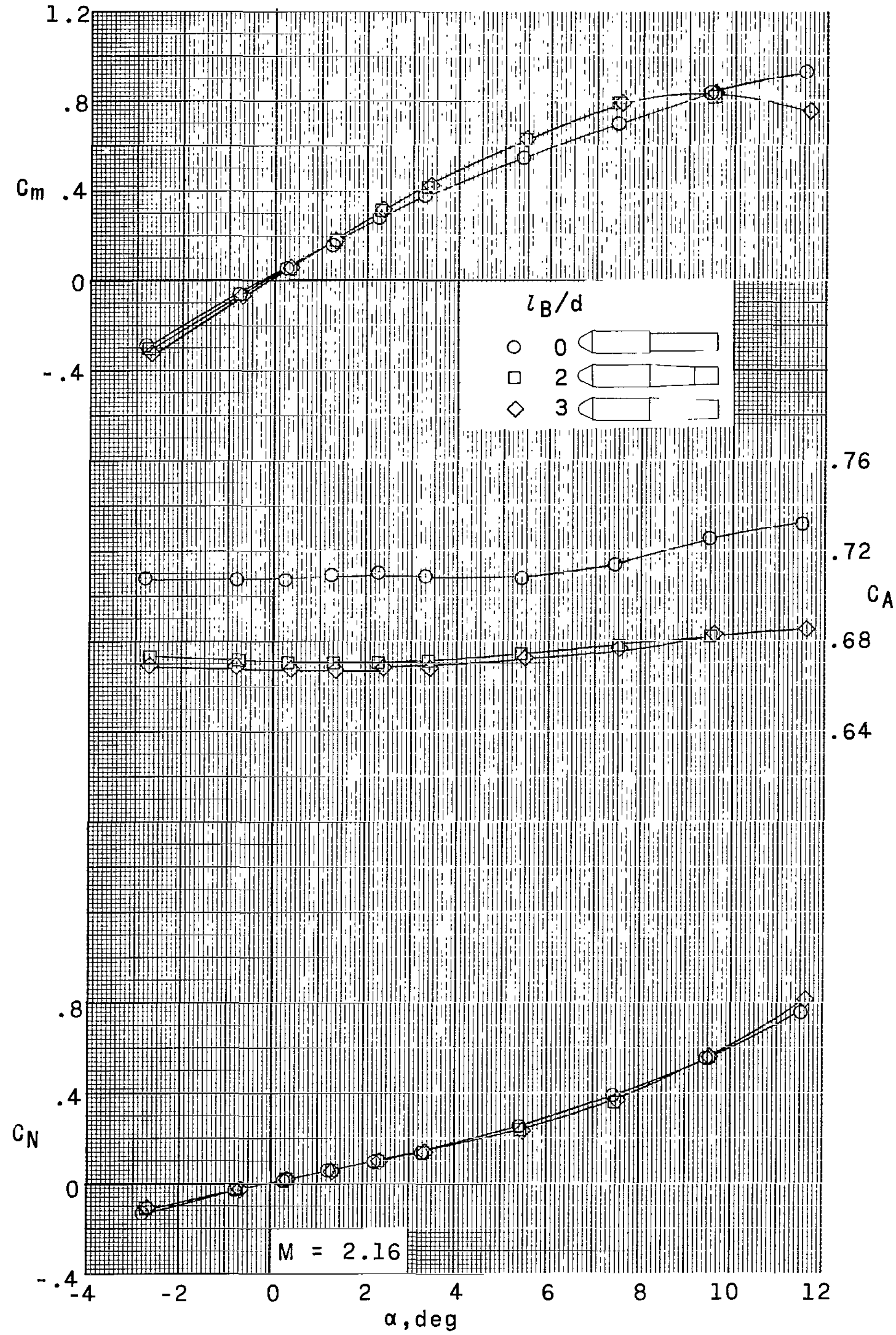

(b) Continued.

Figure 9.- Continued.

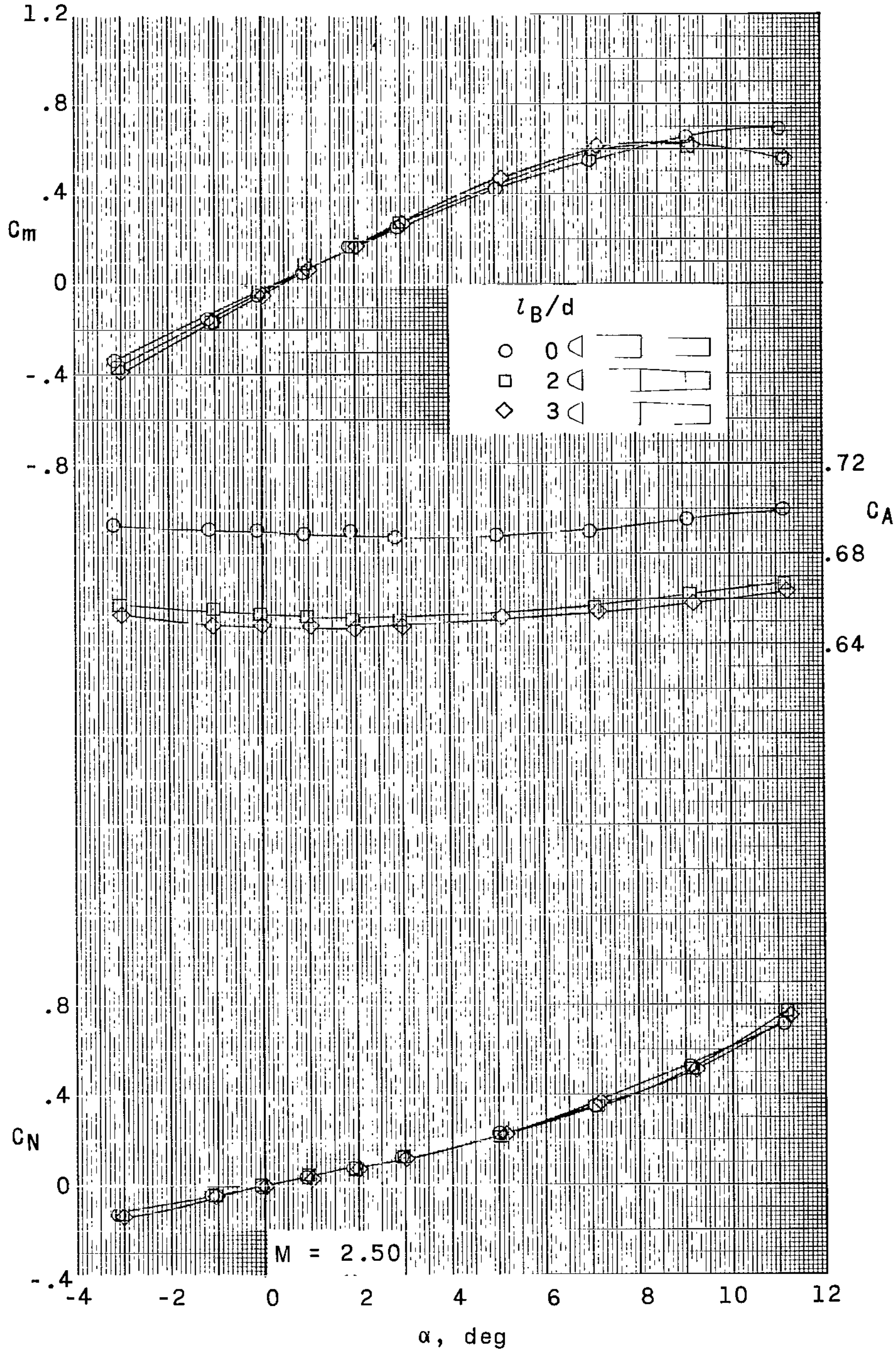

(b) Continued.

Figure 9.- Continued.

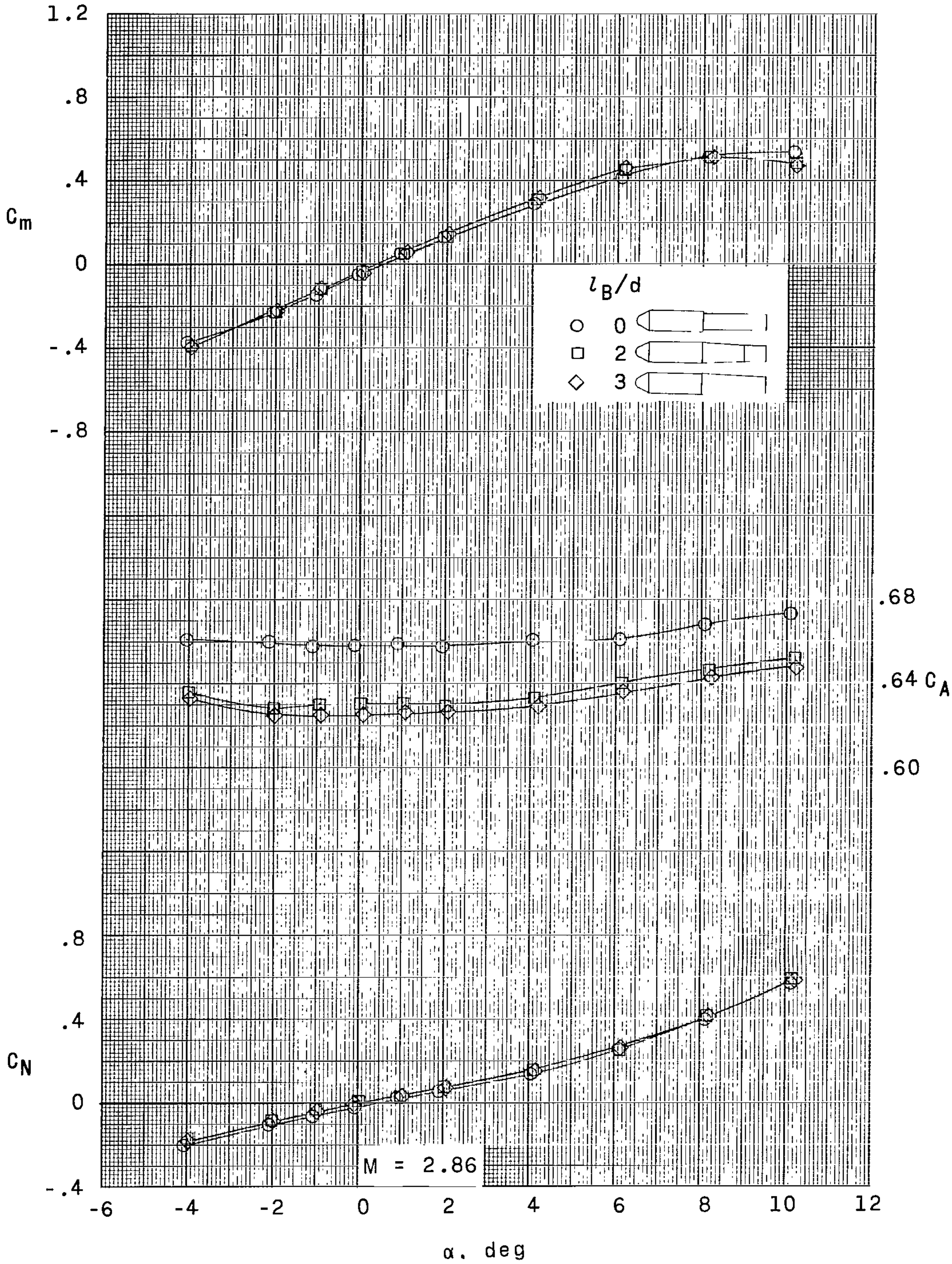

(b) Concluded.

Figure 9.- Concluded.

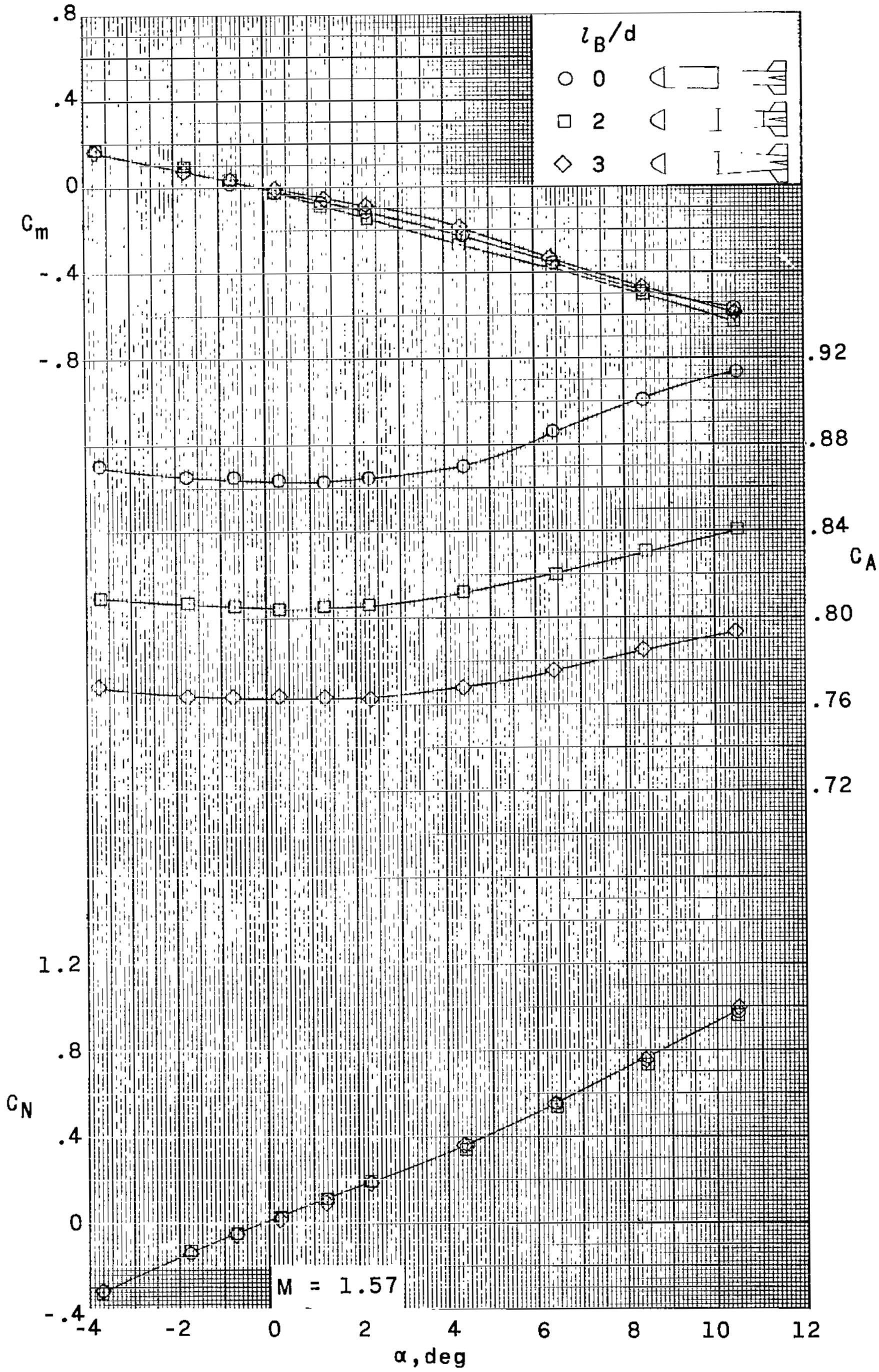

(a) $d_a/d = 0.55$.

Figure 10.- Aerodynamic characteristics in pitch. Intermediate first stage; small fins.

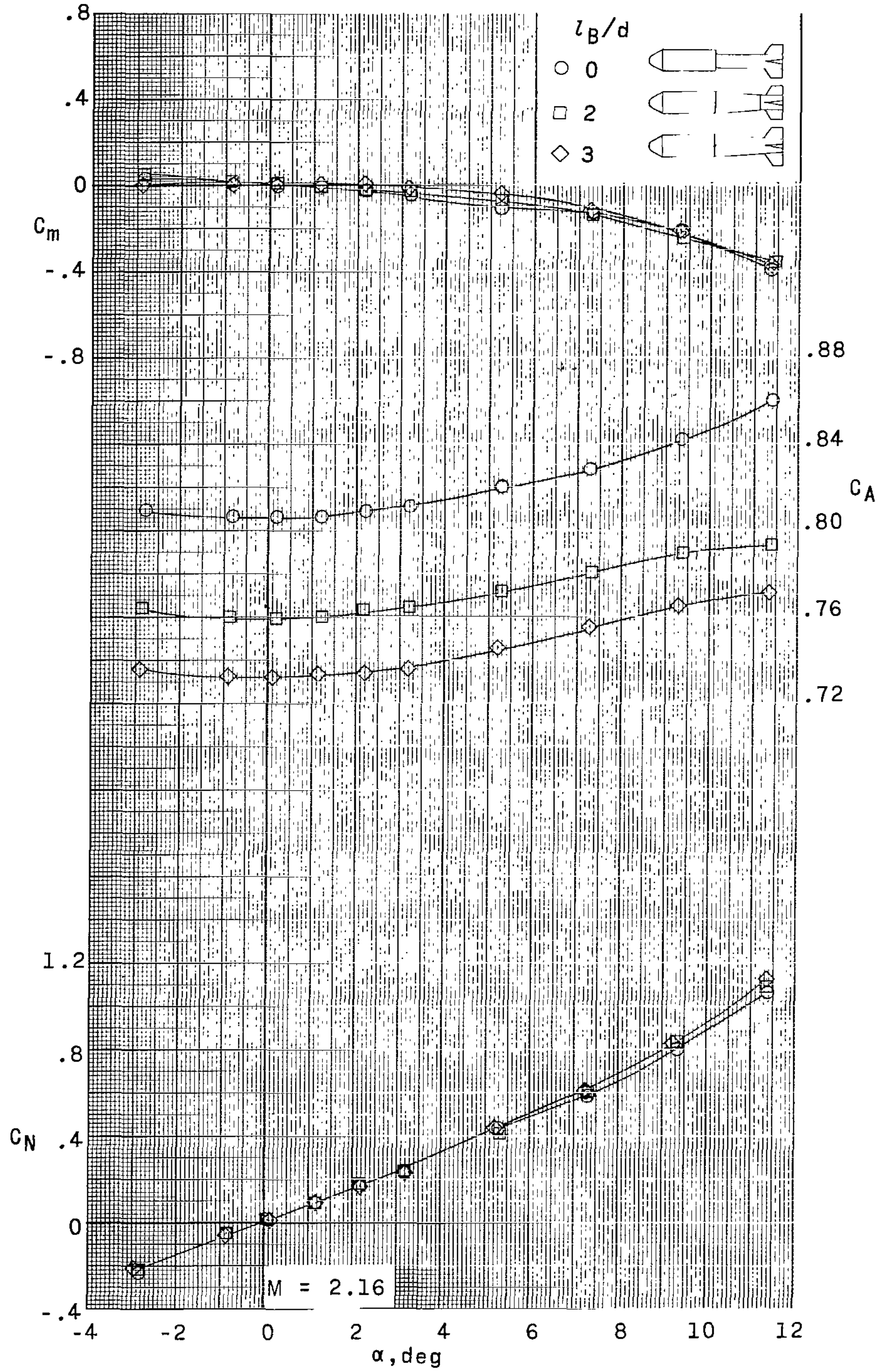

(a) Continued.

Figure 10.- Continued.

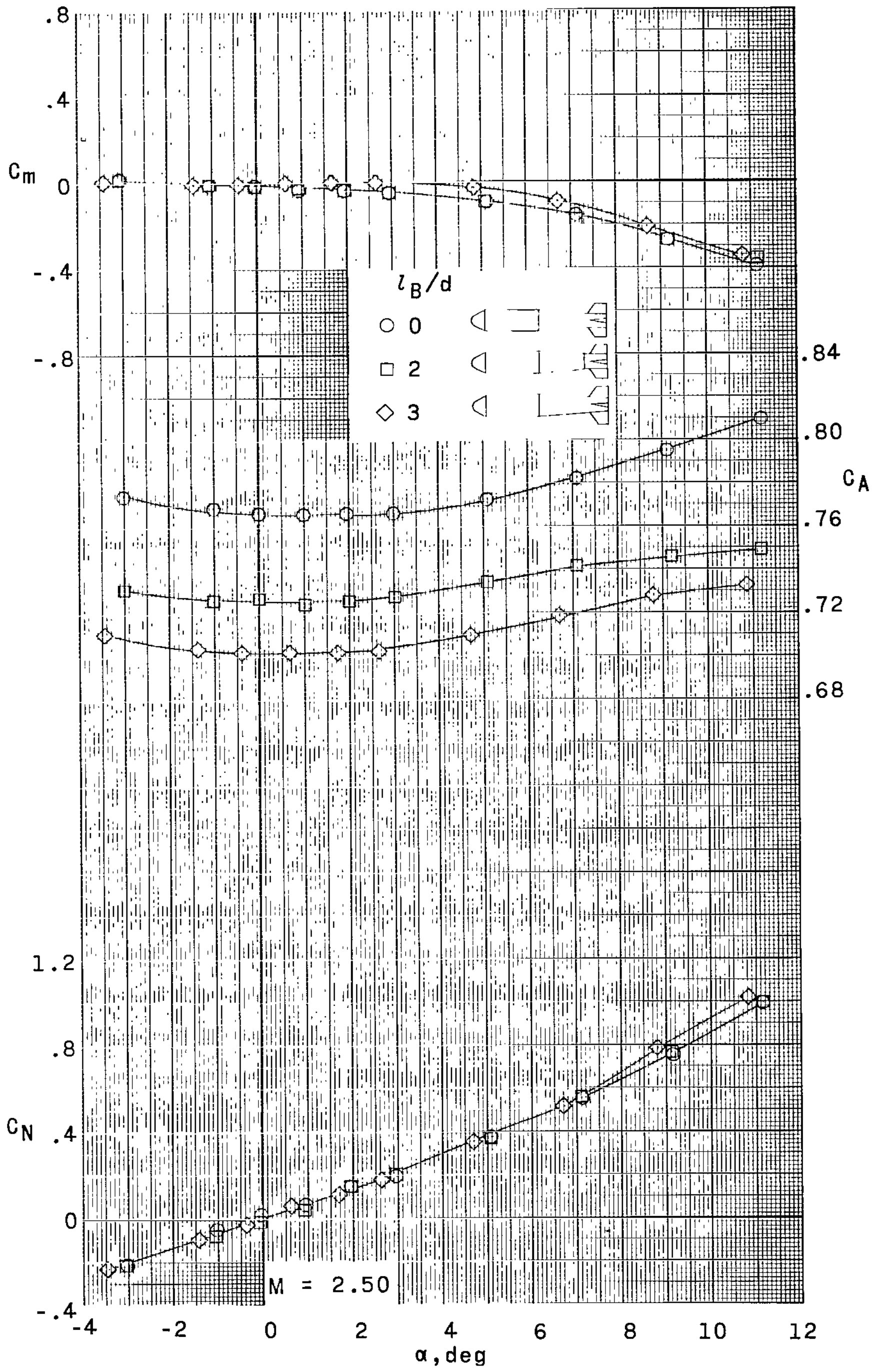

(a) Continued.

Figure 10.- Continued.

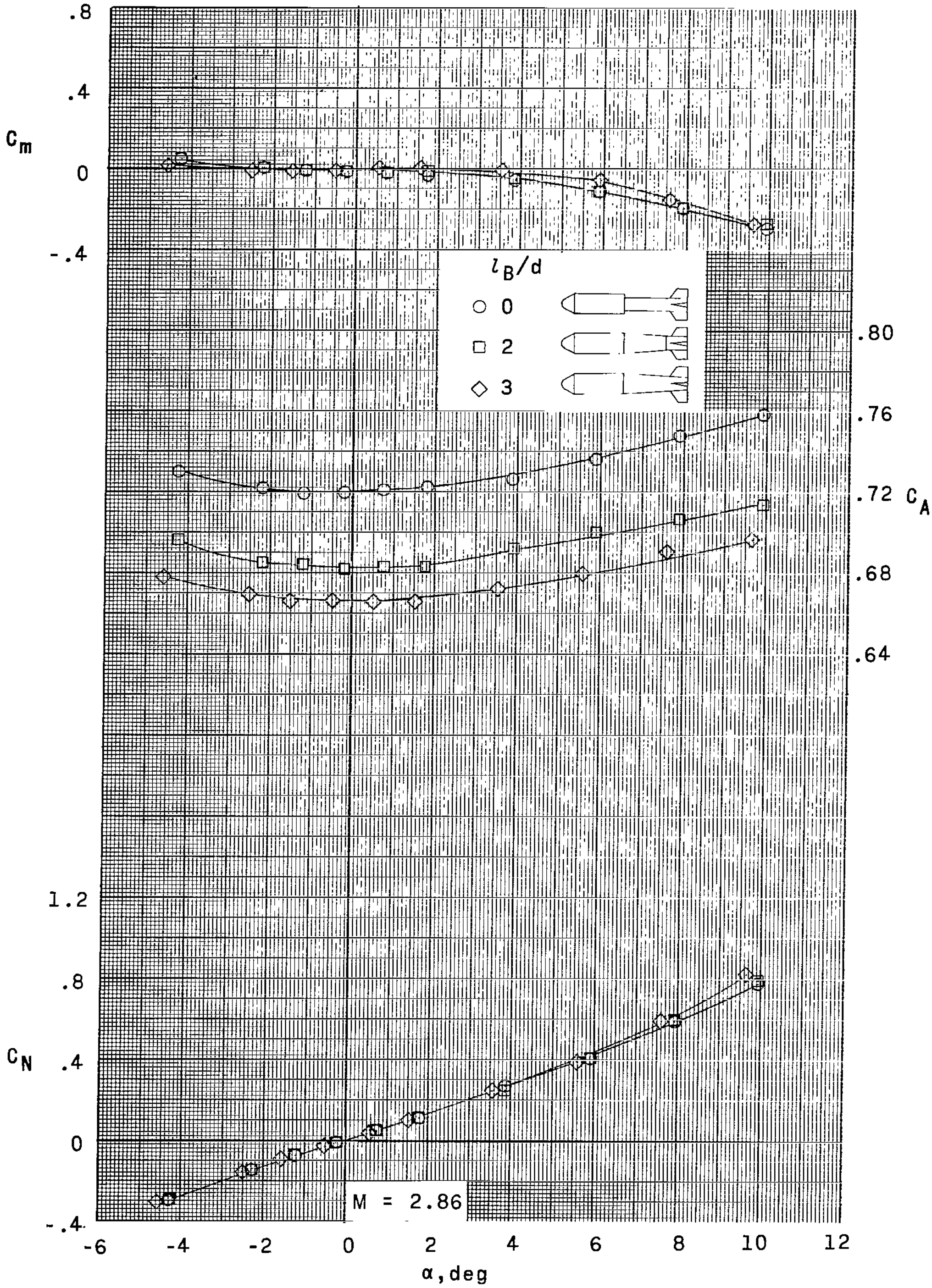

(a) Concluded.

Figure 10.- Continued.

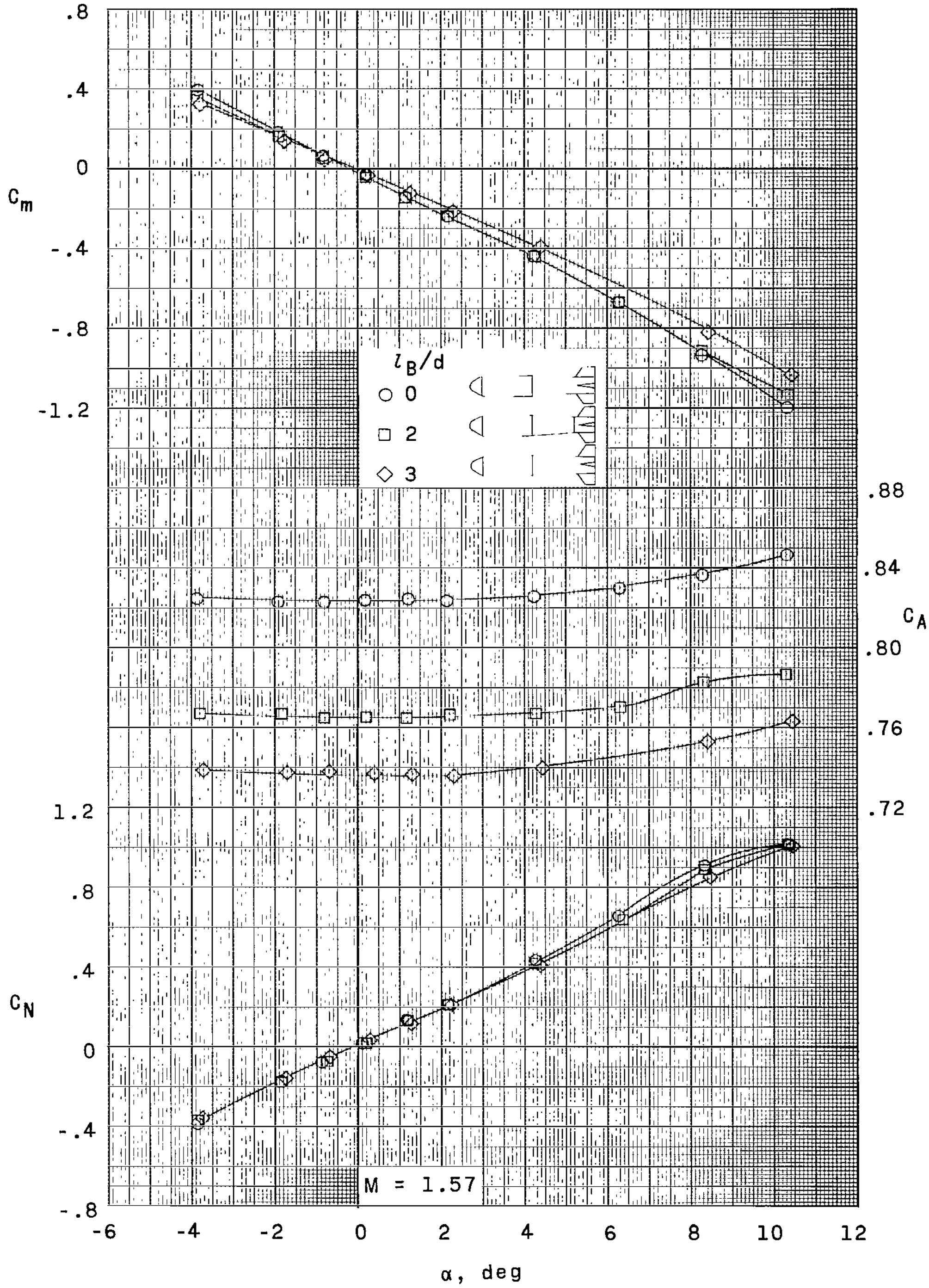

(b) $d_a/d = 0.75$.

Figure 10.- Continued.

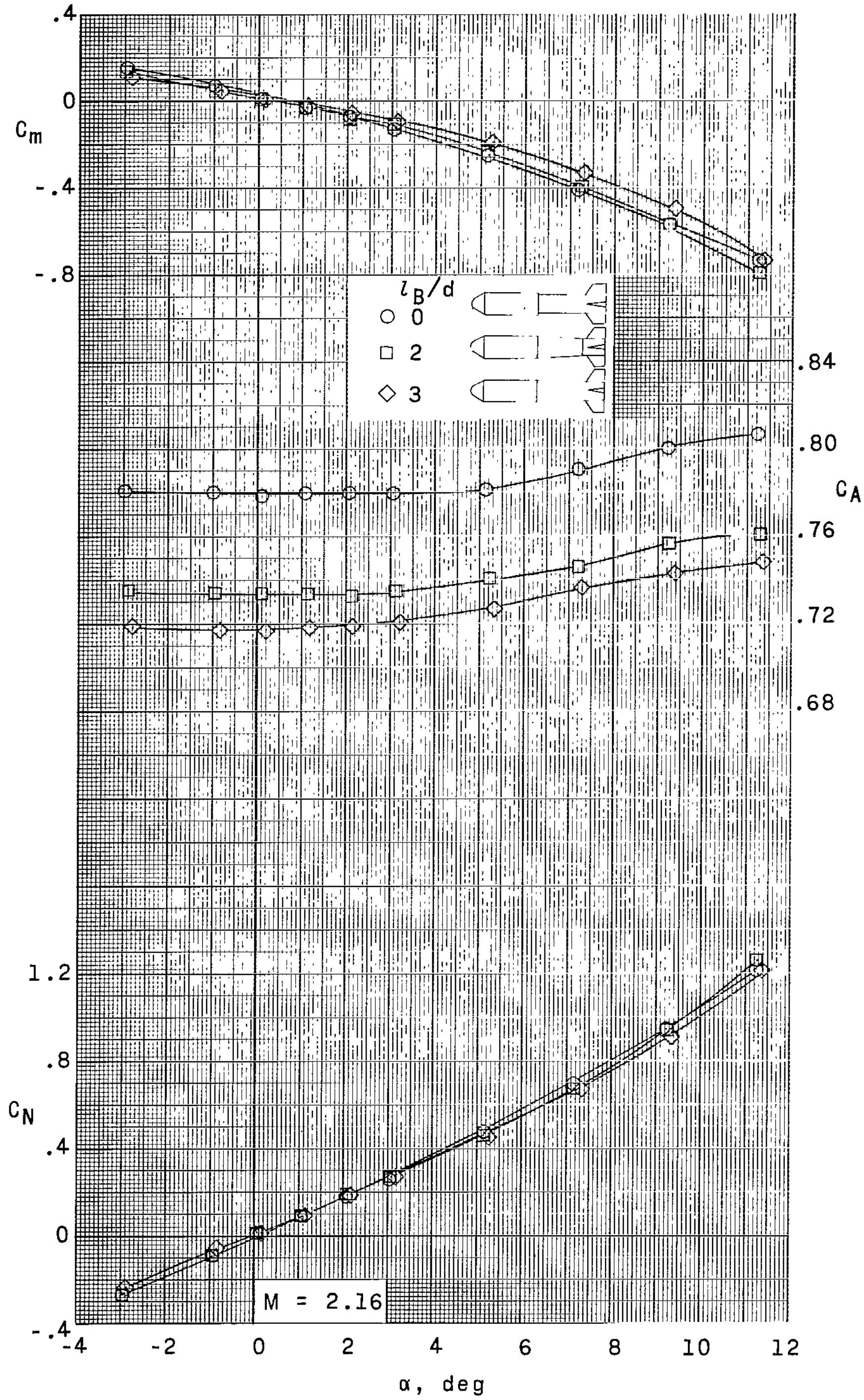

(b) Continued.

Figure 10.- Continued.

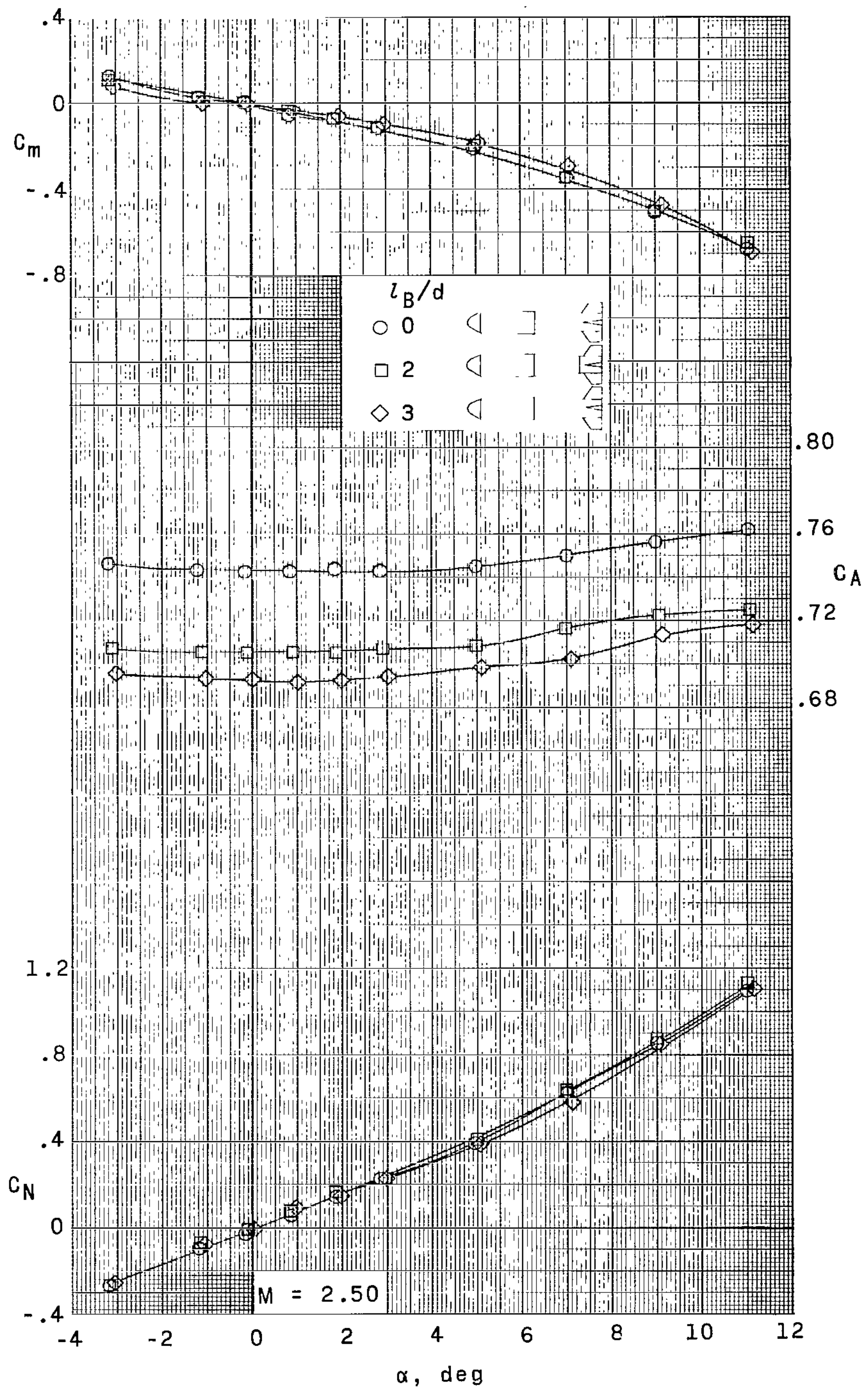

(b) Continued.

Figure 10.- Continued.

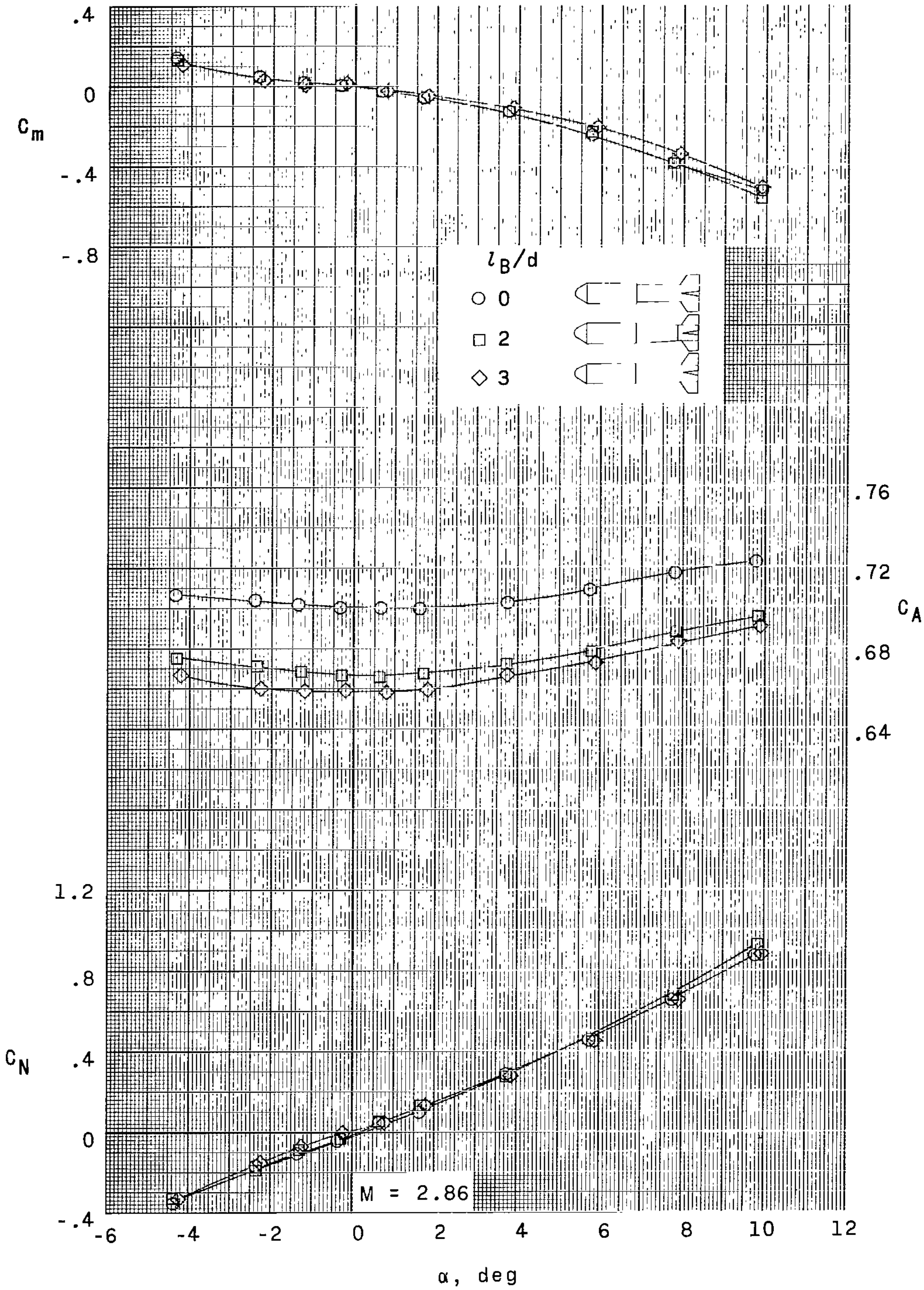

(b) Concluded.

Figure 10.- Concluded.

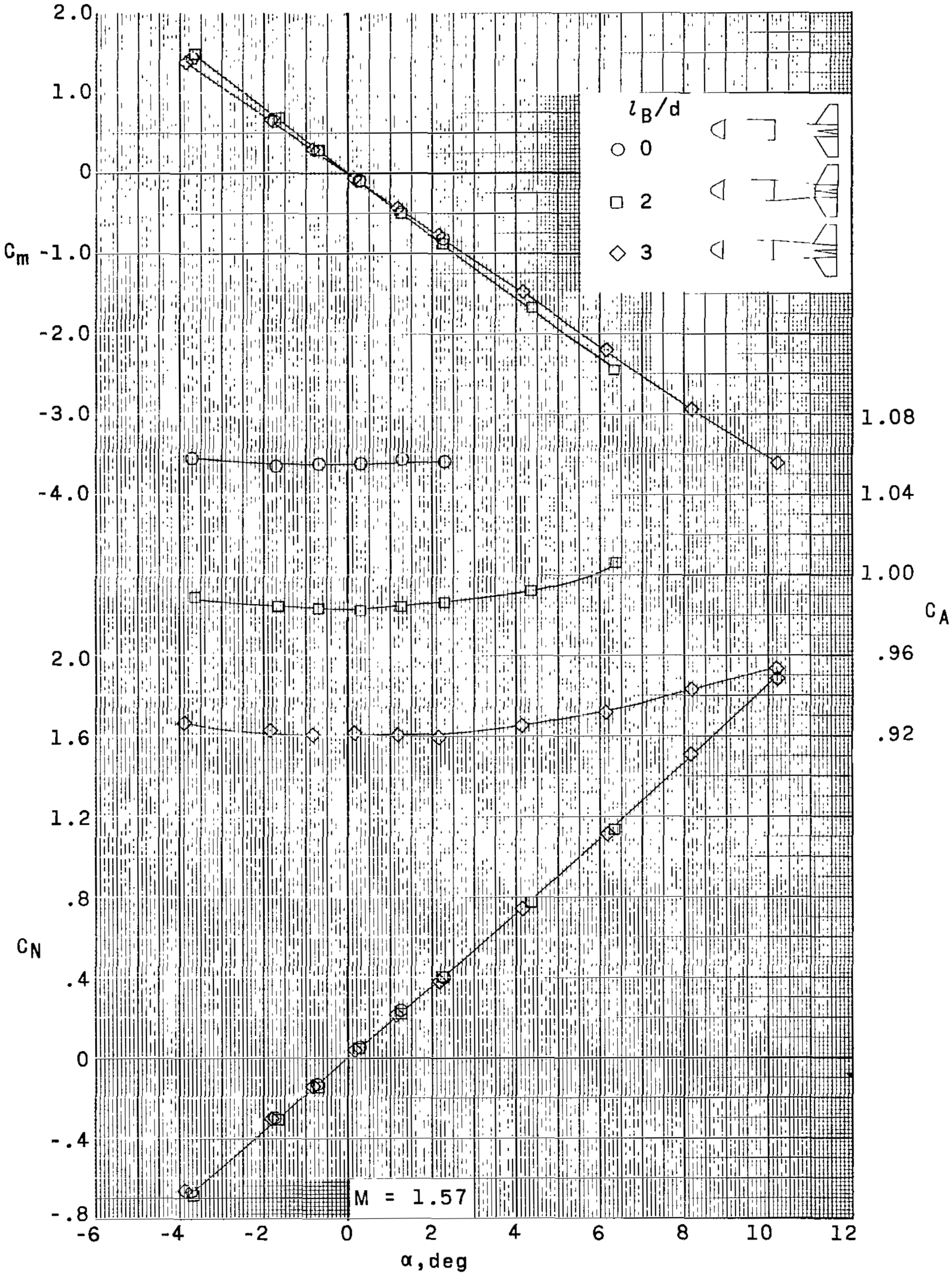

(a) $d_a/d = 0.55$.

Figure 11.- Aerodynamic characteristics in pitch. Intermediate first stage; large fins.

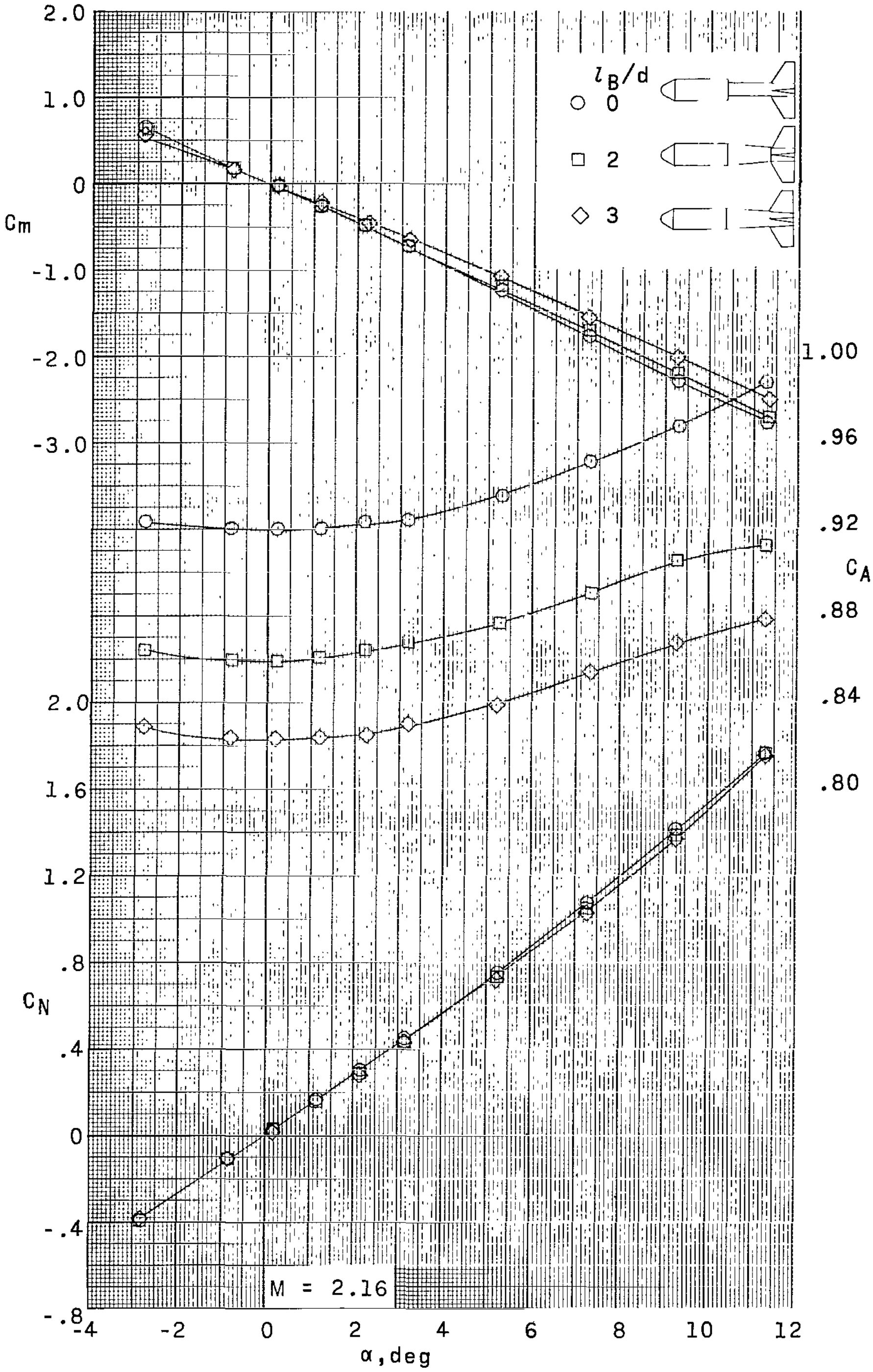

(a) Continued.

Figure 11.- Continued.

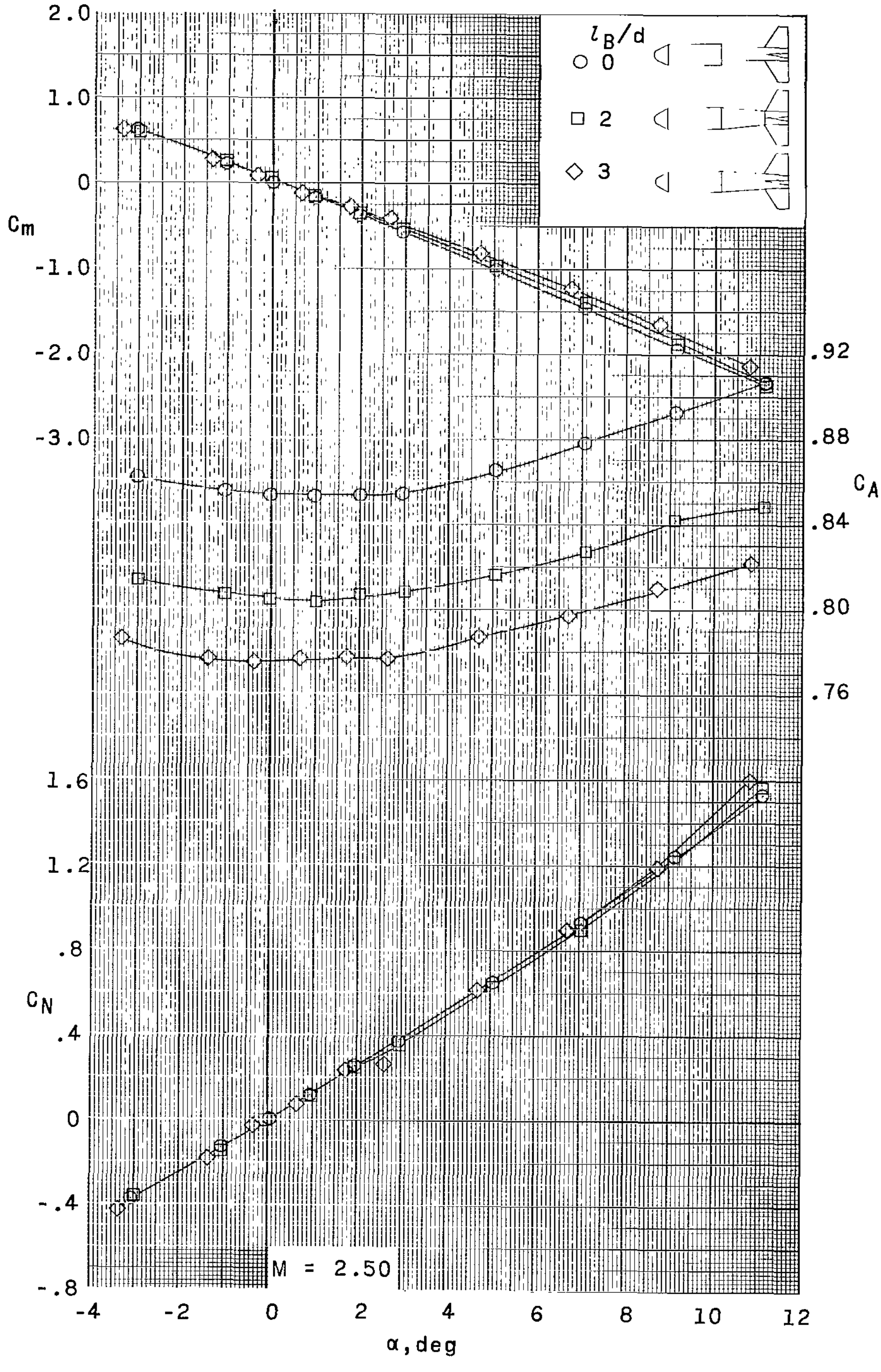

(a) Continued.

Figure 11.- Continued.

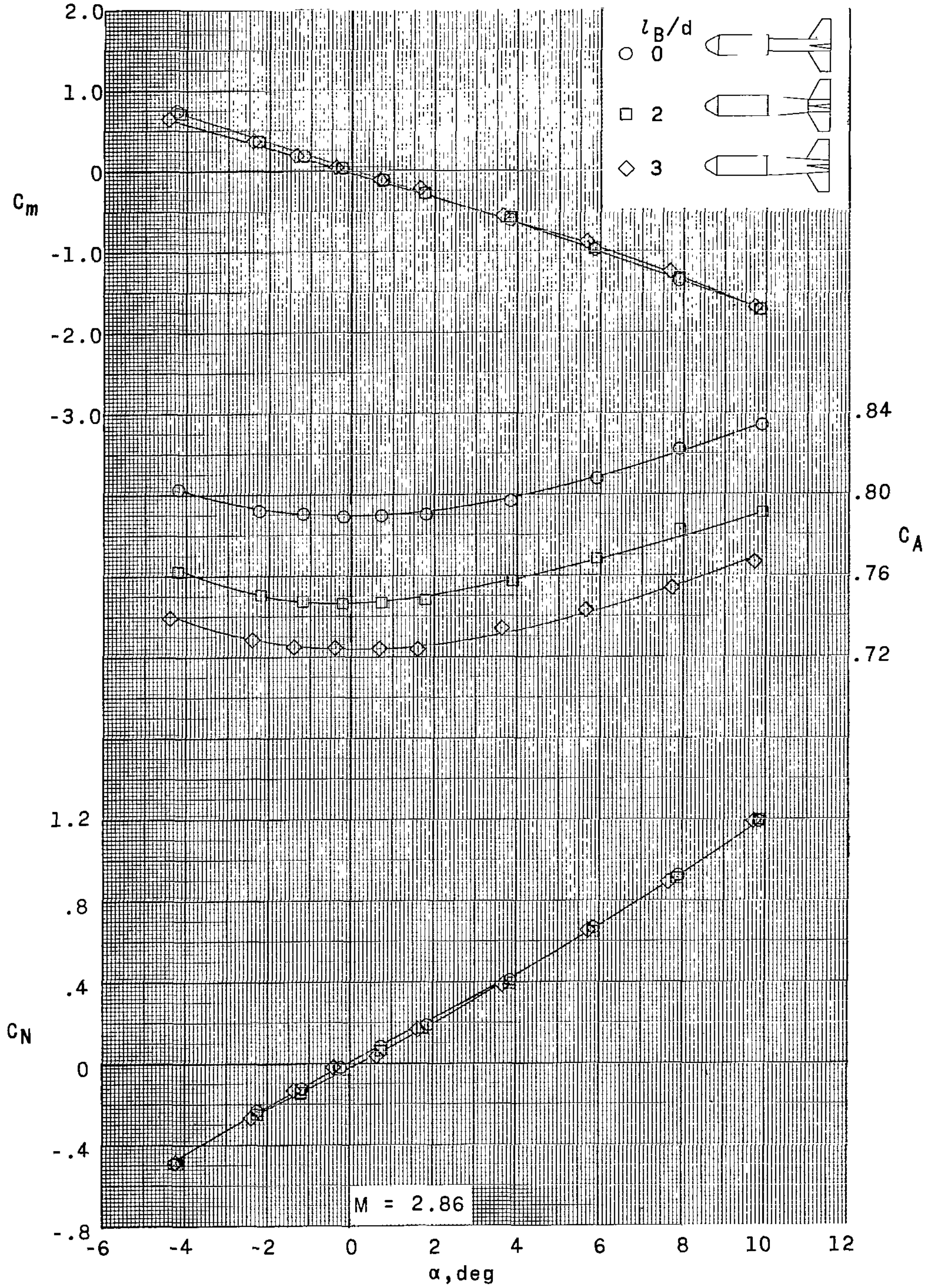

(a) Concluded.

Figure 11.- Continued.

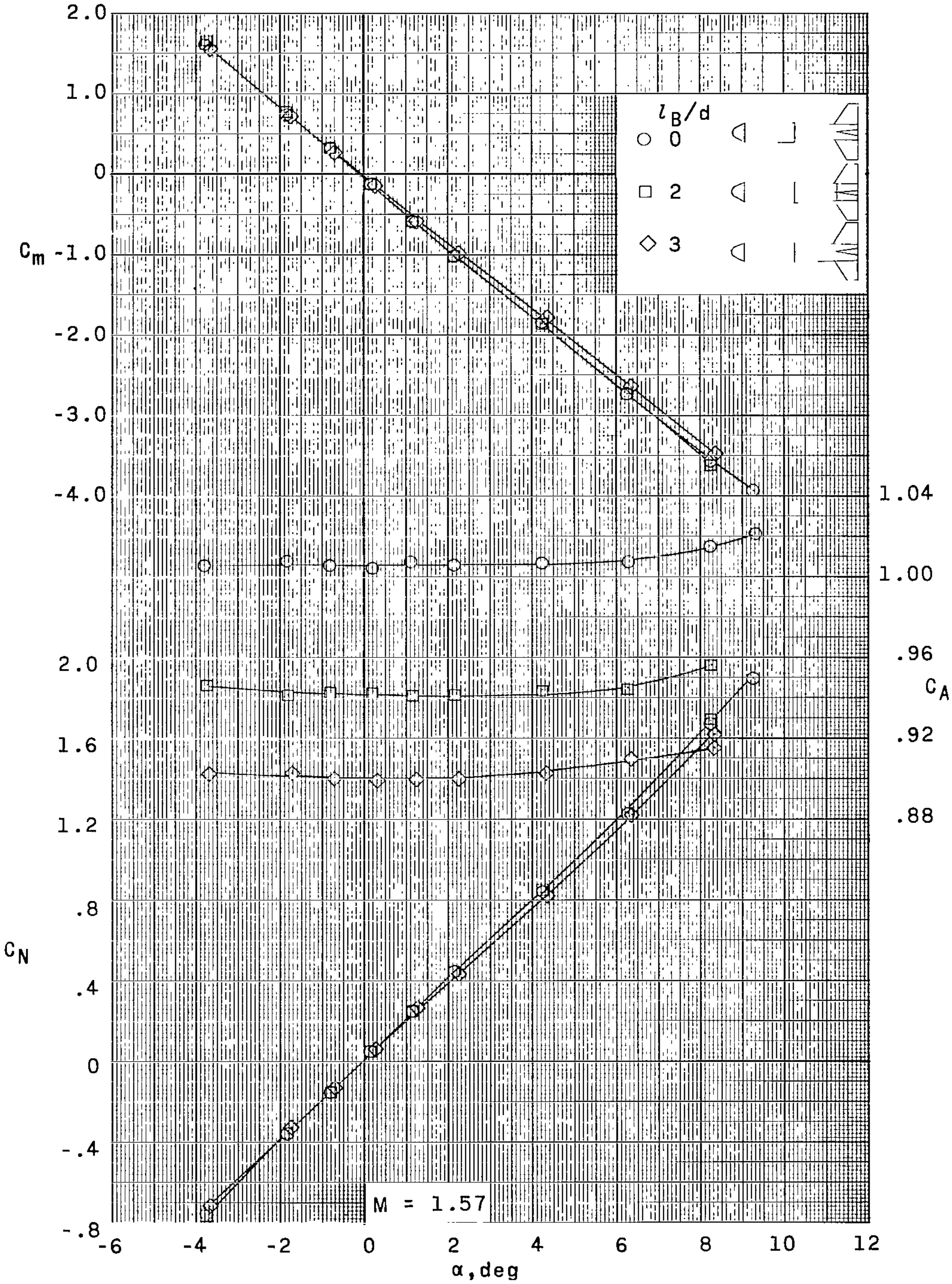

(b) $d_a/d = 0.75$.

Figure 11.- Continued.

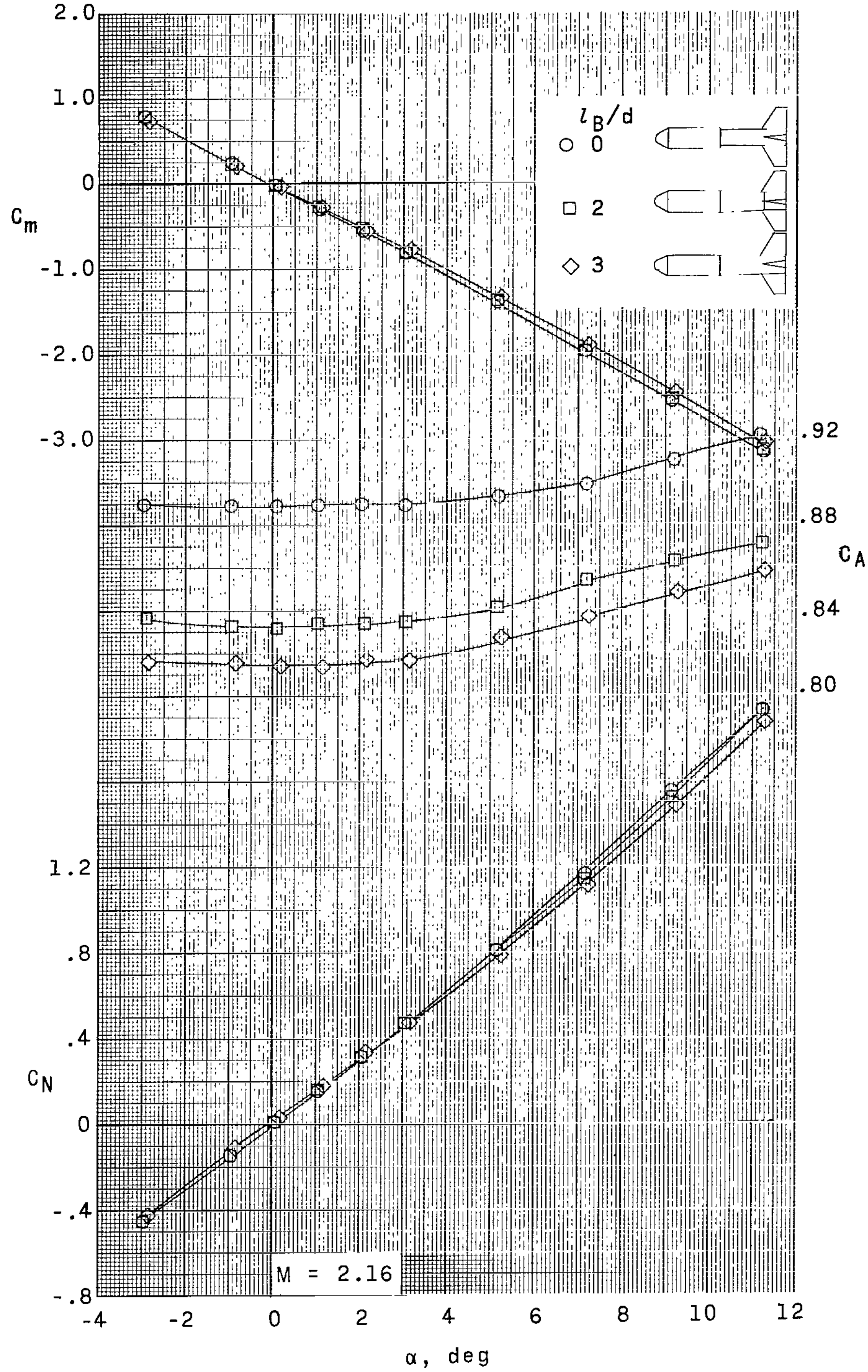

(b) Continued.

Figure 11.- Continued.

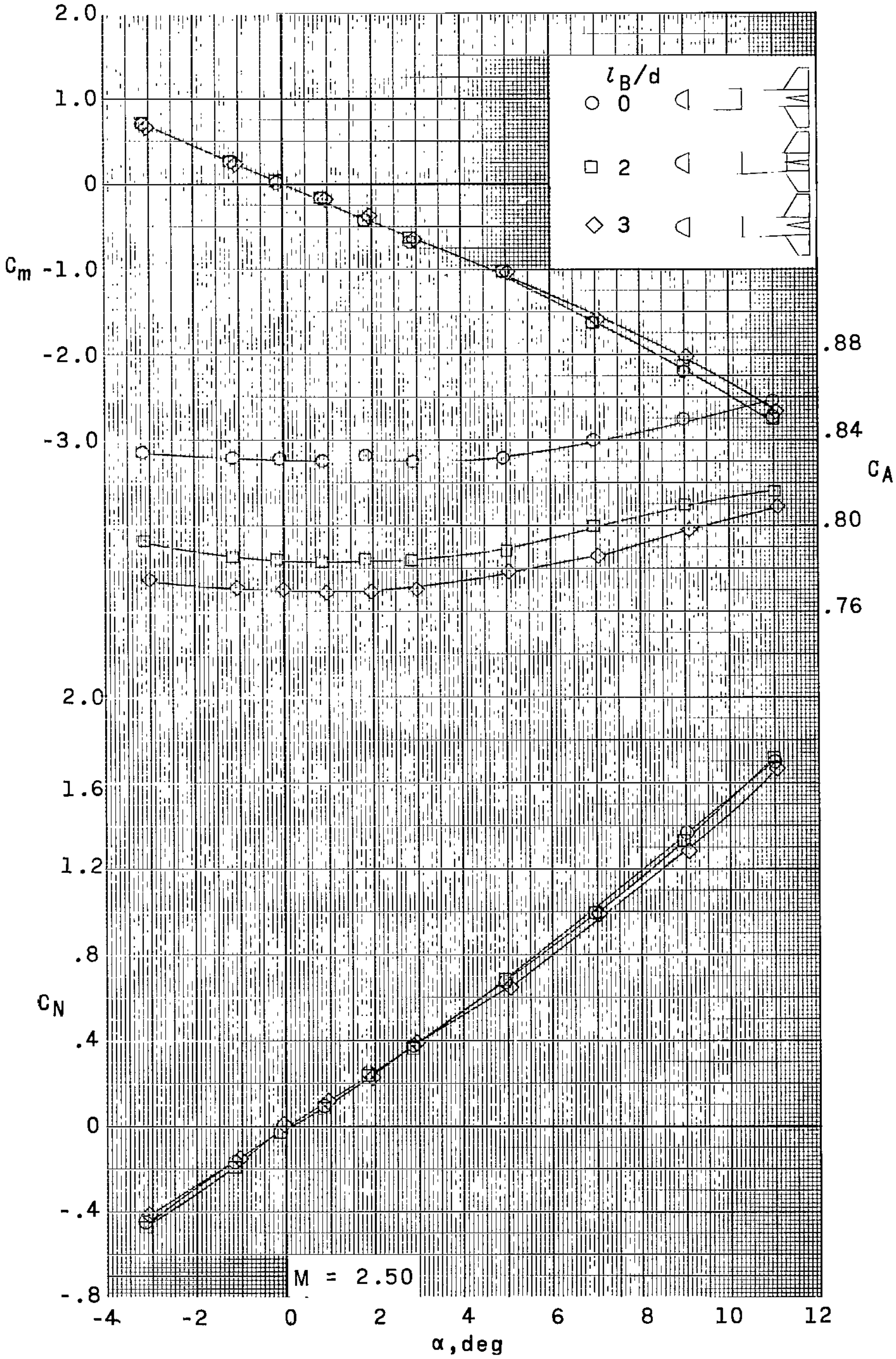

(b) Continued.

Figure 11.- Continued.

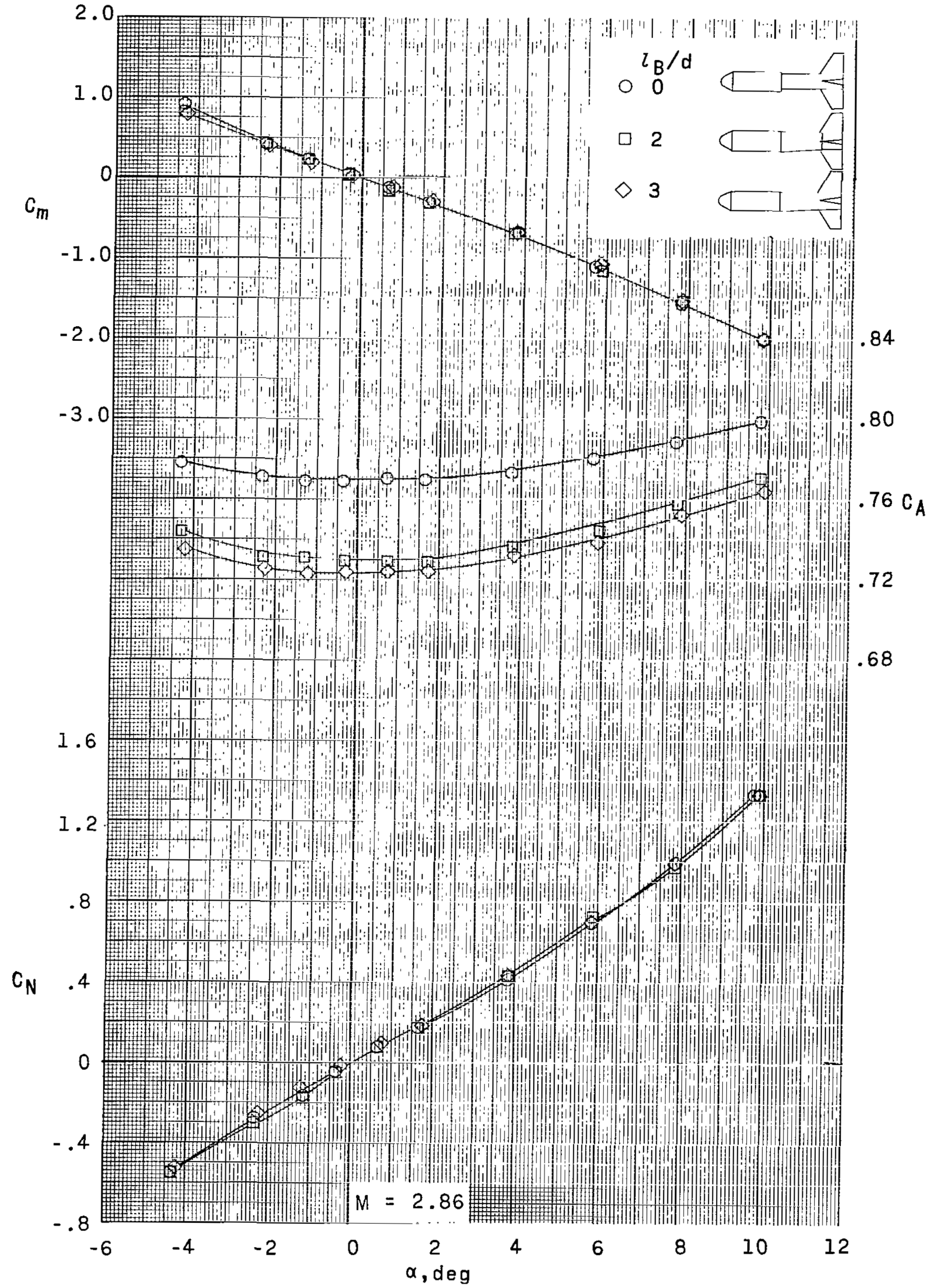

(b) Concluded.

Figure 11.- Concluded.

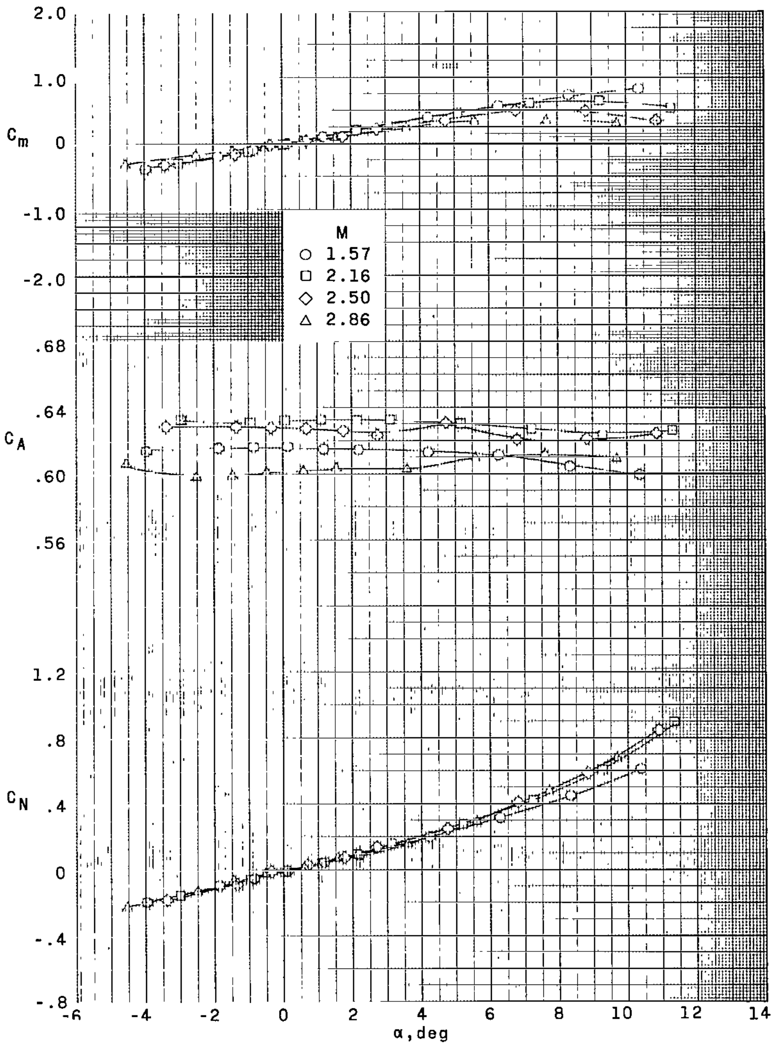

(a) Fins off.

Figure 12.- Aerodynamic characteristics in pitch. Intermediate first stage; $d_a/d = 1.00$.

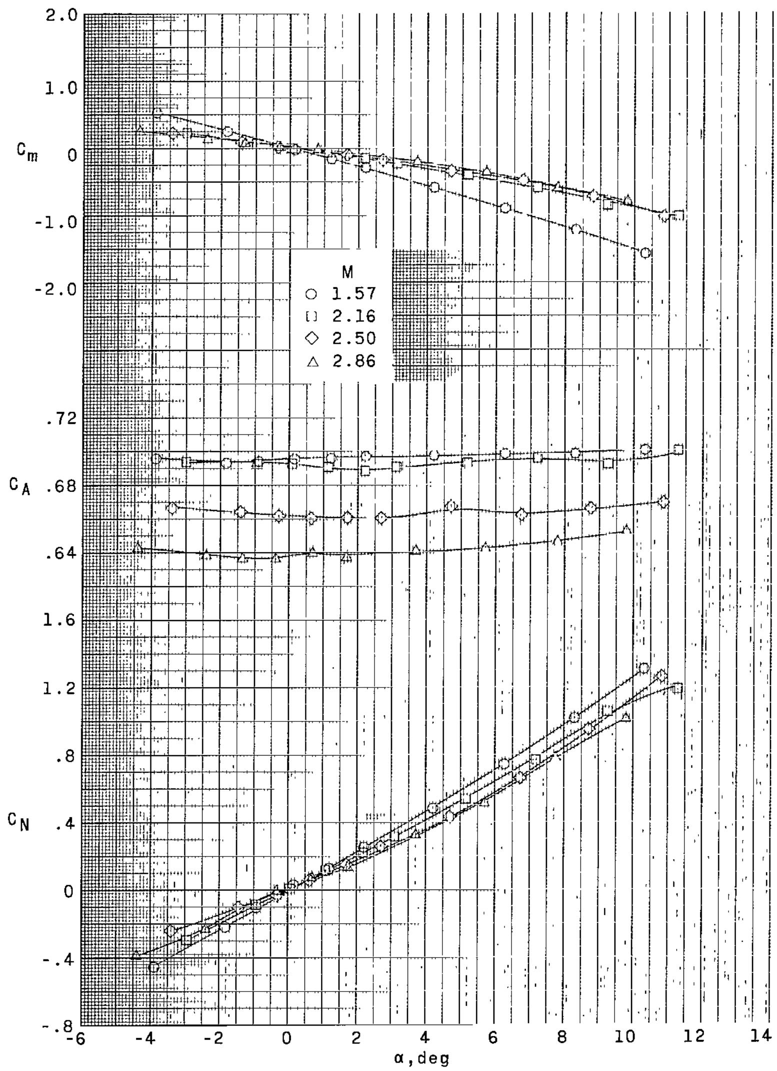

(b) Small fins.

Figure 12.- Continued.

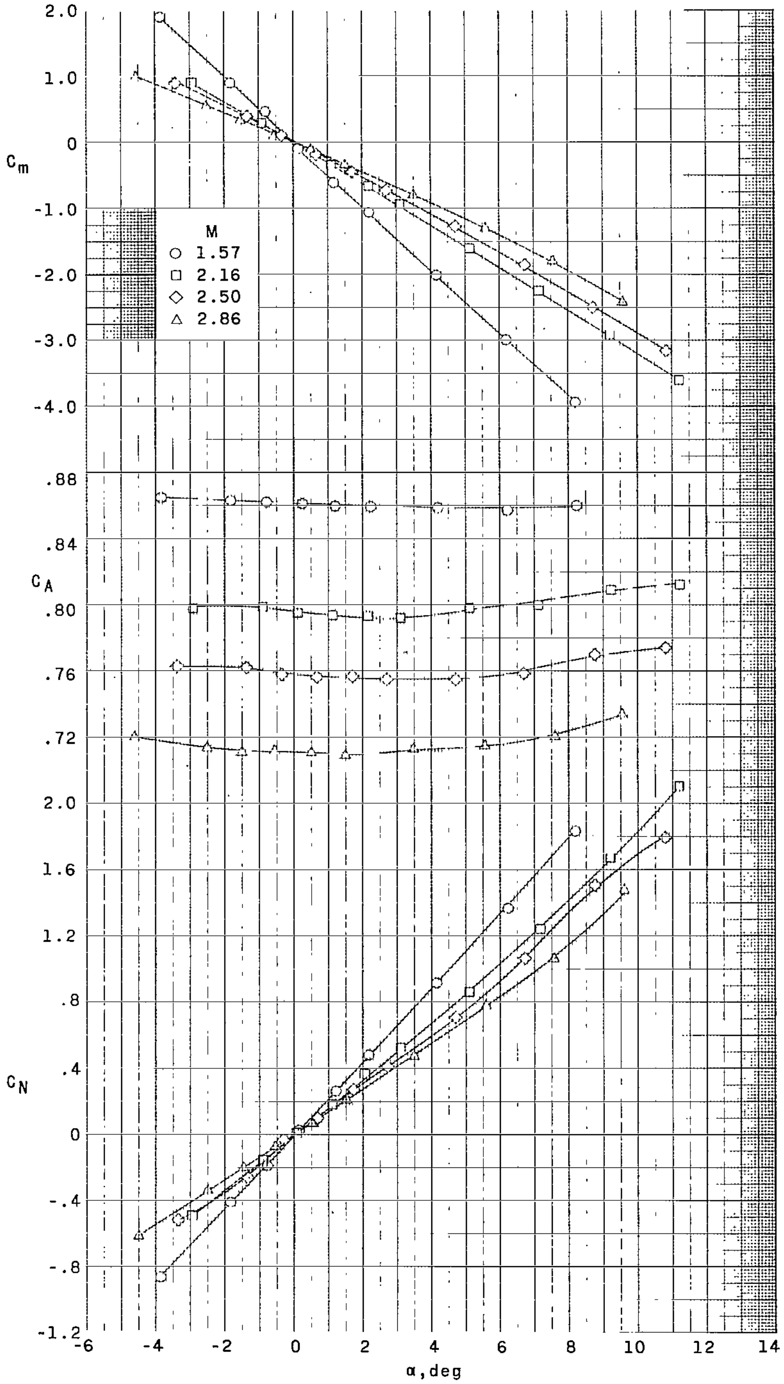

(c) Large fins.

Figure 12.- Concluded.

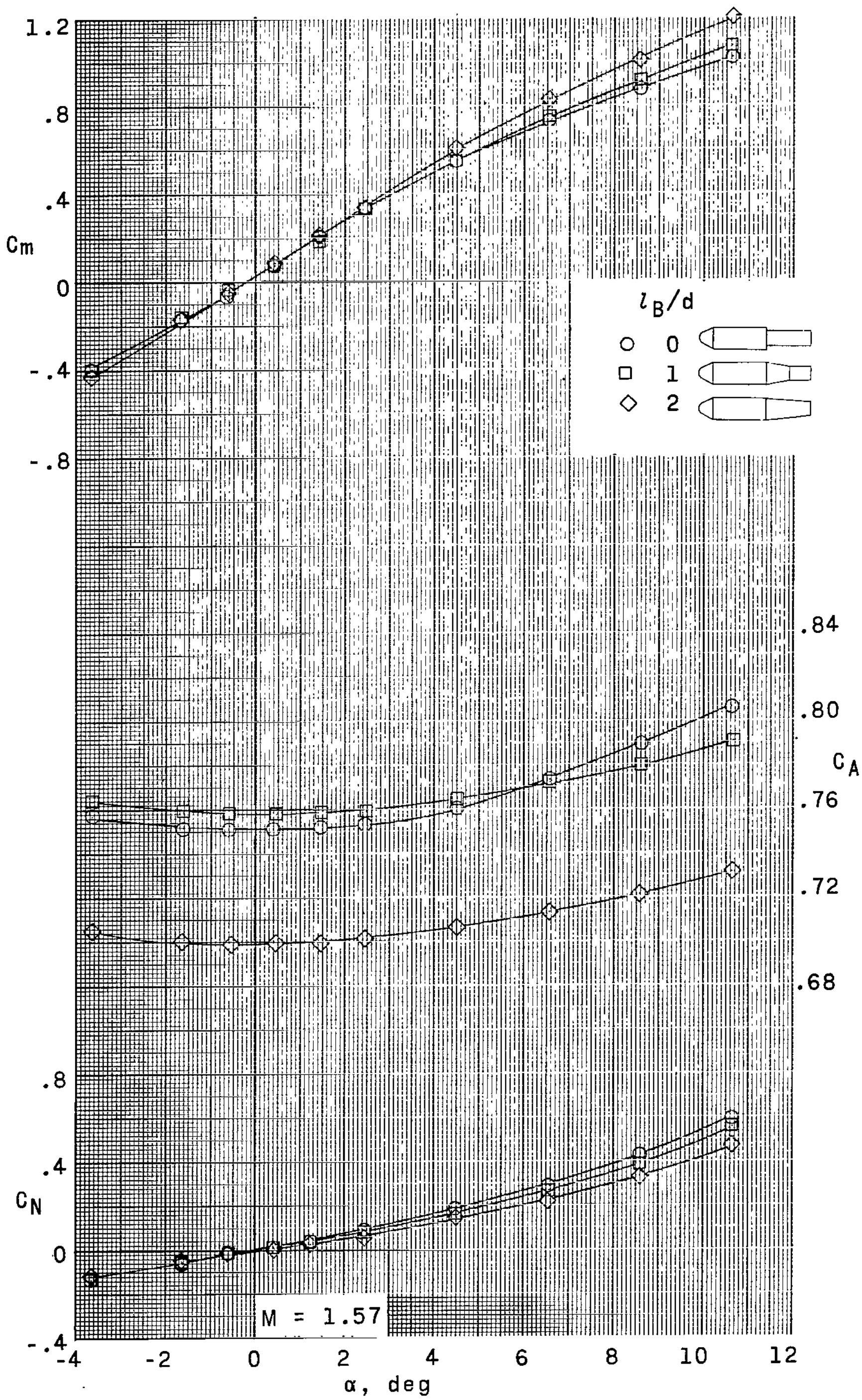

(a) $d_a/d = 0.55$.

Figure 13.- Aerodynamic characteristics in pitch. Short first stage; fins off.

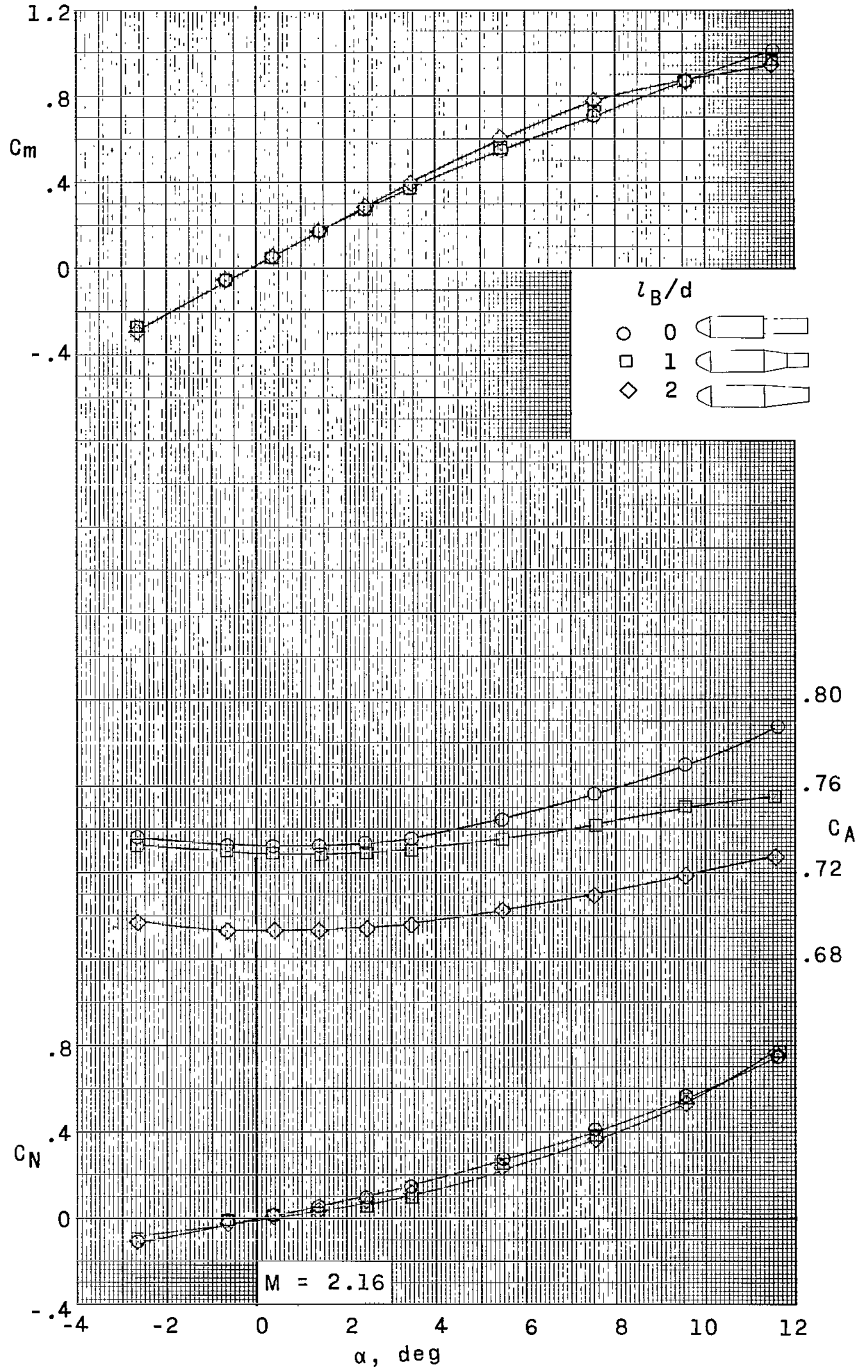

(a) Continued.

Figure 13.- Continued.

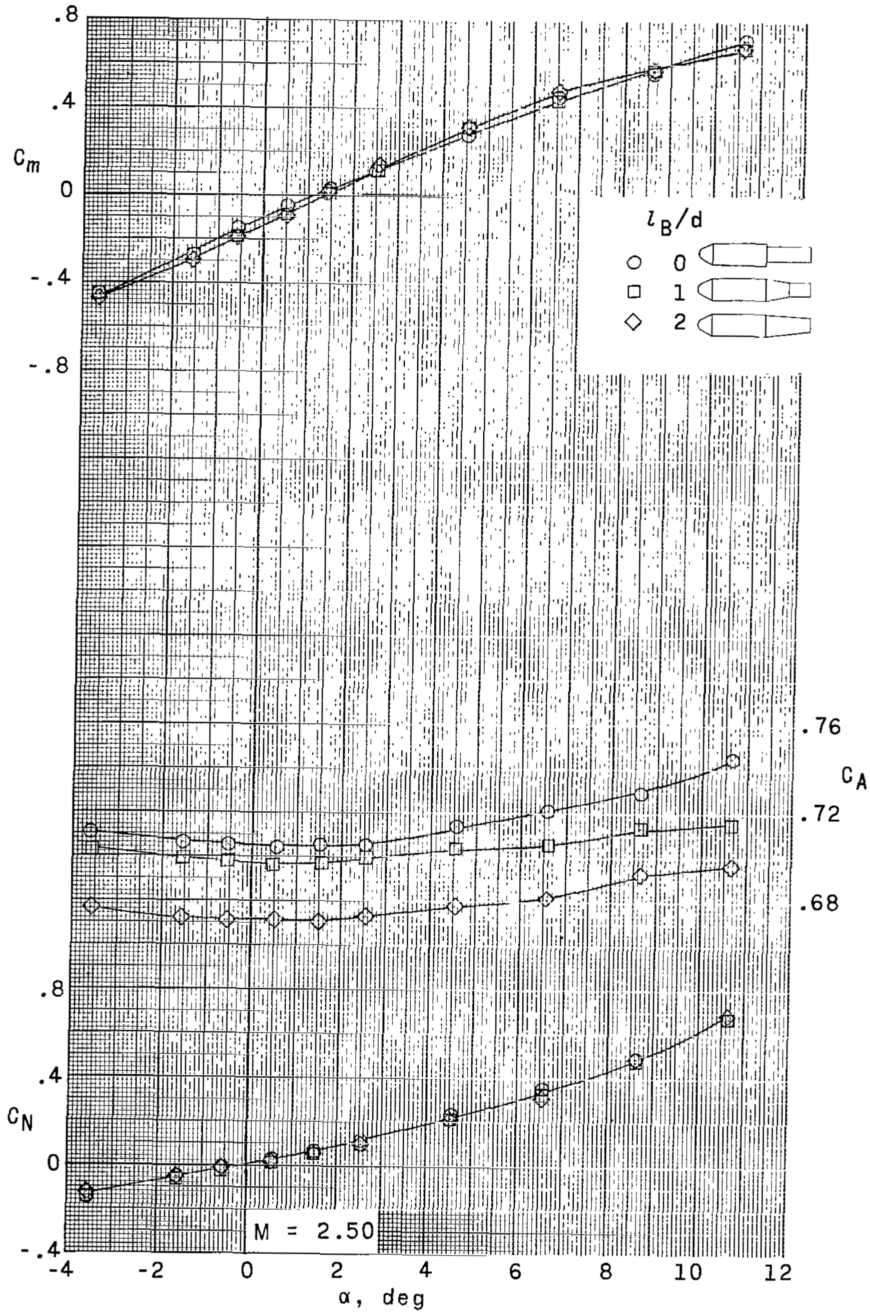

(a) Continued.

Figure 13.- Continued.

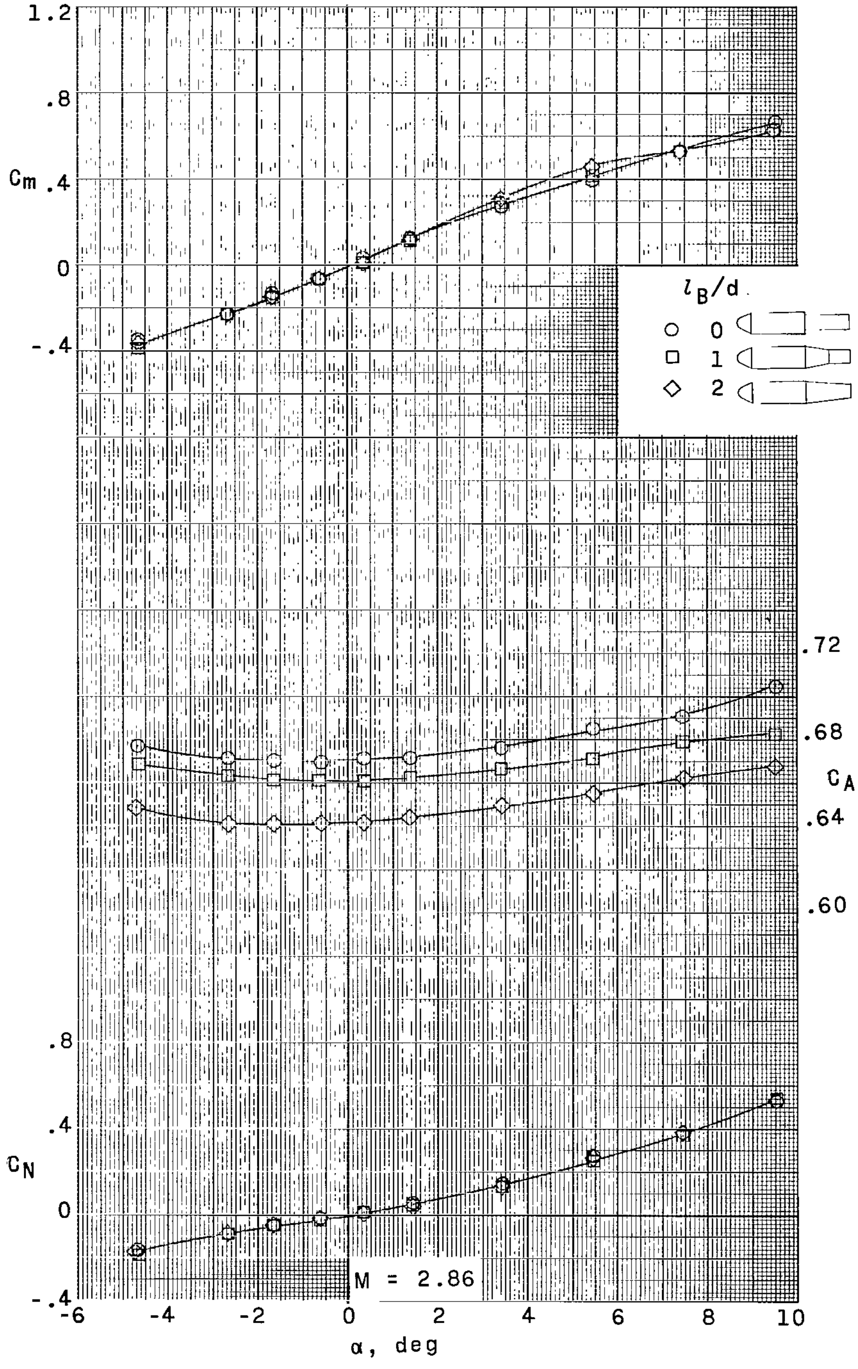

(a) Concluded.

Figure 13.- Continued.

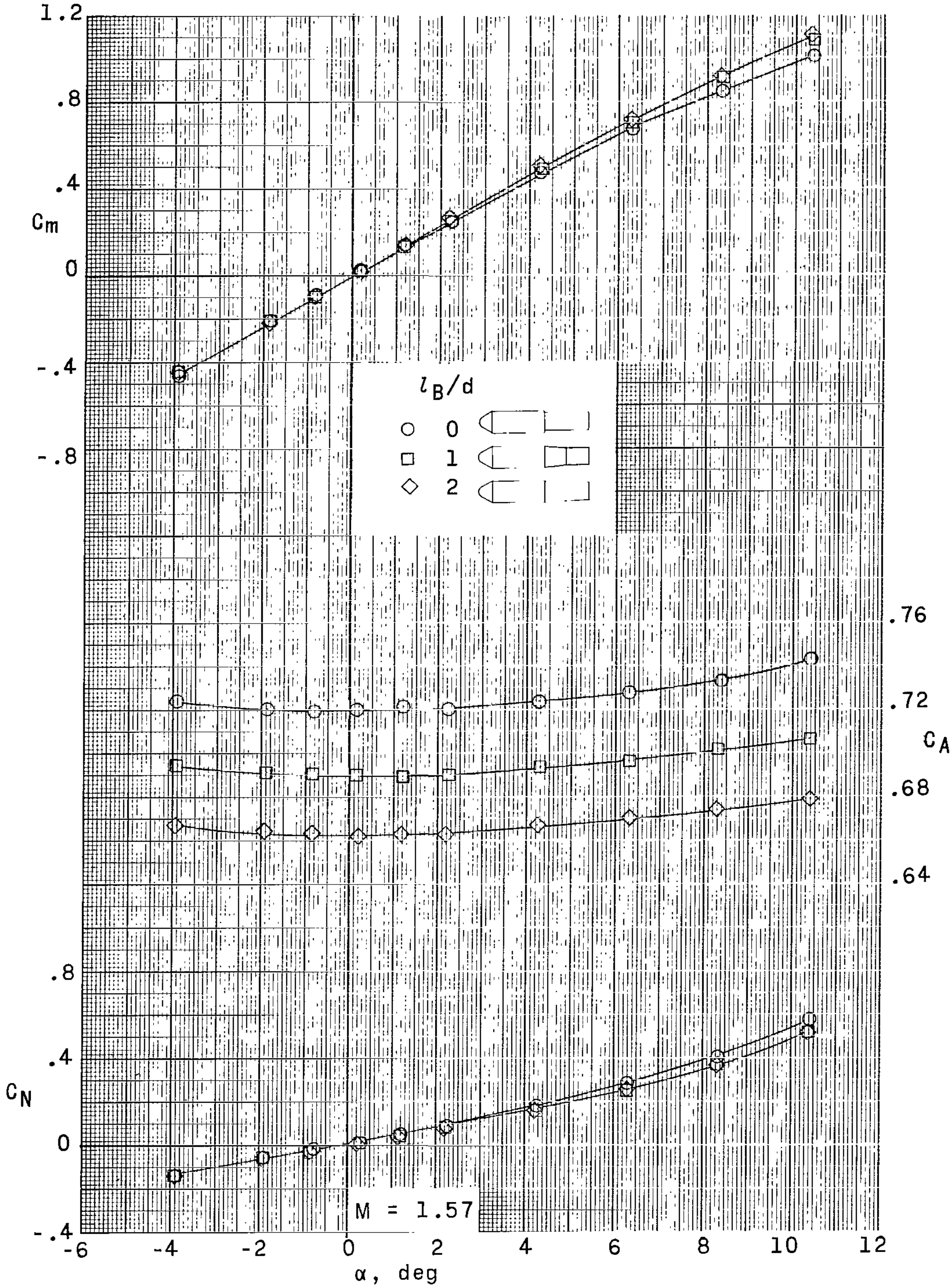

(b) $d_a/d = 0.75$.

Figure 13.- Continued.

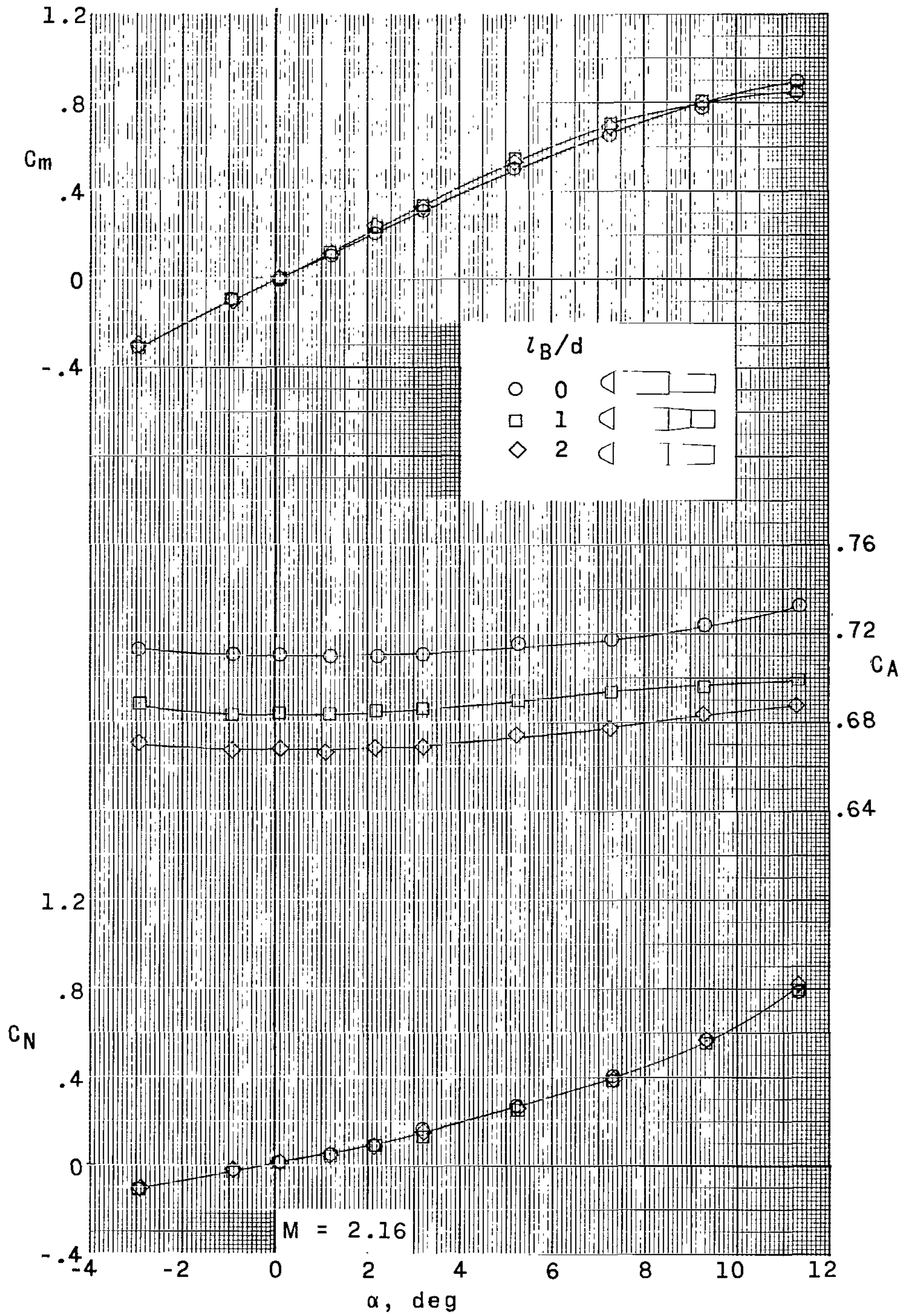

(b) Continued.

Figure 13.- Continued.

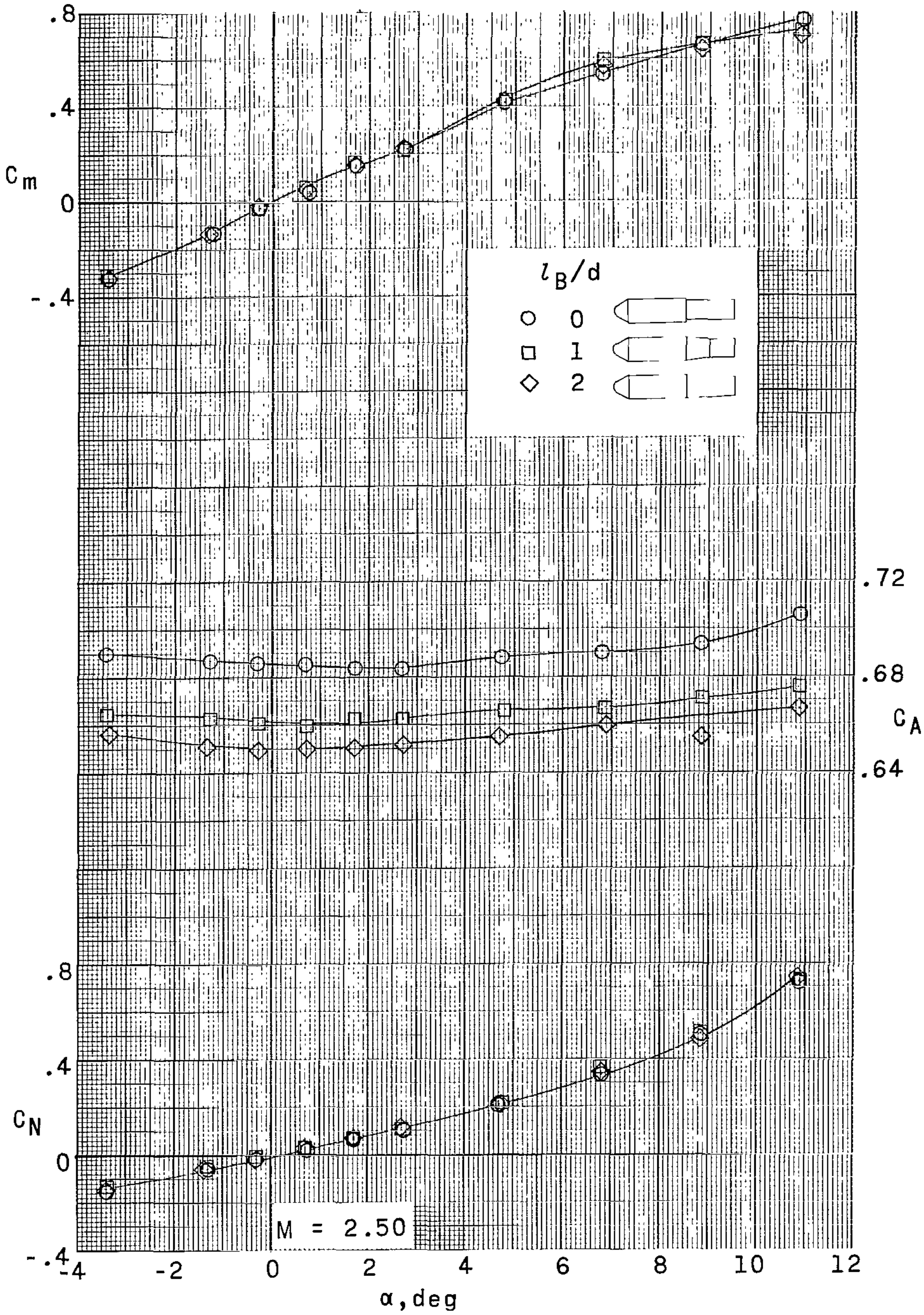

(b) Continued.

Figure 13.- Continued.

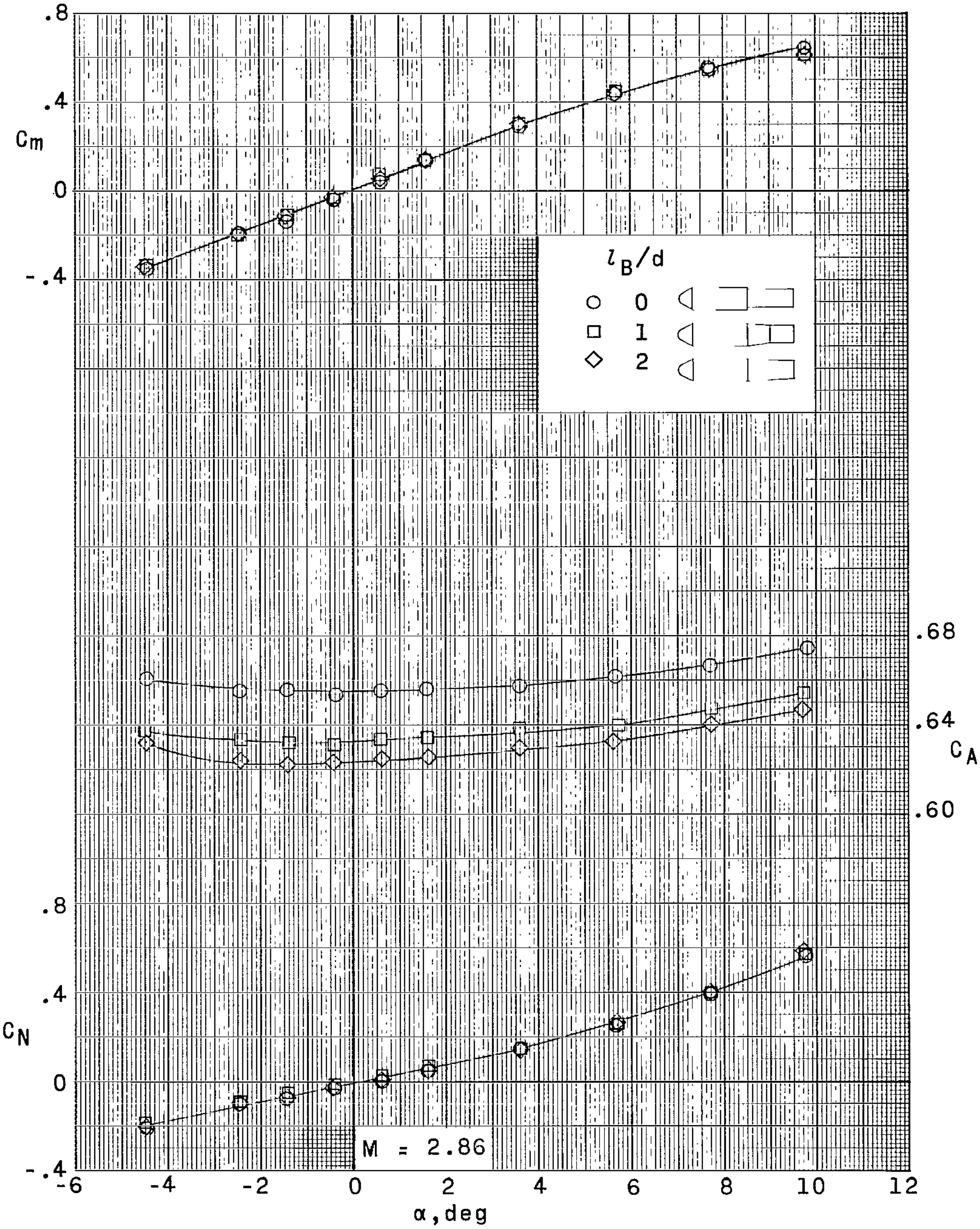

(b) Concluded.

Figure 13.- Concluded.

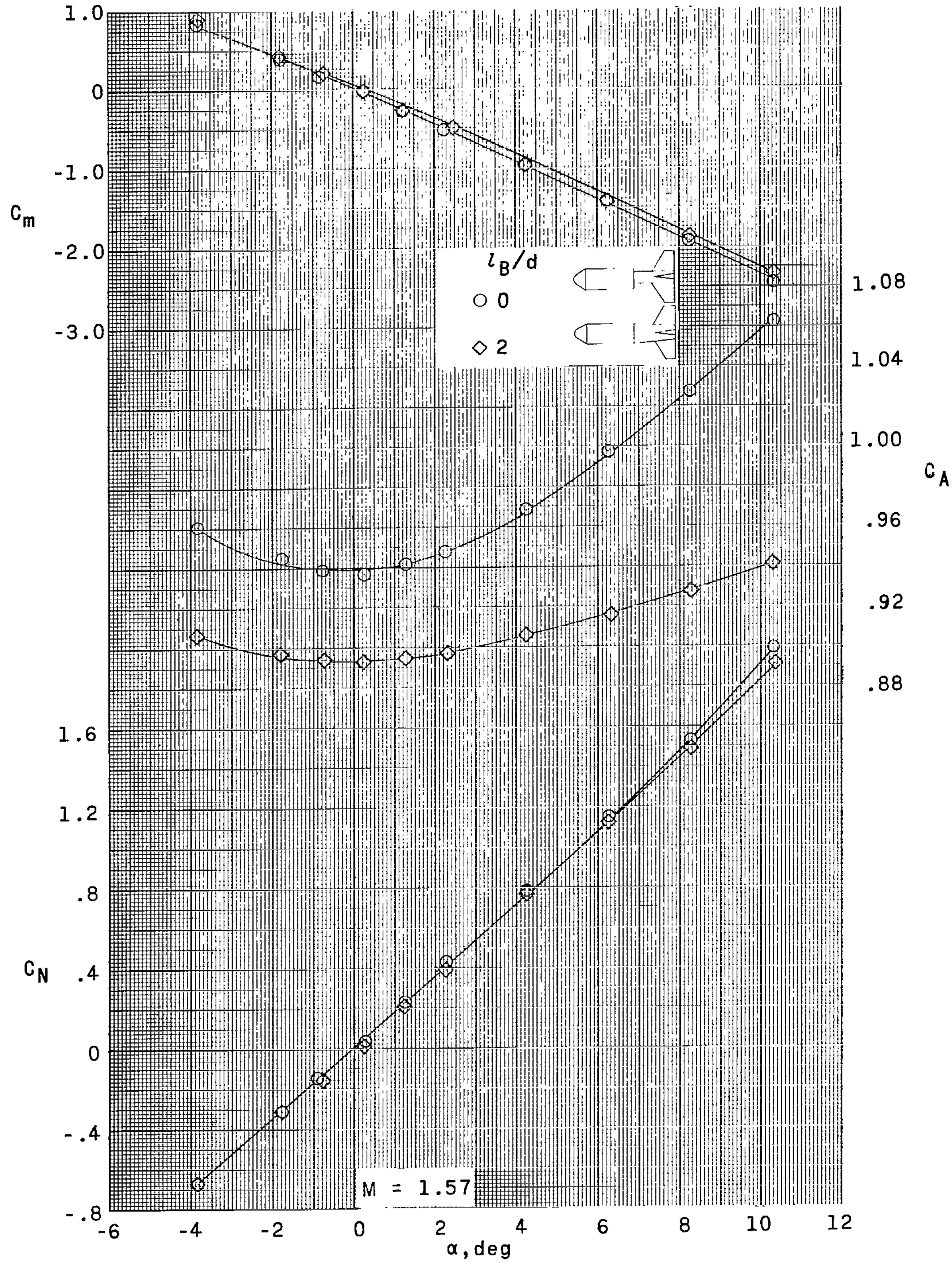

(a) $d_a/d = 0.55$.

Figure 14.- Aerodynamic characteristics in pitch. Short first stage; large fins.

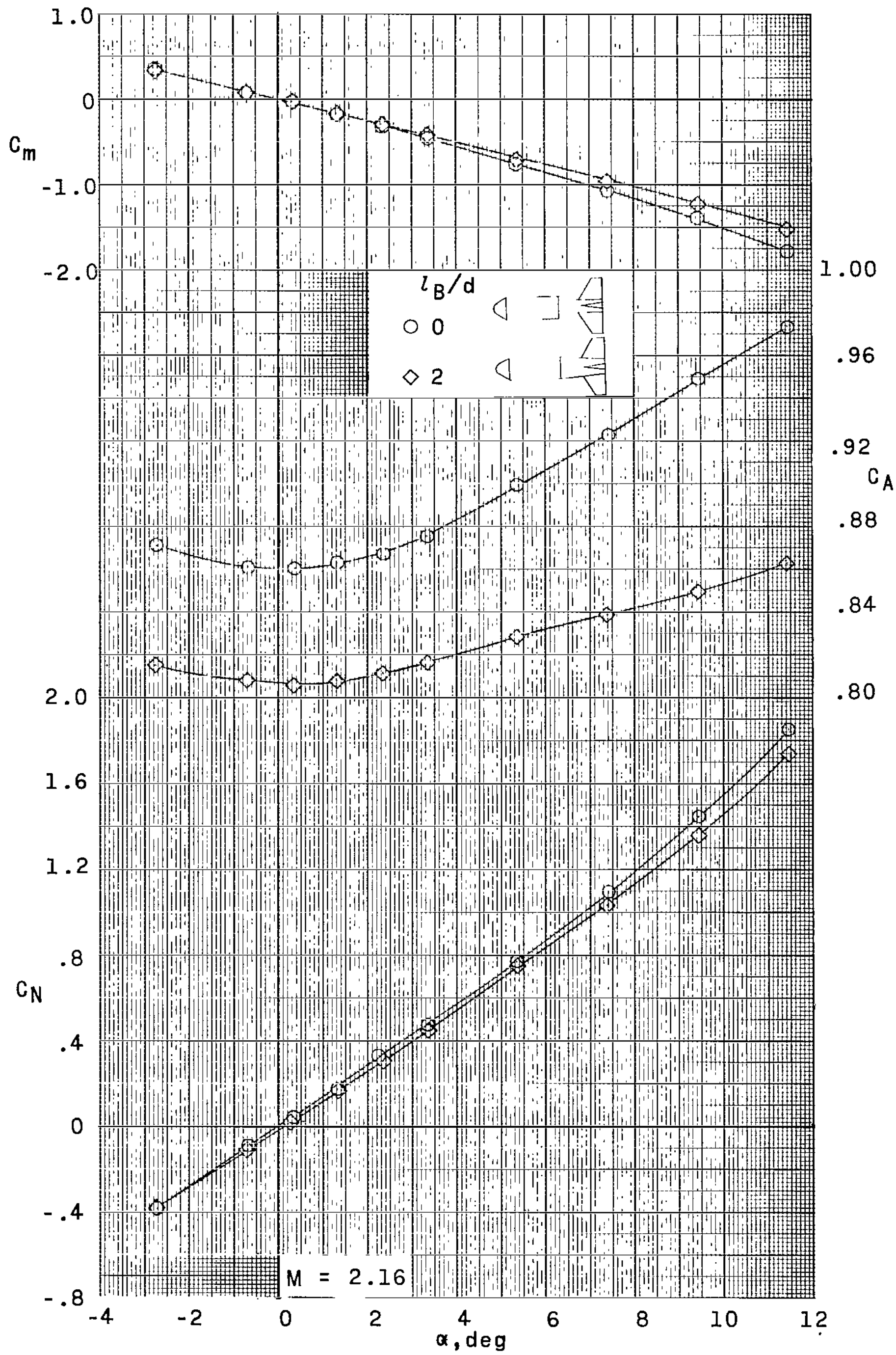

(a) Continued.

Figure 14.- Continued.

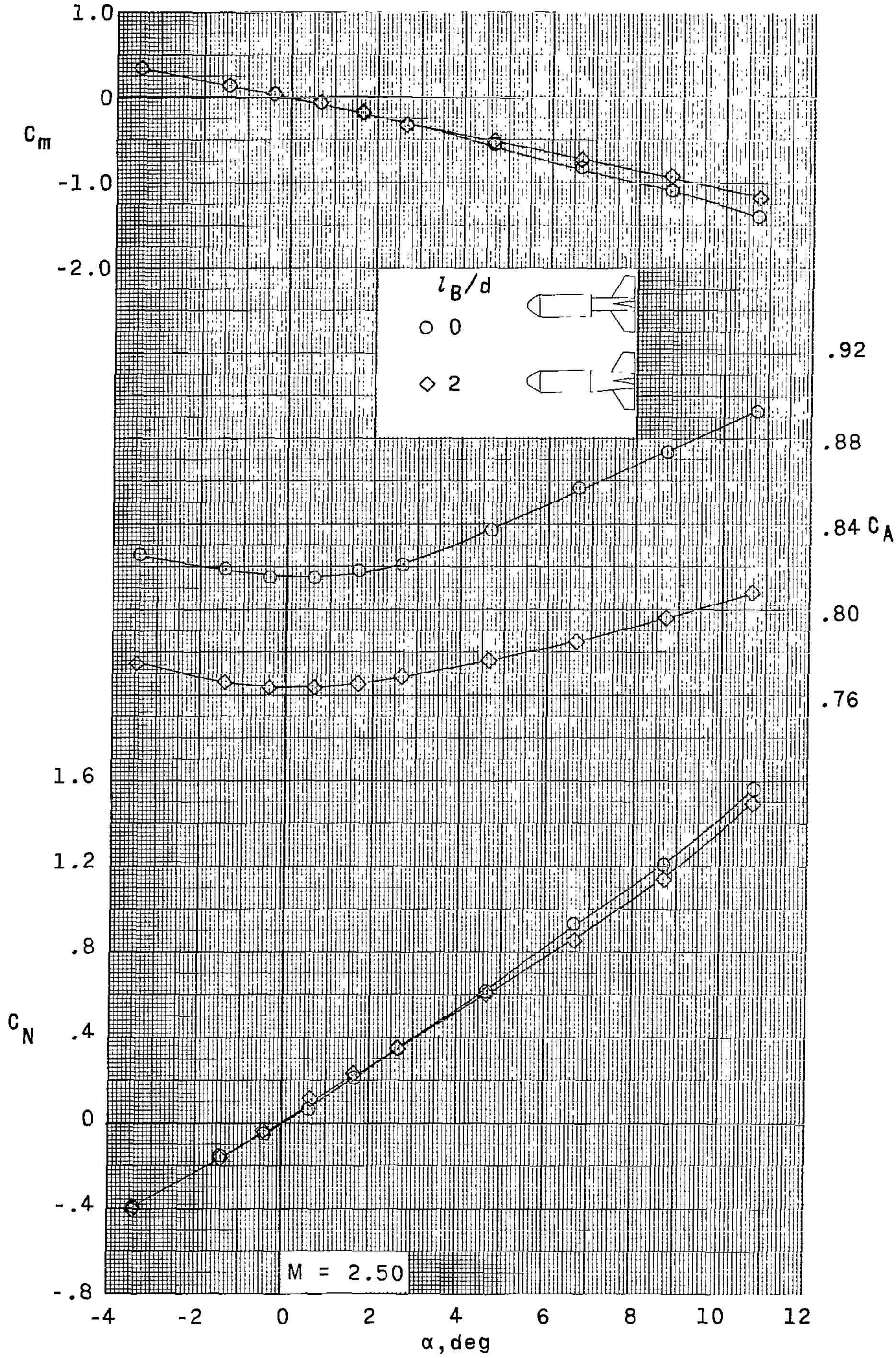

(a) Continued.

Figure 14.- Continued.

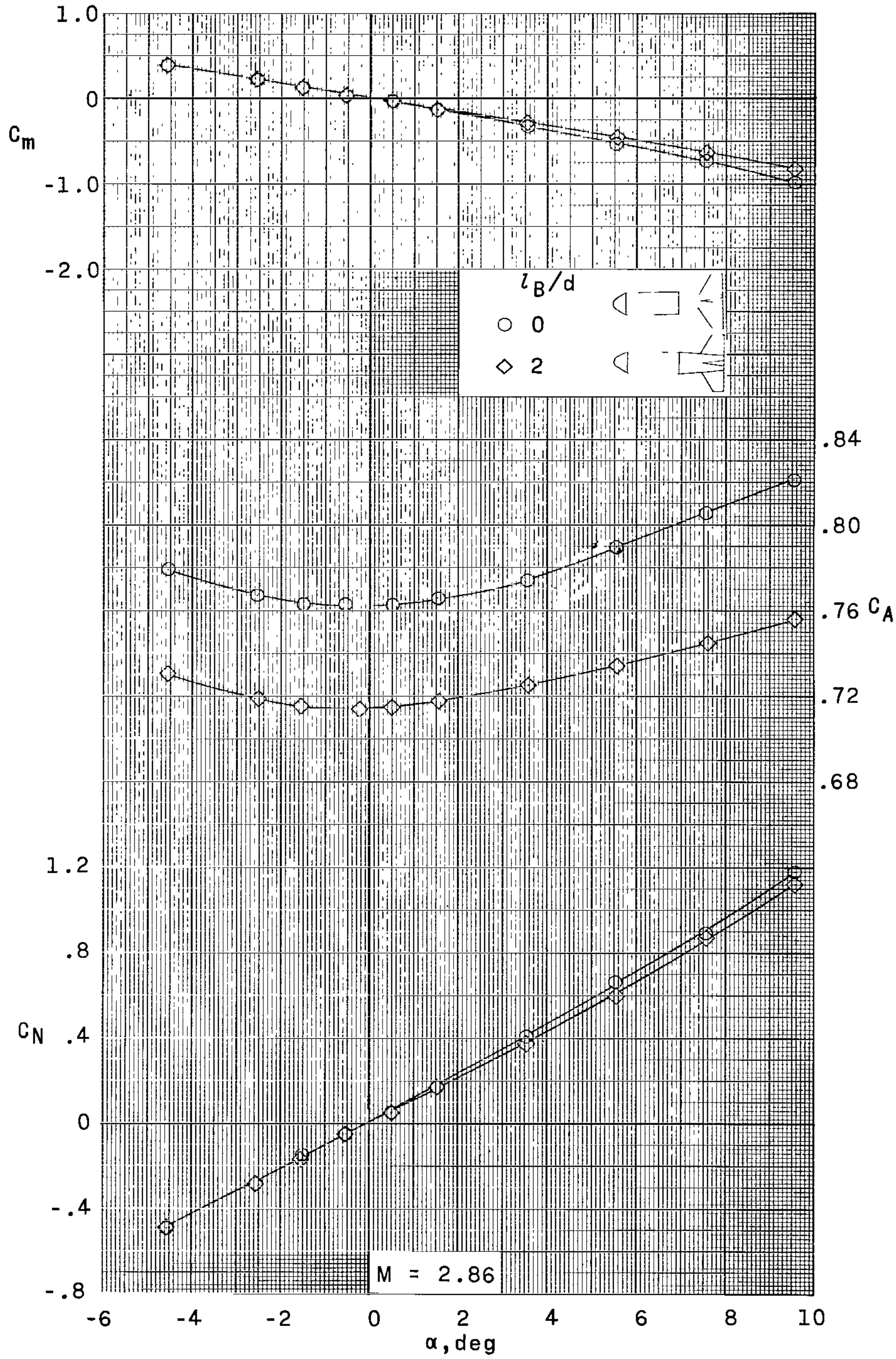

(a) Concluded.

Figure 14.- Continued.

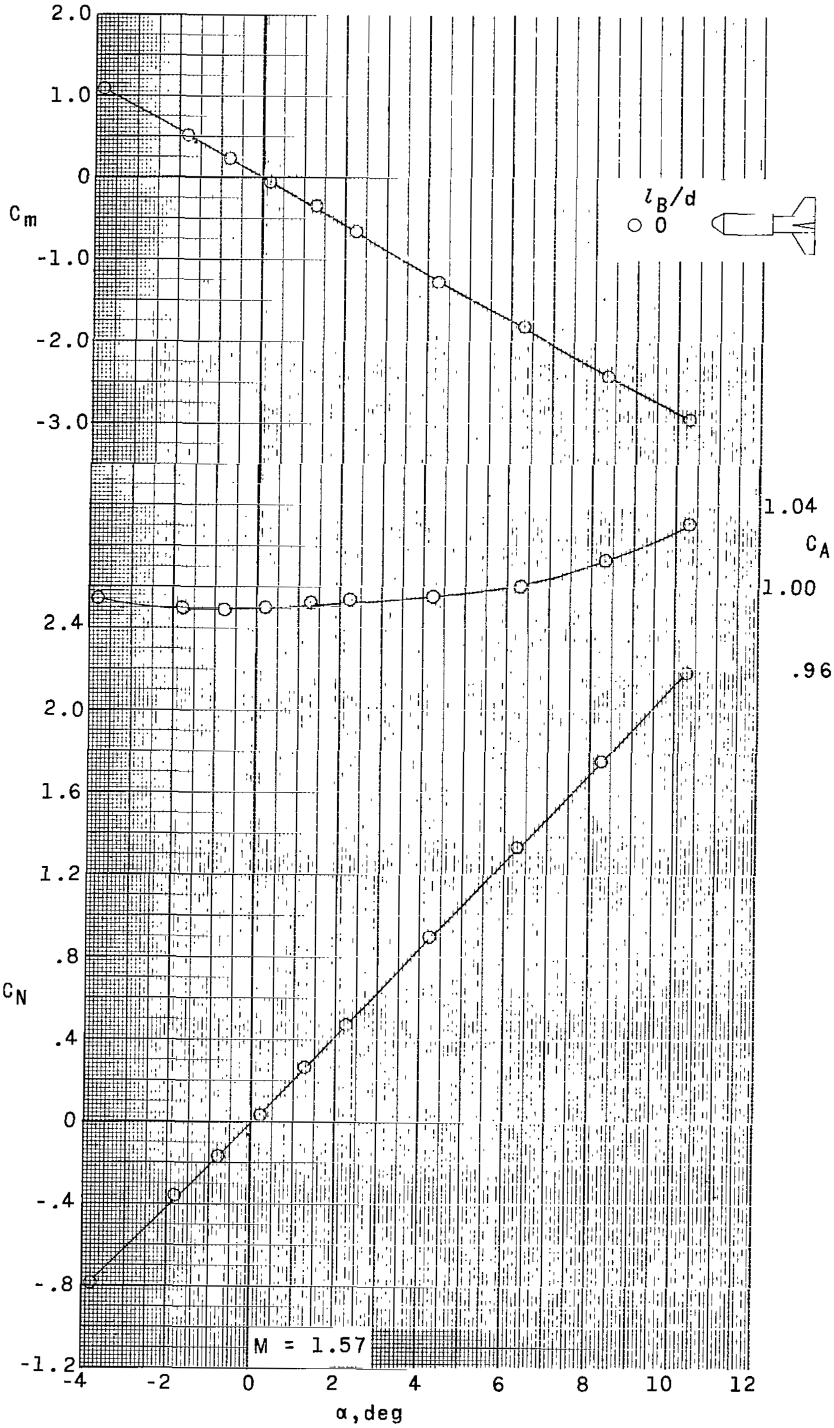

(b) $d_a/d = 0.75$.

Figure 14.- Continued.

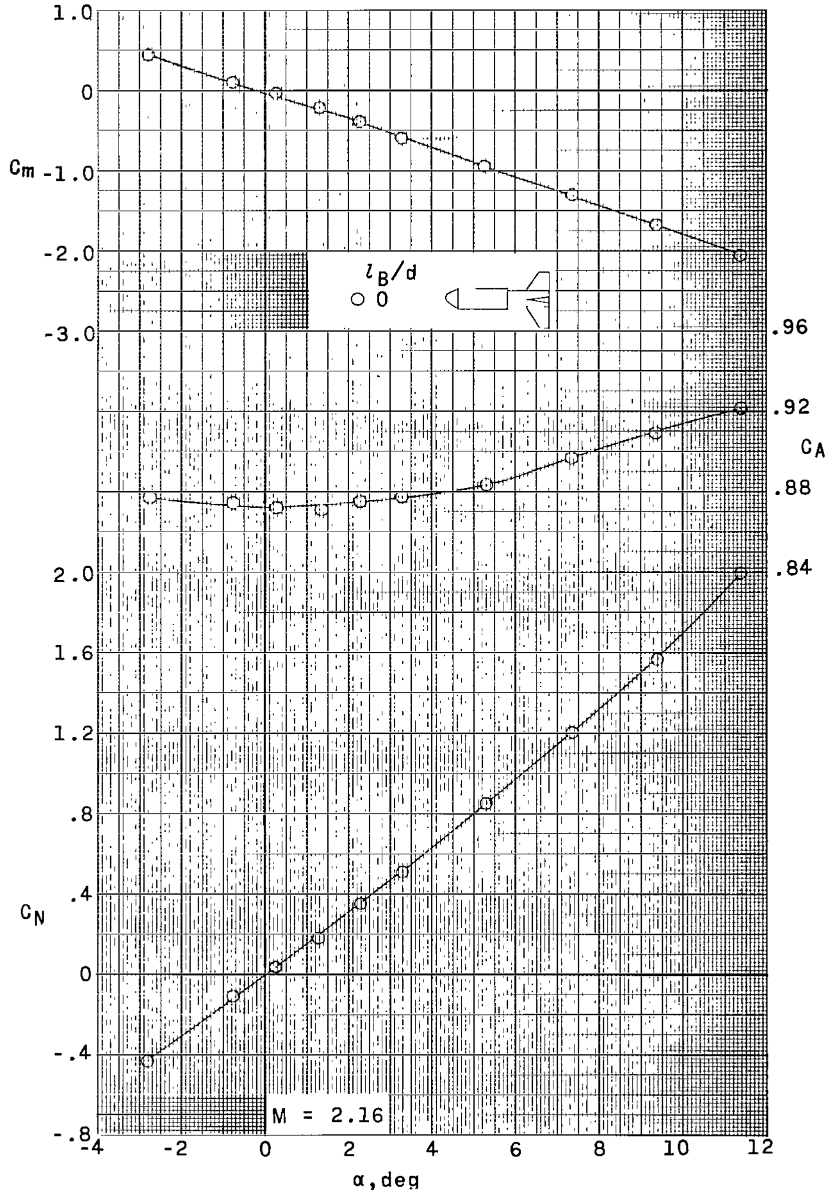

(b) Continued.

Figure 14.- Continued.

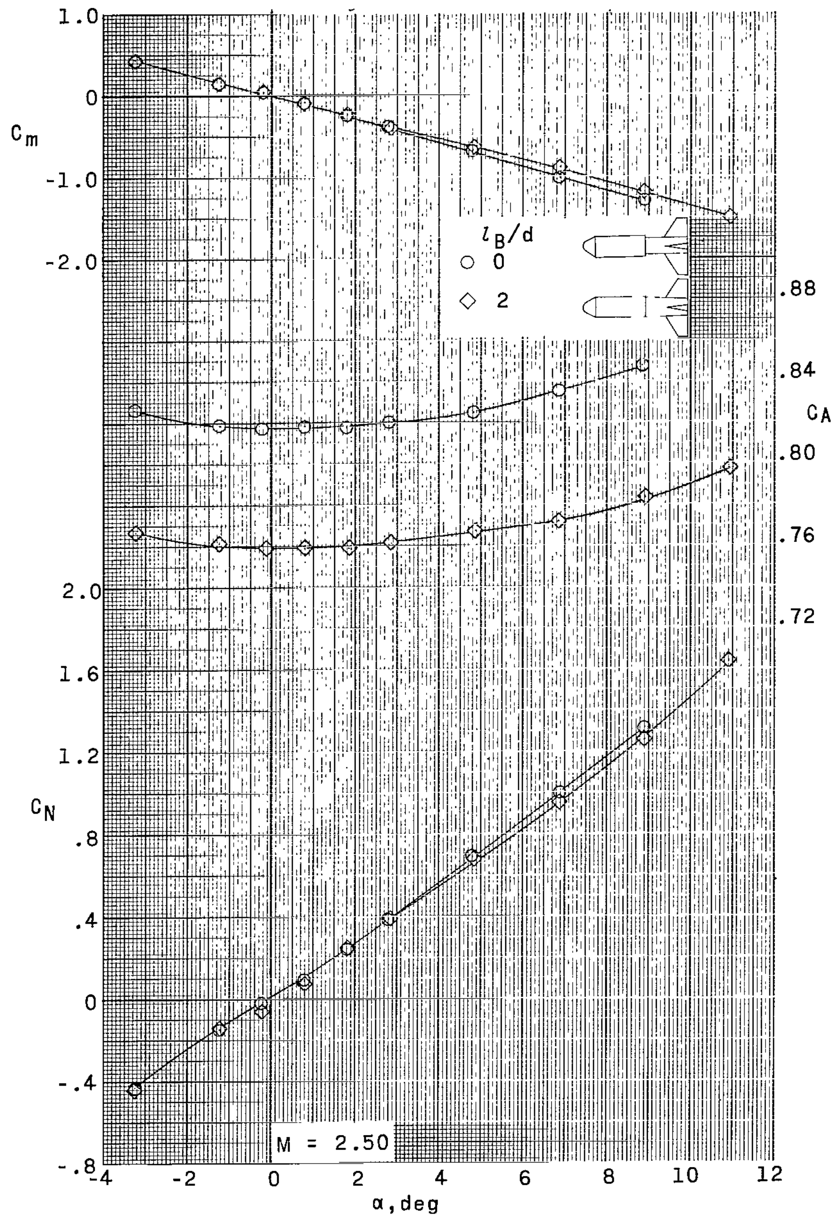

(b) Continued.

Figure 14.- Continued.

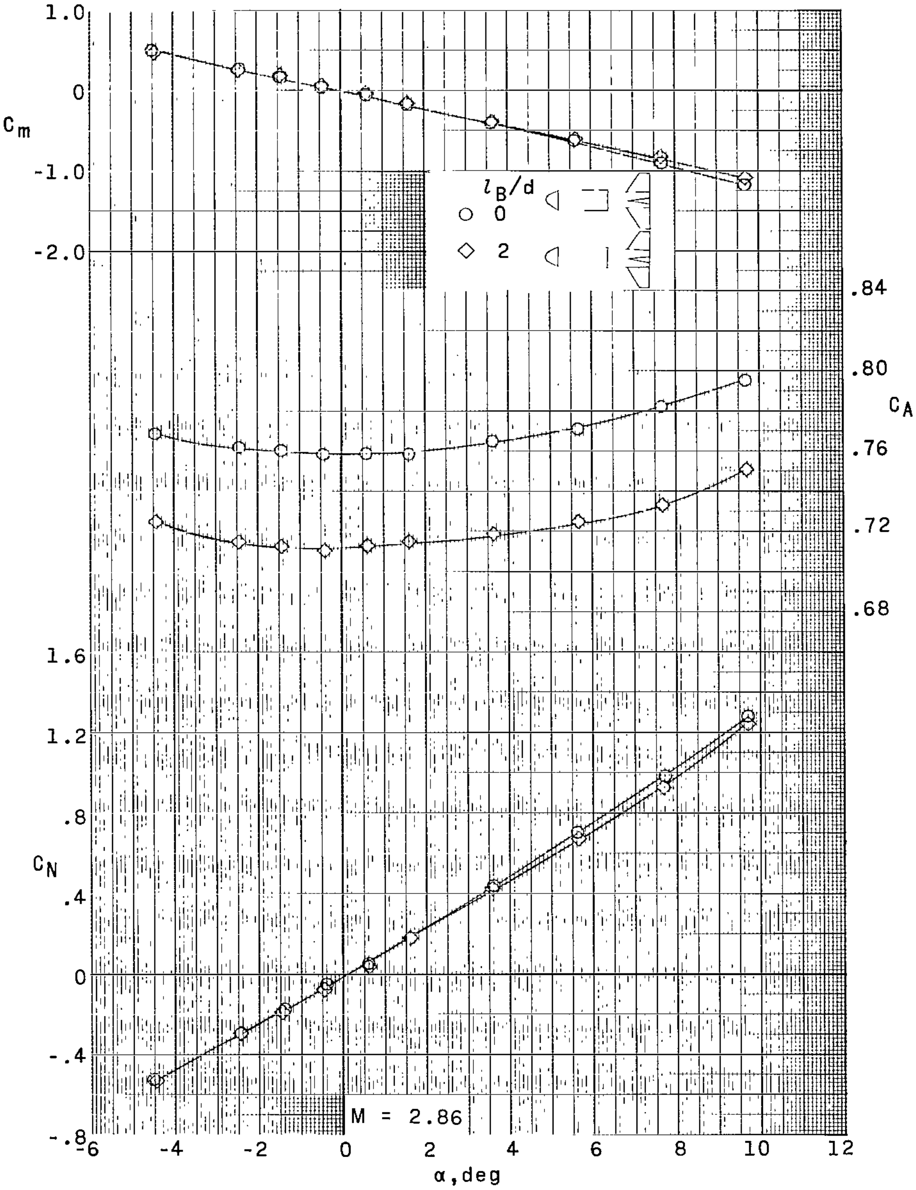

(b) Concluded.

Figure 14.- Concluded.

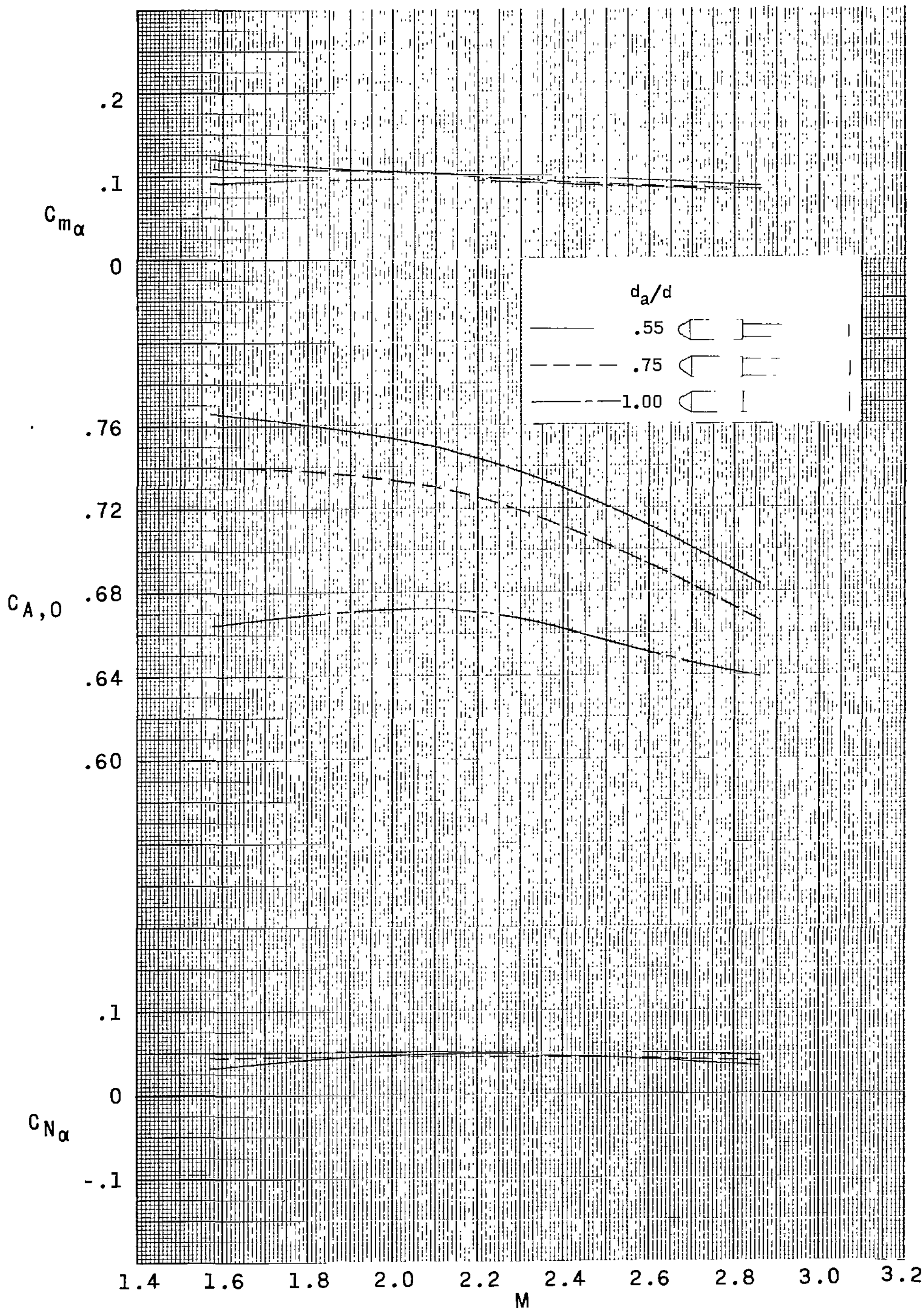

(a) Long first stage.

Figure 15.- Effect of ratio of first-stage diameter to second-stage diameter on longitudinal aerodynamic parameters. Fins off; $l_B/d = 0$.

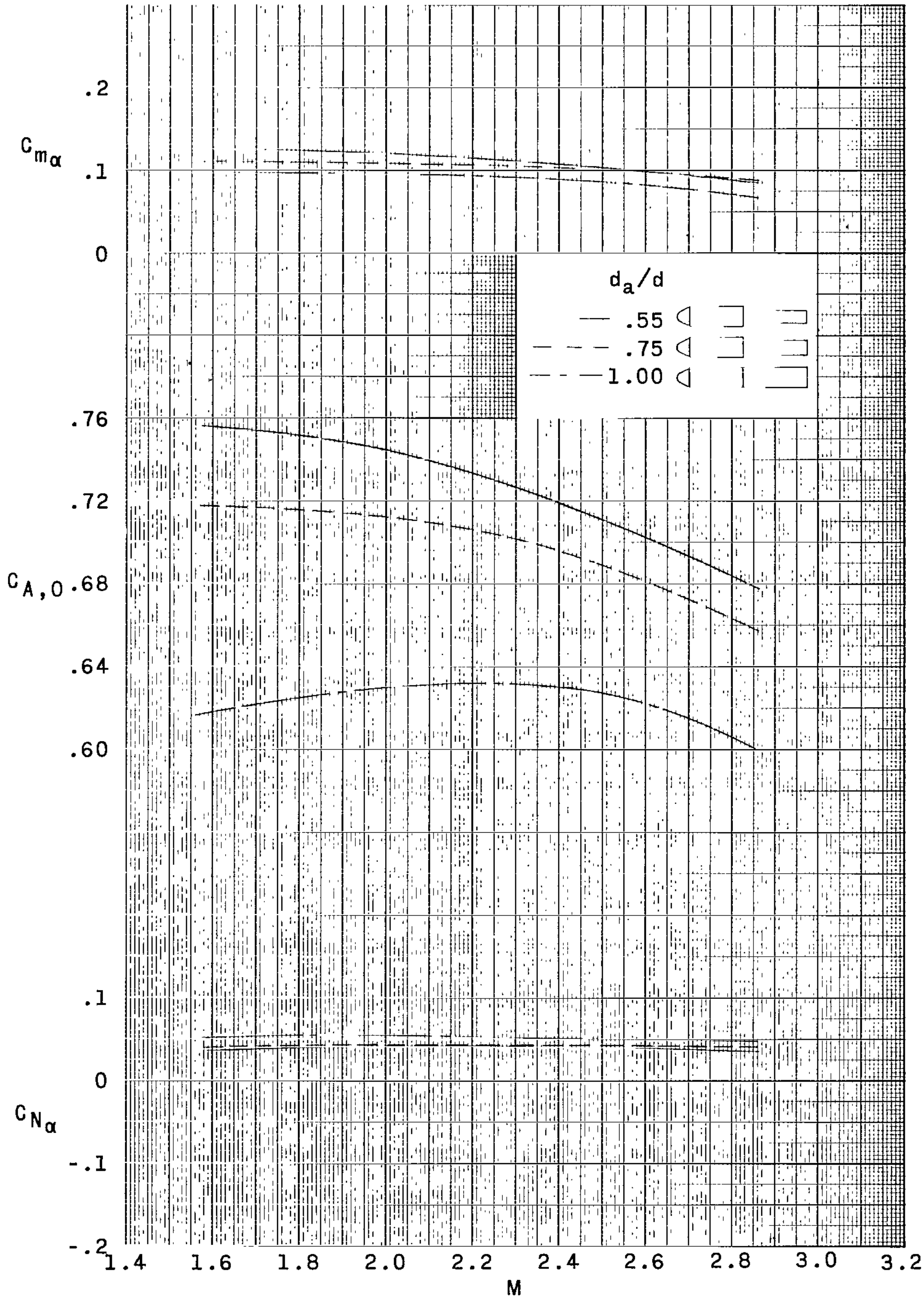

(b) Intermediate first stage.

Figure 15.- Continued.

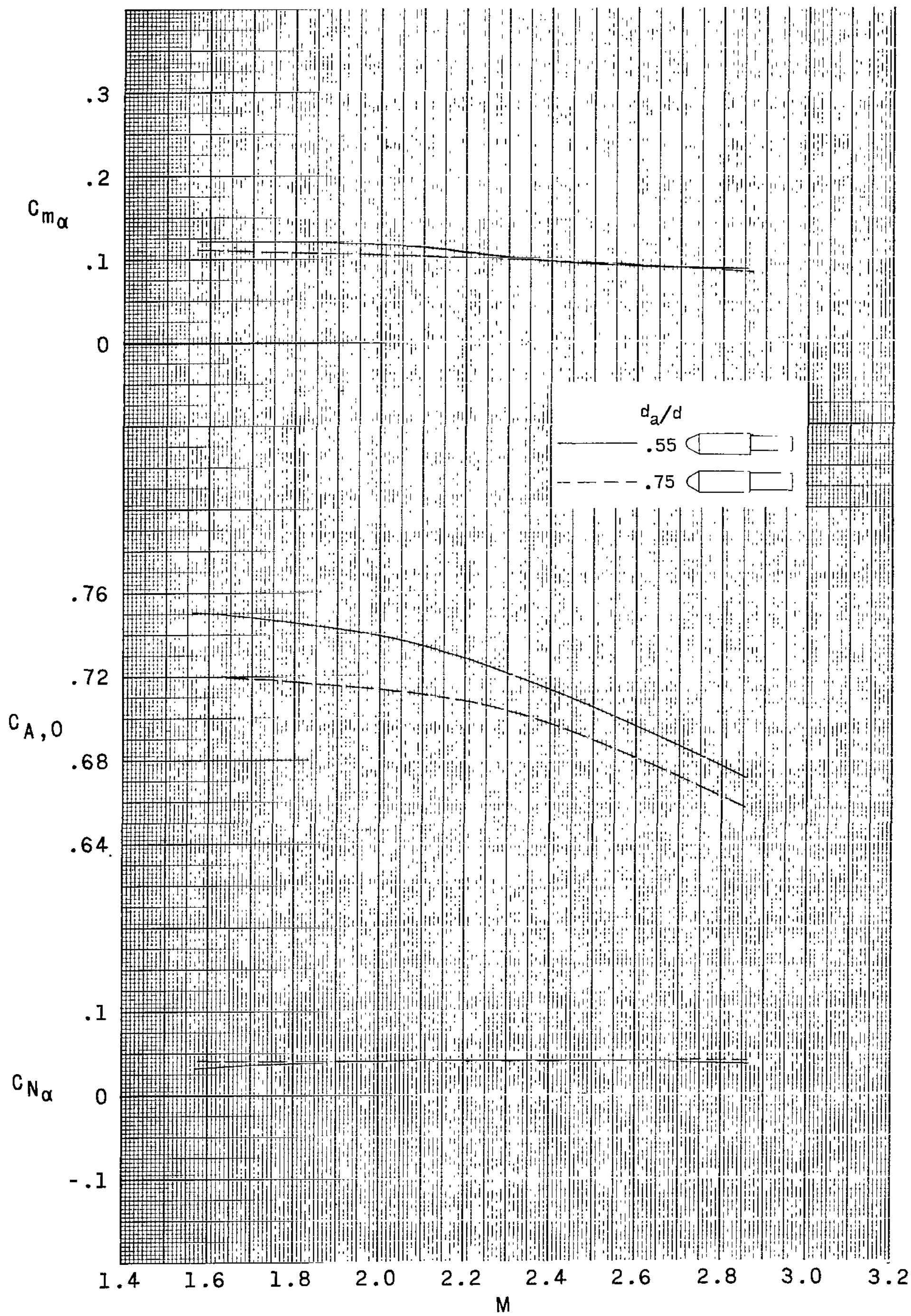

(c) Short first stage.

Figure 15.- Concluded.

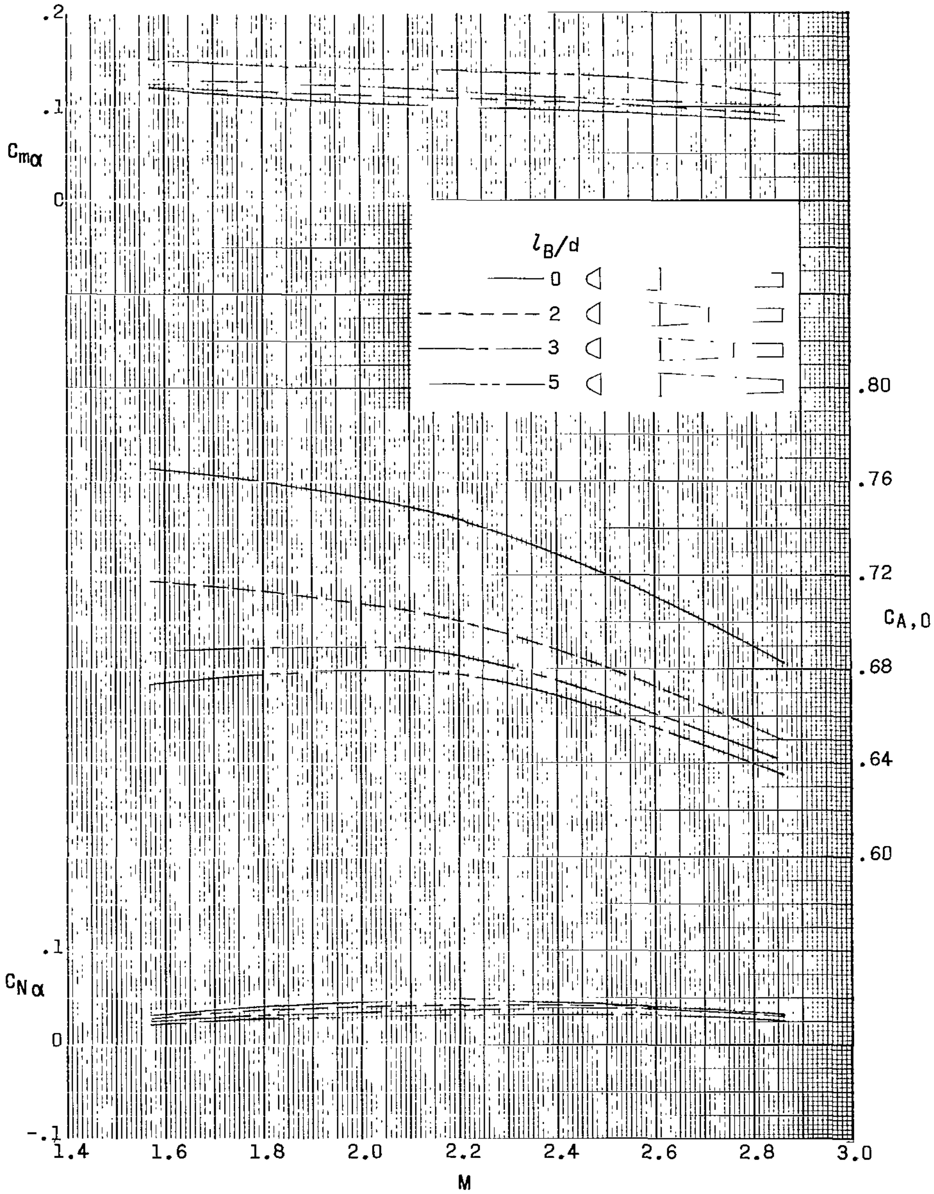

(a) Long first stage.

Figure 16.- Effect of boattail length on longitudinal aerodynamic parameters. Fins off; $d_a/d = 0.55$.

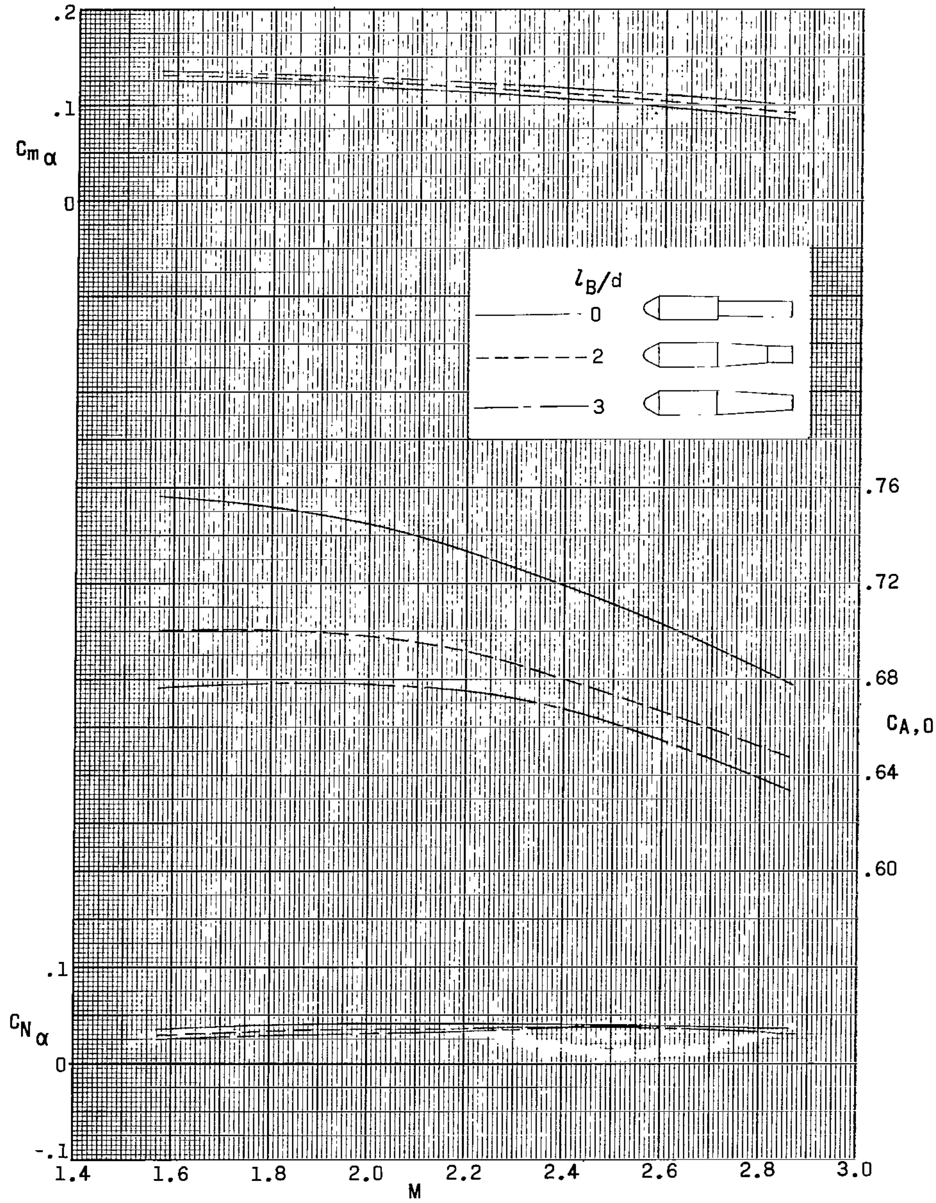

(b) Intermediate first stage.

Figure 16.- Continued.

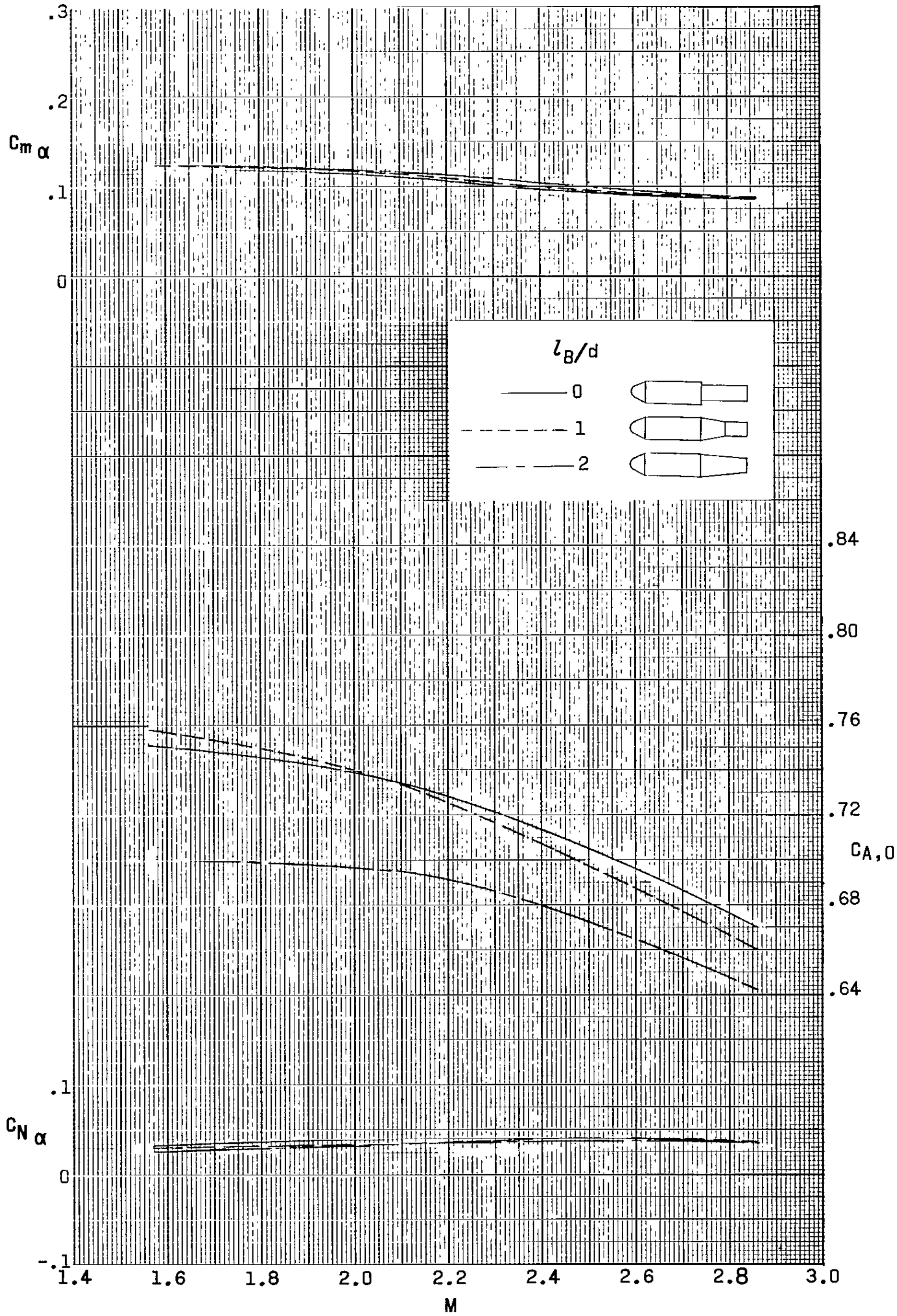

(c) Short first stage.

Figure 16.- Concluded.

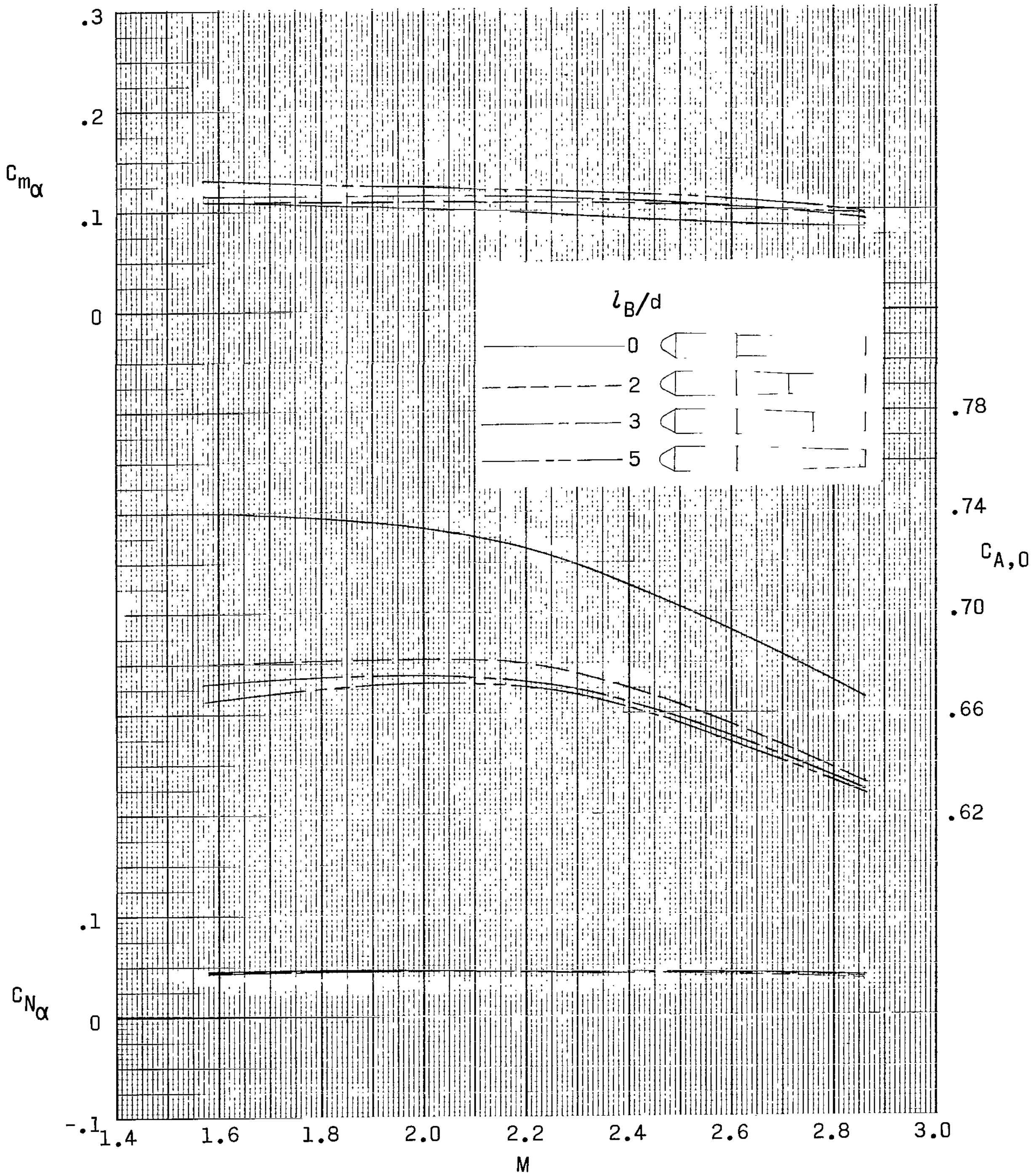

(a) Long first-stage configuration.

Figure 17.- Effect of boattail length on longitudinal aerodynamic parameters. Fins off; $d_a/d = 0.75$.

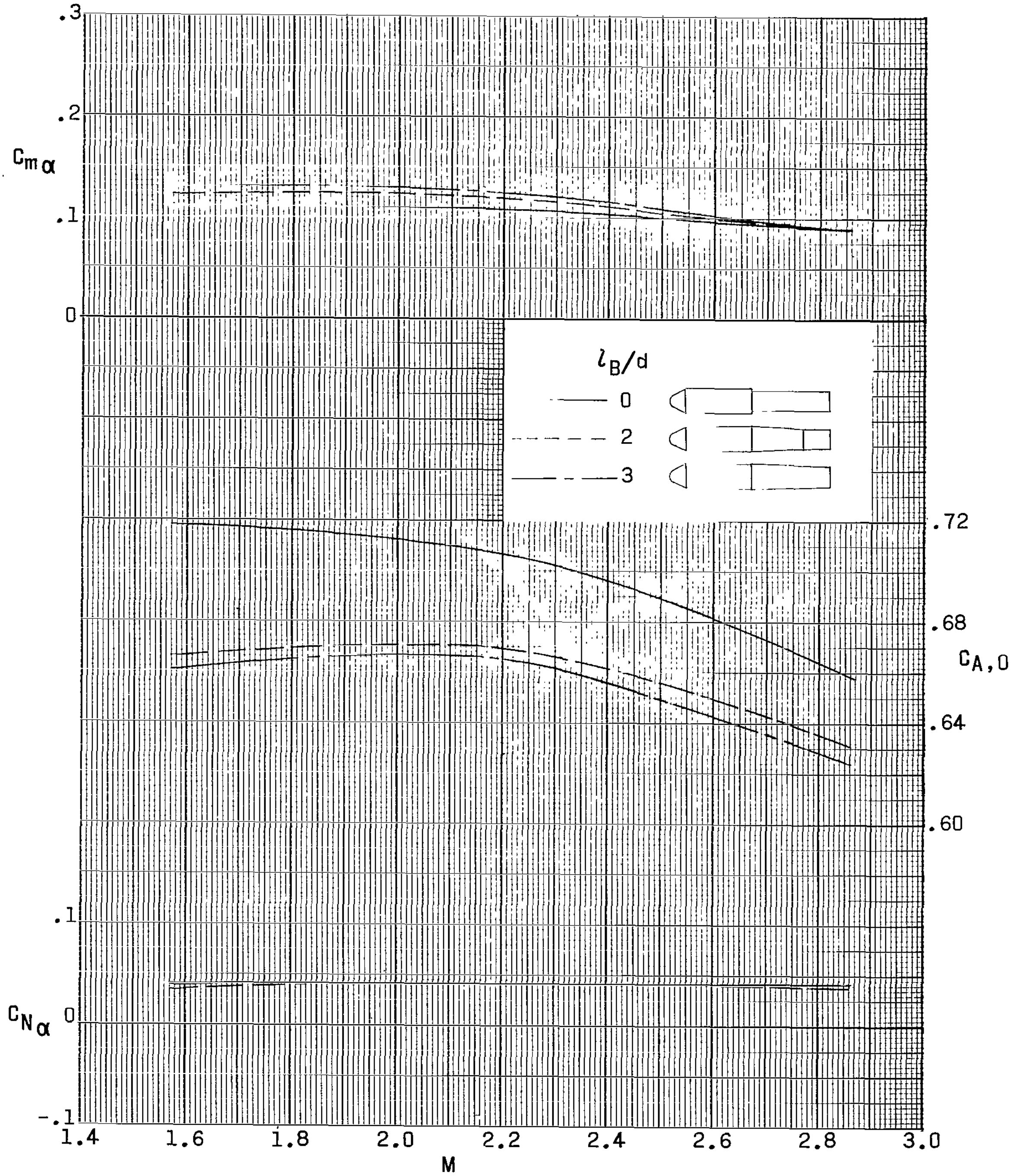

(b) Intermediate first stage.

Figure 17.- Continued.

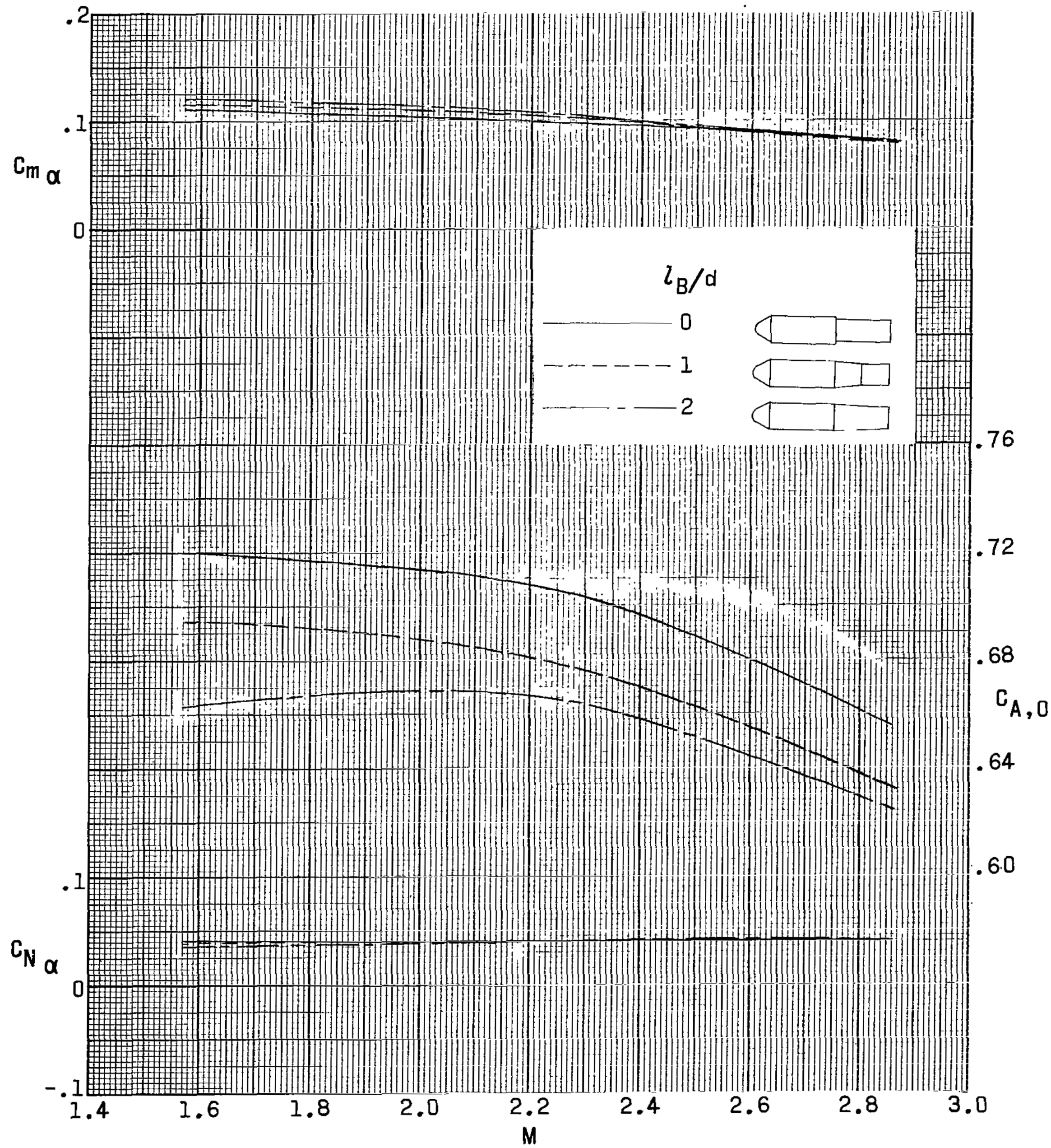

(c) Short first stage.

Figure 17.- Concluded.

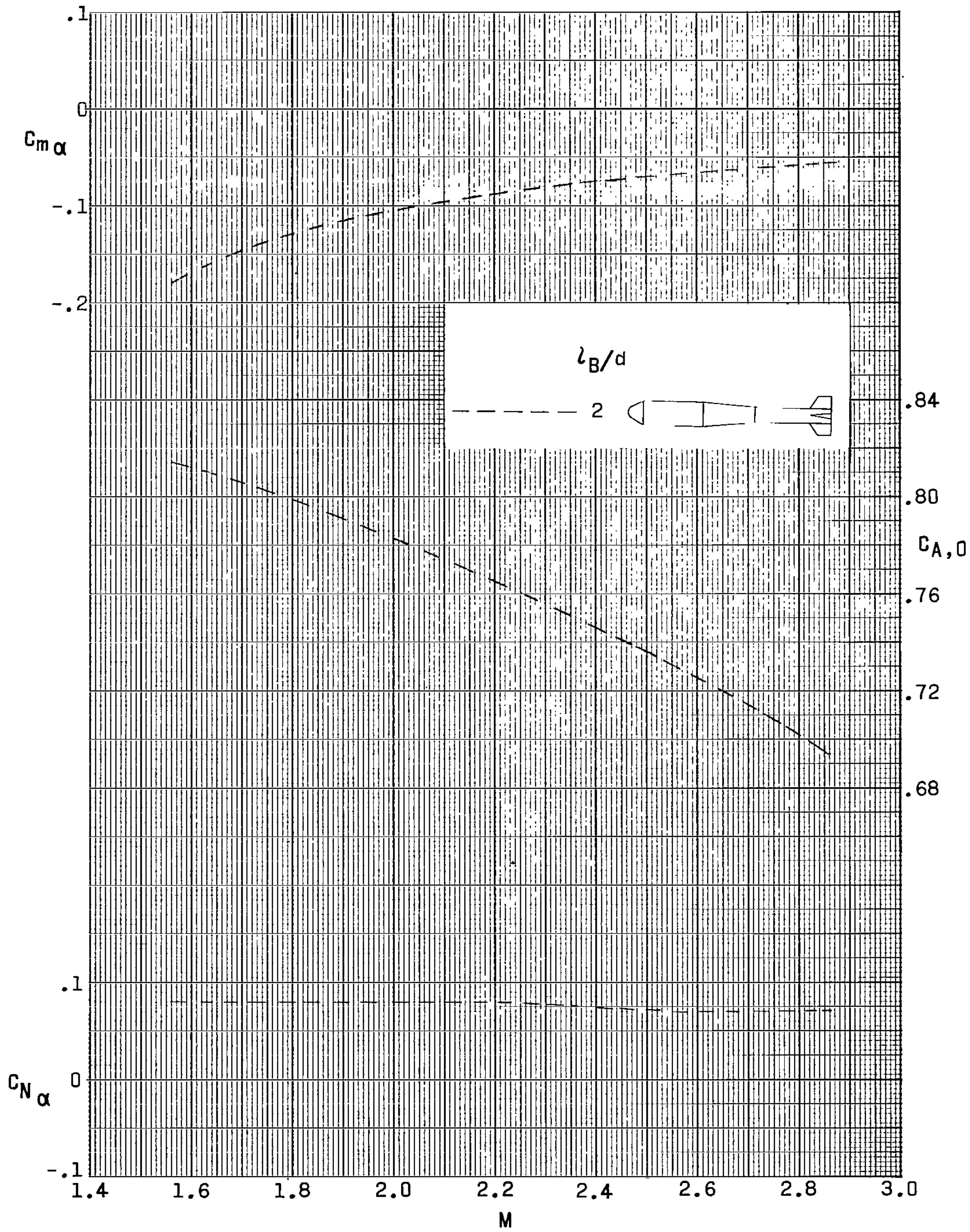

(a) Long first stage.

Figure 18.- Effect of boattail length on longitudinal aerodynamic parameters. Small fins; $d_a/d = 0.55$.

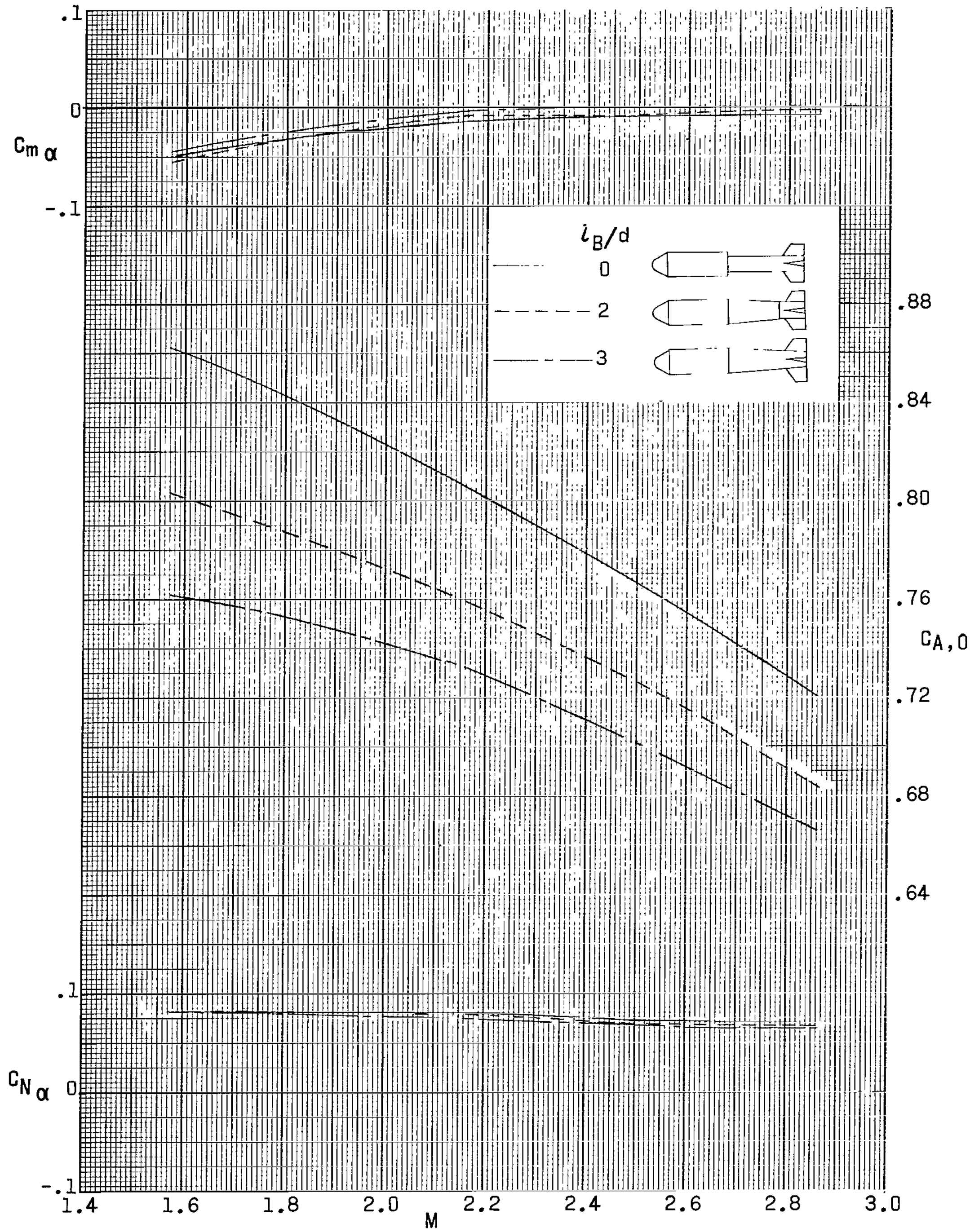

(b) Intermediate first stage.

Figure 18.- Concluded.

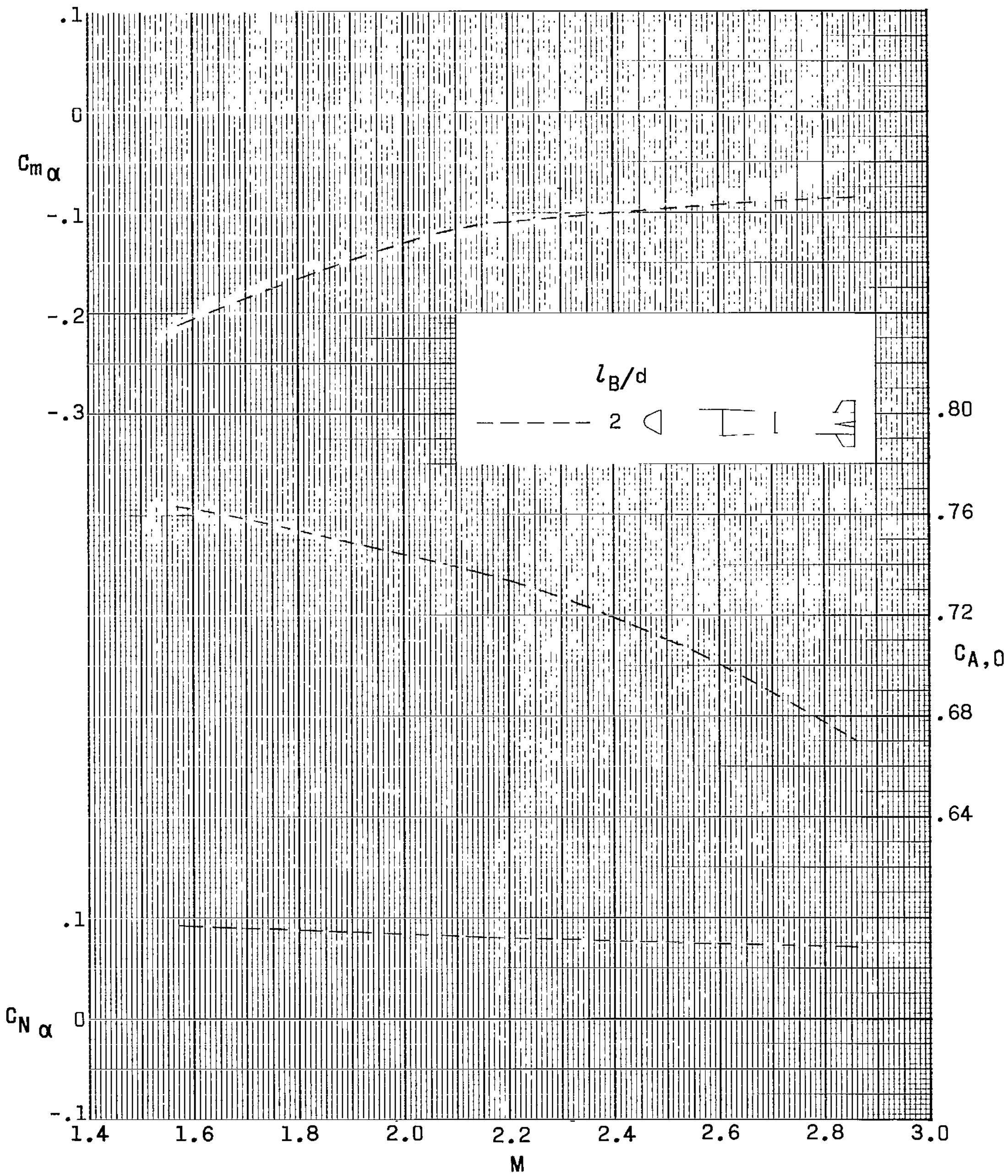

(a) Long first stage.

Figure 19.- Effect of boattail length on longitudinal aerodynamic parameters. Small fins; $d_a/d = 0.75$.

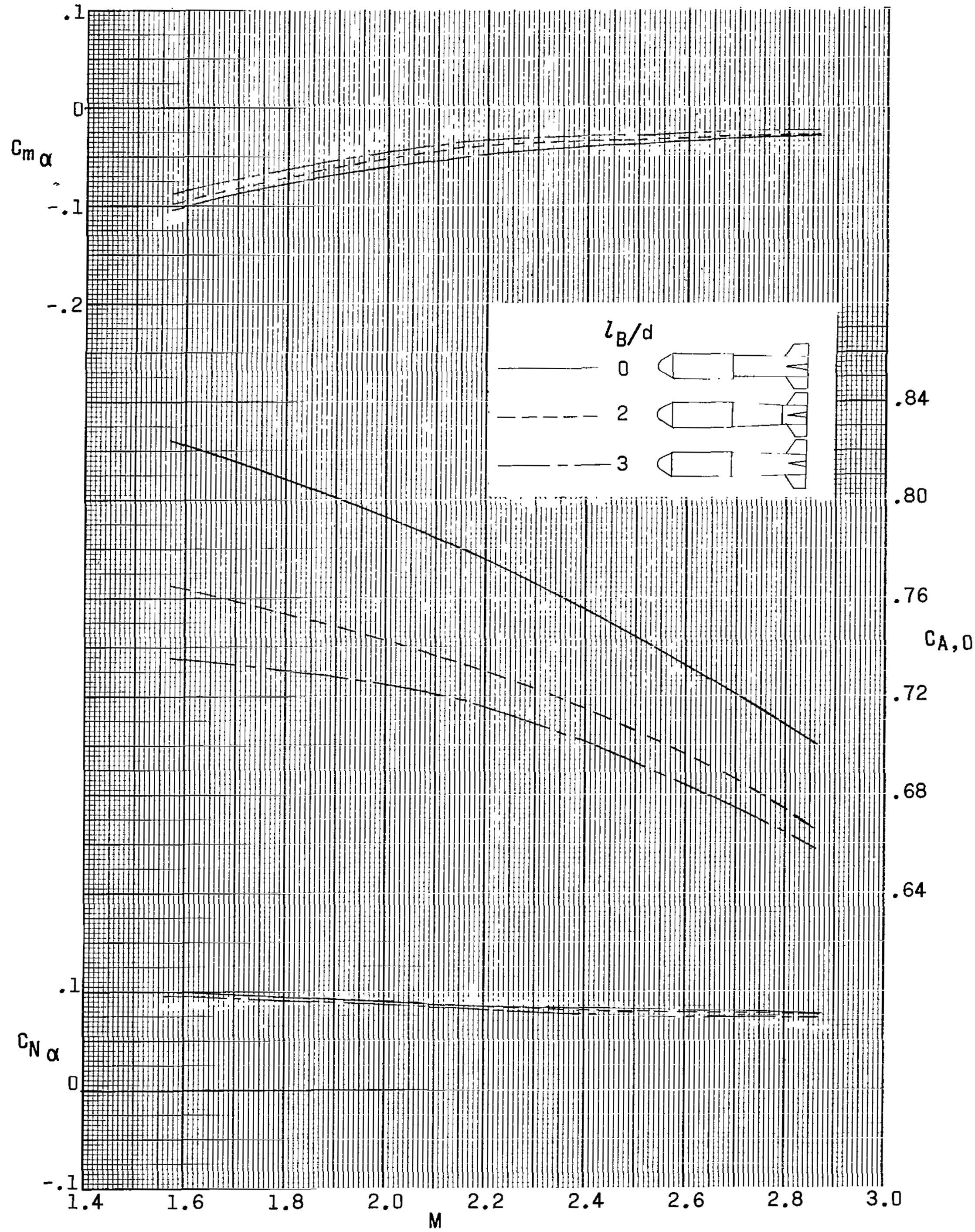

(b) Intermediate first stage.

Figure 19.- Concluded.

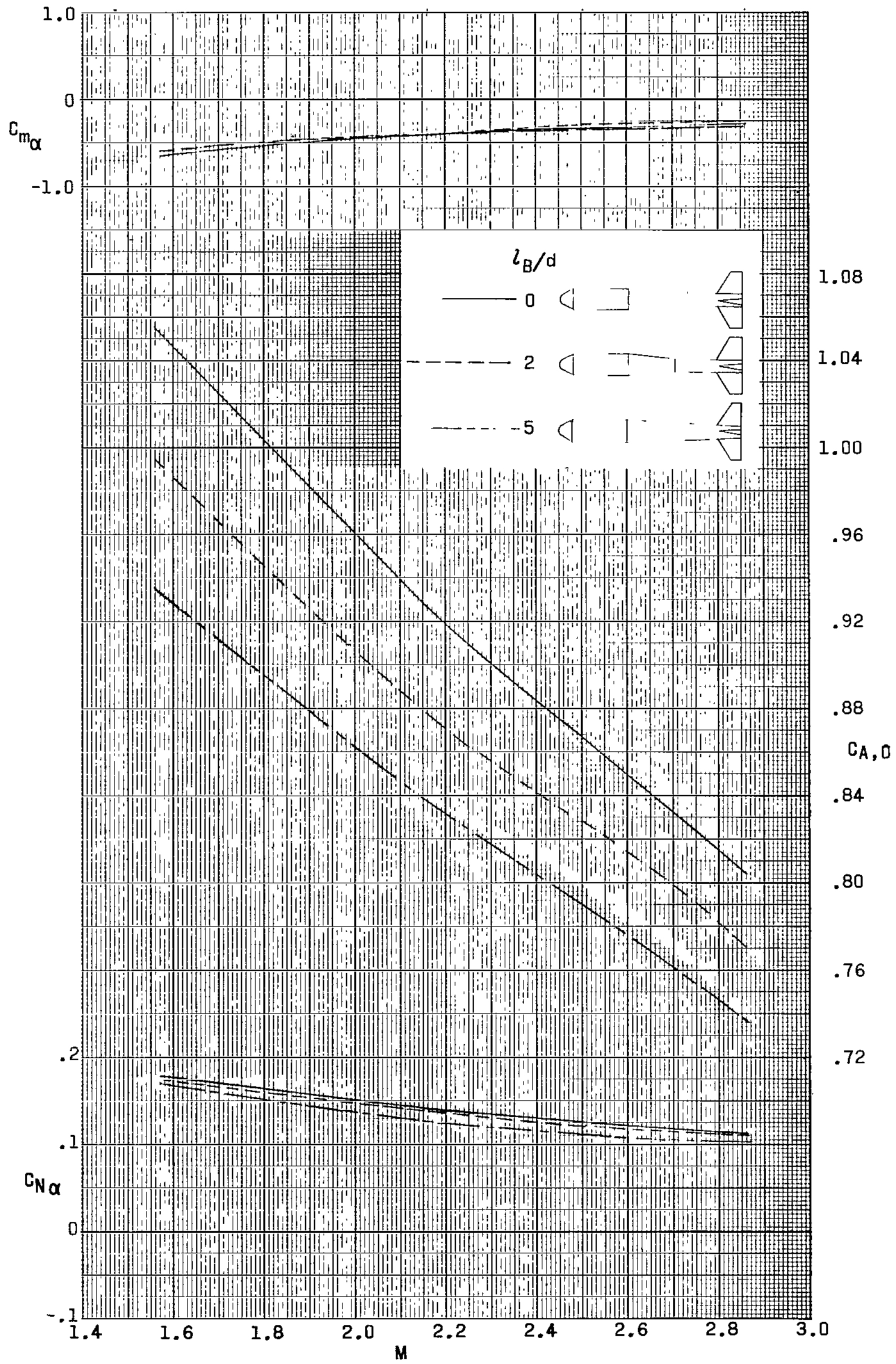

(a) Long first stage.

Figure 20.- Effect of boattail length on longitudinal aerodynamic parameters. Large fins; $d_a/d = 0.55$.

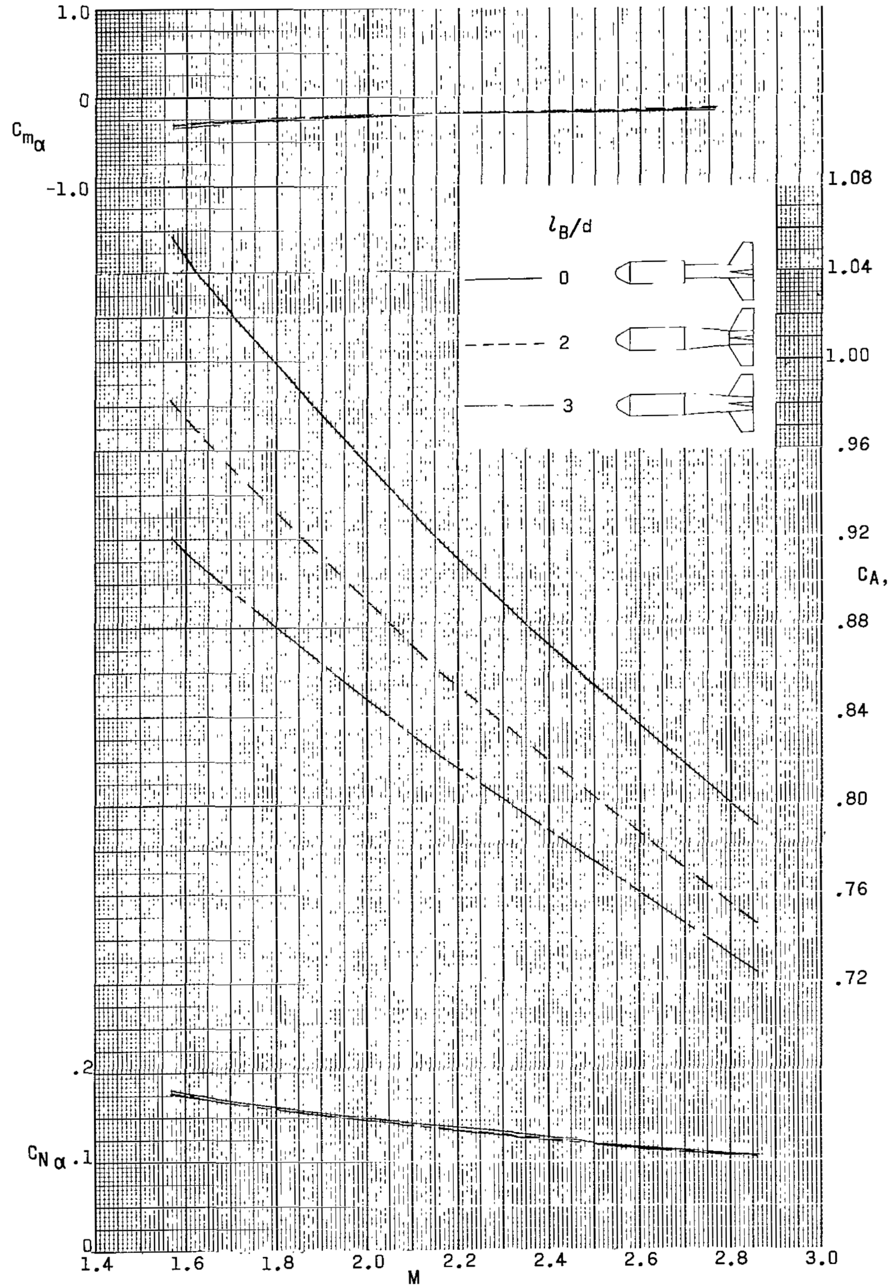

(b) Intermediate first stage.

Figure 20.- Continued.

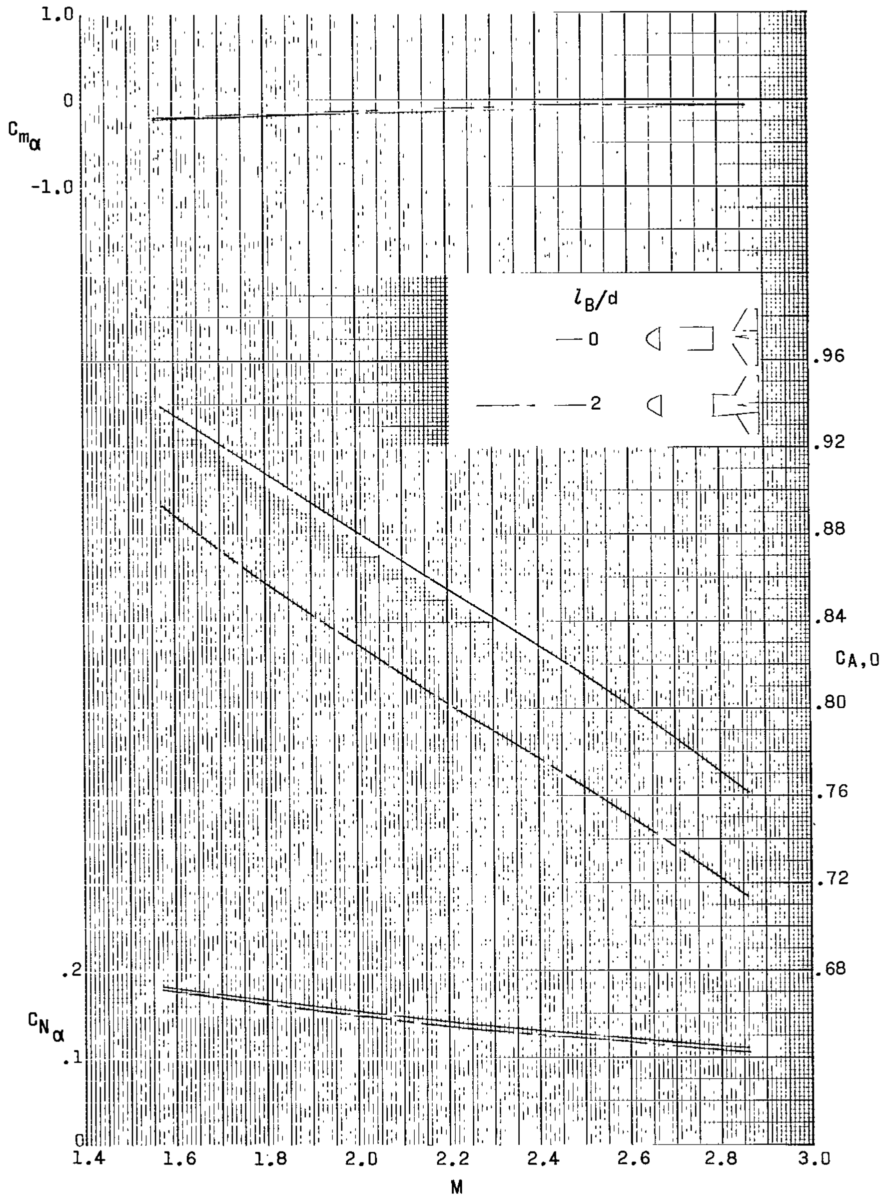

(c) Short first stage.

Figure 20.- Concluded.

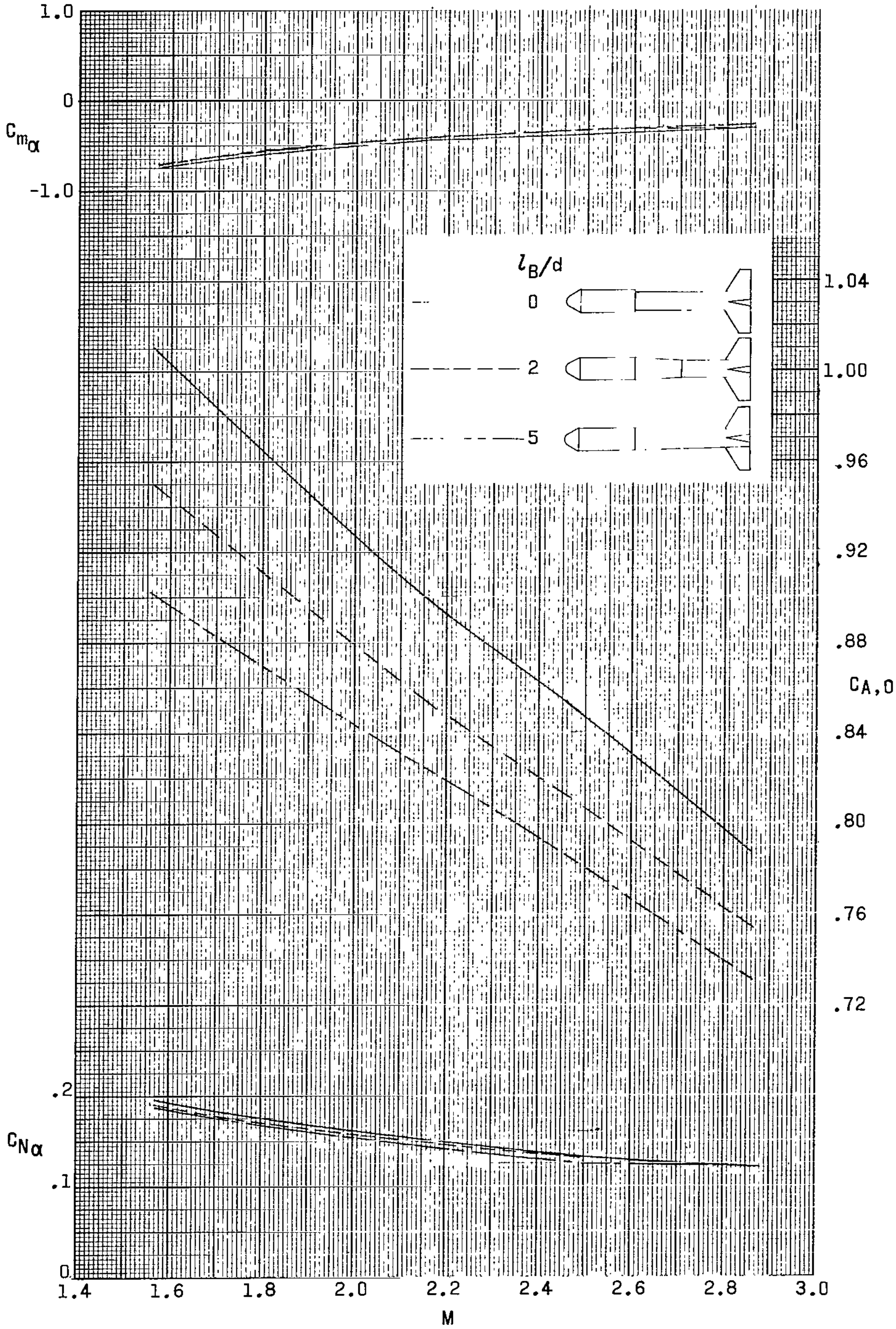

(a) Long first stage.

Figure 21.- Effect of boattail length on longitudinal aerodynamic parameters. Large fins; $d_a/d = 0.75$.

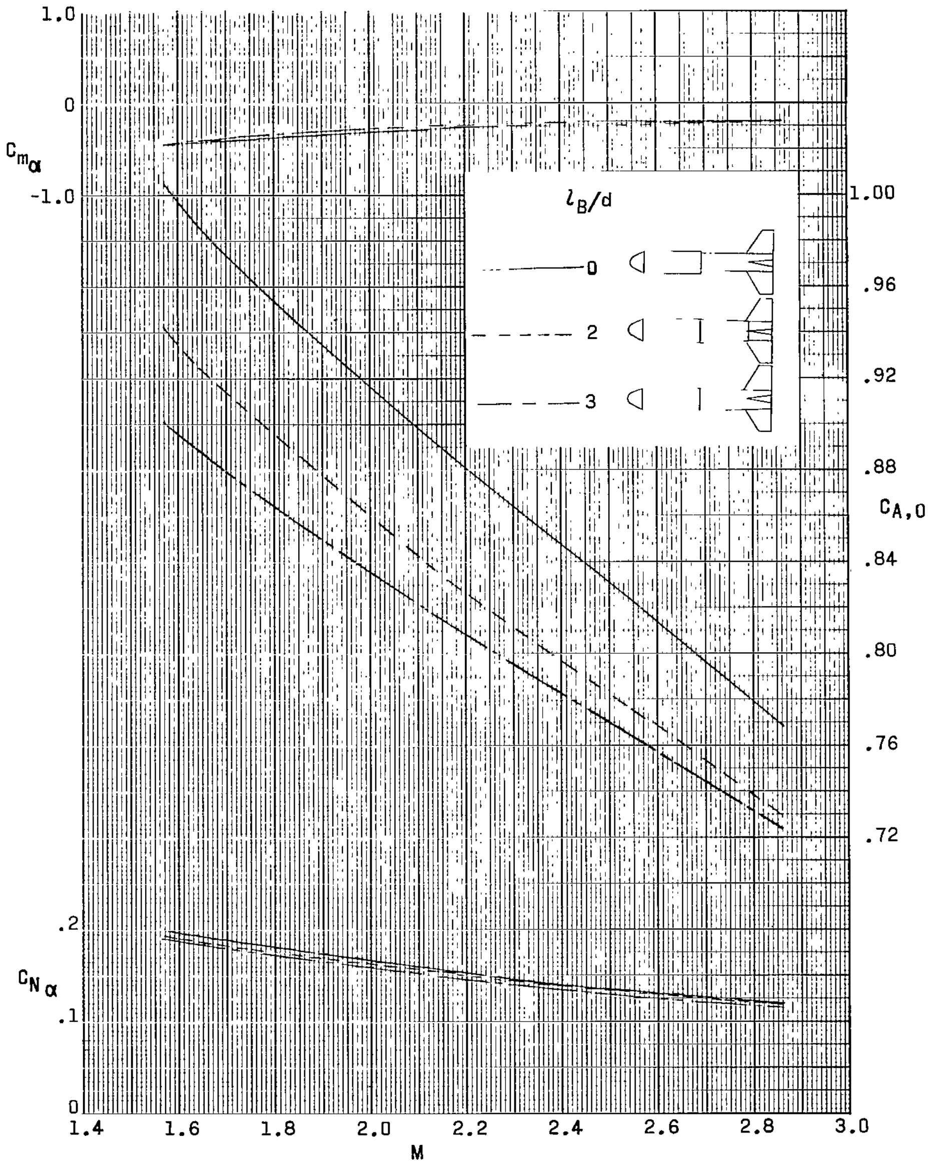

(b) Intermediate first stage.

Figure 21.- Continued.

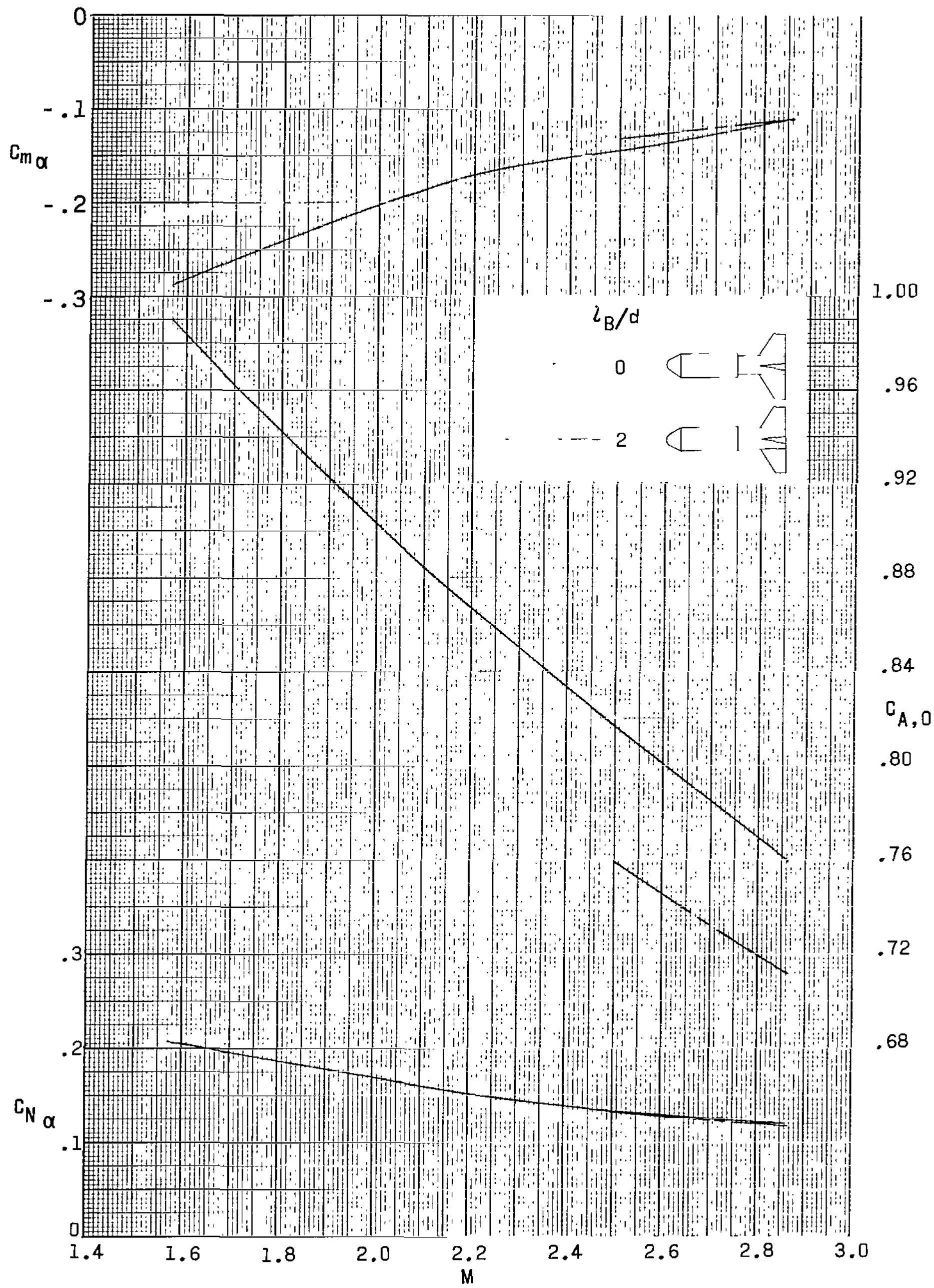

(c) Short first stage.

Figure 21.- Concluded.

NASA-Langley, 1965 L-3589

2/22/85
8

"The aeronautical and space activities of the United States shall be conducted so as to contribute . . . to the expansion of human knowledge of phenomena in the atmosphere and space. The Administration shall provide for the widest practicable and appropriate dissemination of information concerning its activities and the results thereof."

—NATIONAL AERONAUTICS AND SPACE ACT OF 1958

NASA SCIENTIFIC AND TECHNICAL PUBLICATIONS

TECHNICAL REPORTS: Scientific and technical information considered important, complete, and a lasting contribution to existing knowledge.

TECHNICAL NOTES: Information less broad in scope but nevertheless of importance as a contribution to existing knowledge.

TECHNICAL MEMORANDUMS: Information receiving limited distribution because of preliminary data, security classification, or other reasons.

CONTRACTOR REPORTS: Technical information generated in connection with a NASA contract or grant and released under NASA auspices.

TECHNICAL TRANSLATIONS: Information published in a foreign language considered to merit NASA distribution in English.

TECHNICAL REPRINTS: Information derived from NASA activities and initially published in the form of journal articles.

SPECIAL PUBLICATIONS: Information derived from or of value to NASA activities but not necessarily reporting the results of individual NASA-programmed scientific efforts. Publications include conference proceedings, monographs, data compilations, handbooks, sourcebooks, and special bibliographies.

Details on the availability of these publications may be obtained from:

SCIENTIFIC AND TECHNICAL INFORMATION DIVISION

NATIONAL AERONAUTICS AND SPACE ADMINISTRATION

Washington, D.C. 20546